



INVESTICE DO ROZVOJE VZDĚLÁVÁNÍ

Tisk této publikace byl podpořen z projektu:
„Tvorba mezinárodního vědeckého týmu a zapojování do vědeckých sítí v oblasti nanotechnologií a nekonvenčního tváření materiálu“,
reg. č. **CZ.1.07/2.3.00/20.0038**
podporovaného Operačním programem Vzdělávání pro konkurenceschopnost, spolufinancovaného z Evropského sociálního fondu a ze státního rozpočtu České republiky.

Autor:	kolektiv autorů
Pracoviště:	VŠB-Technická univerzita Ostrava Fakulta strojní
Název:	Sborník příspěvků z workshopu „The EU Framework Programmes - Our Future“
Místo, rok:	Ostrava, 2014
Počet stran:	95
Vydala:	Vysoká škola báňská – Technická univerzita Ostrava, FS, Katedra mechanické technologie

Za obsah příspěvků odpovídají jednotliví autoři.

Vysoká škola báňská – Technická univerzita Ostrava, 2014

ISBN 978-80-248-3477-1



Nanotým VŠB – TU Ostrava
CZ.1.07/2.3.00/20.0038

Nanotým VŠB – TU Ostrava CZ.1.07/2.3.00/20.0038



WORKSHOP

„The EU Framework Programmes - Our Future“

6. – 8. února 2014

Sborník příspěvků

Hotel Sepetná, Ostravice, Česká republika
2014

Project name: Creation of an international team of scientists and participation in scientific networks in the sphere of nanotechnology and unconventional forming material.

Program: Operational Programme Education for Competitiveness

Priority Programme: 2 - Tertiary Education, Research and Development

Support area: 2.3 - Human resources in research and development

Registration number: CZ.1.07/2.3.00/20.0038

Project start date: 1. June 2011

Project closing date: 31. May 2014

Project applicant: VŠB - TU Ostrava

Project partner: COMTES FHT a.s.

Administrative team: Main project manager – prof. Ing. Stanislav Ruzs, CSc.
Project coordinator – Ing. Jan Kedroň
Finance manager – Ing. Stanislav Tylšar

**Nanoteam VSB – TU Ostrava
CZ.1.07/2.3.00/20.0038**

**WORKSHOP
„The EU Framework Programmes – Our Future“**

Proceedings

**6th – 8th February 2014
Hotel Sepetná
Ostravice, Czech Republic**

VŠB – Technical University of Ostrava, Faculty of Mechanical Engineering, Department of Mechanical Technology, 2014



euROPEAN
social fund in the
czech republic



EUROPEAN UNION



MINISTRY OF EDUCATION,
YOUTH AND SPORTS



OP Education
for Competitiveness

INVESTMENTS IN EDUCATION DEVELOPMENT

Evaluation of seasoning of strip from low-carbon steel

Radek ČADA

VŠB – Technical University of Ostrava, 17. Listopadu 15, CZ 708 33 Ostrava-Poruba, Czech Republic,
radek.cada@vsb.cz

Abstract

Contribution concerns evaluation of formability of strip from low-carbon steel DC04, which is mostly used in Czech Republic for production of intricate deep stampings. The properties of strip were fully evaluated by tensile tests and by cupping tests according to Erichsen. The tests were carried out 2, 4, 6, 8, 10 and 12 months after the date of steel strip production. It is concluded that stored steel strip is suitable for the cases of drawing of flat stampings, where pressure-tension, eventually combined mechanical schemes of deformations occur.

Keywords

Formability, strip, steel, tensile test, cupping test, seasoning

1. INTRODUCTION

In Czech Republic the strips from steel DC04, which are produced in joint-stock company VSŽ Ocel' Košice, are often used for production of intricate or deep stampings. The standardized properties of this steel are guaranteed 6 months after the date of production. With regard to the fact, that in finishing enterprises these strips are sometimes stored even some months whereby their formability decreases as a rule, the evaluation of seasoning upon formability of mentioned steel strip at normal temperature was carried out.

2. TESTED MATERIAL

For detailed evaluation of properties the coil of sheet-metal from steel DC04 with dimensions 0.85 x 280 mm (heat No. 5494, coil No. 549403/3), made by cold rolling in joint stock company VSŽ Ocel' Košice, Slovak Republic, was chosen. This steel represents especially deep-drawing grade of steel. The strip was delivered recrystallizationally annealed and additionally light cold re-rolled.

2.1 Evaluation of chemical composition

Evaluation of chemical composition of chosen steel was carried out by dust exhausting method with the use of spectrometer GDS-750 QDP. The results of analysis are in Table 1. It is seen, that delivered strip from steel DC04 fulfilled the demands on chemical composition according to Czech State Standard (ČSN) 41 1305.



Table 1 Chemical analysis results of heat No. 43952 of strip from steel DC04

C (wt. %)	Mn (wt. %)	Si (wt. %)	P (wt. %)	S (wt. %)	Al (wt. %)
0.013	0.344	0.00	0.018	0.013	0.069

2.2 Metallography judgment

The mean degree of contamination of steel DC04 by non-metallic inclusions was less than 1 according to Czech State Standard 42 0471, which gives evidence about great fineness of their microstructure and from that following good formability.

In order to judge the microstructure of sheet the metallographic samples from thickness of sheet-metal etched by 3 % Nital solution, i. e. 3 % solution of nitric acid HNO₃ (density 1.4 g/cm³) in ethyl alcohol C₂H₅OH, were carried out. Felt polishing and etching were generally three times repeated. The photographs of etched metallographic samples were carried out on microscope Neophot 2 (Carl Zeiss Jena). On photographs the ferrite grain with lamellar pearlite on grain lines was visible.

At steel DC04 the ferrite grain size of 9.5 according to the Czech State Standard 42 0462 was found out. The shape of ferrite grains at all tested steels was flattened, lens-shaped, the longer axes were in sheet-metal plane. The ferrite grains were extended in direction of rolling with dimensions heterogeneity less than 2 numbers according to scale of Czech State Standard 42 0462.

The grain-size in sheet metal for pressing and deep drawing is often of great importance if the best use is to be made of the material. Grain-size can affect both the working of the part under the press and the final properties achieved in the finished component. It is often taken as a general rule that the larger the grain-size the more ductile is the material and the easier it is to work. However if the grain-size is too large a rough surface is developed during pressing known as an orange-peel effect. Hence there is usually an optimum grain grain-size for material to make any particular part depending on the severity of the working operation and on the importance or otherwise of achieving a smooth surface finish.

The optimum grain-size for autobody quality steel has been established over the years as around ASTM 7. This results in a good balance between formability requirements and manufacturing limitations in the steel mill necessary for economic production.

Grain-size influence tensile strength and to a less significant extent elongation in addition to the yield strength and strain-hardening characteristic and it is felt that it could have a more significant effect on autobody press-shop performance than some other properties such as anisotropy.

At steel DC04 the highest degree of cementite presence was found out 1/1A-C according to Czech State Standard 42 0469, i. e. non uniform layout of formations with dimensions approximately 10 µm at grain lines and in grains and small formations, arranged to the direction of forming.

3. PROPERTIES OF STRIP FROM STEEL DC04 DURING STORAGE

For evaluation of the influence of storage time on formability of steel strip DC04 the properties of this steel were evaluated 2, 4, 6, 8, 10 and 12 months after the date of steel strip production.



3.1 Cupping tests according to Erichsen

By cupping tests according to Czech State Standard 42 0406 at tested steel strip stored 2, 4, 6, 8, 10 and 12 months after the date of its production the mean values of deepening, IE , were found out from five measurements (see Table 2). At all test specimens the zone of localization of plastic deformation had shape of circle or circular arc which gives evidence about homogenous material. From Table 2 is seen, that all measured values of tested strip from steel DC04 fulfilled the demand of Czech State Standard 41 1305 for thickness 0.85 mm ($IE = \text{min. } 10.30 \text{ mm}$).

Table 2 Results of cupping tests according to Erichsen at tested steel strip

Measurement number	Storage time of strip from steel DC04					
	2 months	4 months	6 months	8 months	10 months	12 months
1	11.25	11.30	11.25	11.10	11.10	11.15
2	11.10	11.20	11.35	11.20	11.25	11.35
3	11.05	11.15	11.15	11.25	11.30	11.45
4	11.05	11.15	11.15	11.25	11.35	11.50
5	11.20	11.25	11.25	11.35	11.35	11.40
Mean value IE (mm)	11.13	11.21	11.23	11.23	11.27	11.37

3.2 Evaluation of mechanical properties

Tensile specimens with initial length of the gauge section $L_0 = 80 \text{ mm}$ and initial width of the gauge section $b_0 = 20 \text{ mm}$ were machined from tested steel parallel, perpendicular and diagonal to the rolling direction. The evaluation was carried out by tensile tests according to Czech State Standard 42 0310. The sheet tensile specimens from the three orientations 0° , 45° , 90° were deformed in INSTRON 1196 (type 2511-320, model No. A212-201, Great Britain) machine at constant crosshead speed in the range $3 \div 30 \text{ MPa}\cdot\text{s}^{-1}$ and at room temperature.

The yield strengths $R_p 0.2$ were found out from tensile diagrams by graphical method according to Czech State Standard 42 0310. The directional values of mechanical properties were calculated like arithmetic means from values measured at five test specimens (see Table 3).

Table 3 Mean values of mechanical properties of strip from steel DC04

Mechanical properties	Storage time of strip from steel DC04					
	2 months	4 months	6 months	8 months	10 months	12 months
$R_p 0.2$ (MPa)	214.56	216.58	187.91	215.99	223.54	216.23
R_m (MPa)	393.71	397.29	390.65	395.62	394.37	382.21
$R_p 0.2/R_m$ (-)	0.545	0.545	0.481	0.546	0.567	0.566
A_{80} (%)	38.6	39.6	39.1	39.0	38.9	39.2
Z (%)	86.4	88.6	86.0	85.9	84.0	84.6
ε_r (-)	0.271	0.272	0.281	0.270	0.271	0.270
C (MPa)	618.03	620.76	641.33	618.42	607.10	588.58

The values of uniform true strain at maximum load, ε_r , were determined according to Czech State Standard 42 0435 using the formula:

$$\varepsilon_r = \frac{L_m - L_0}{L_0} \quad (-) \quad (1)$$



where L_m is the length of the gauge section at maximum load (without unloading), L_0 is the initial length of the gauge section.

3.3 Evaluation of planar anisotropy of mechanical properties

From evaluated directional and mean values of mechanical properties the values of coefficients of planar anisotropy (see Table 4) were calculated according to the additional example:

$$PR_{m(x)} = \frac{R_{m(x)} - R_{m(0)}}{R_{m(0)}} \cdot 100 \quad (\%) \quad (2)$$

where $PR_{m(x)}$ is the coefficient of planar anisotropy of tensile strength for angle x ($^\circ$) in relation to the direction of rolling, $R_{m(x^\circ)}$ is tensile strength for angle x° between tensile axis and rolling direction, $R_{m(0)}$ is tensile strength for angle 0° between tensile axis and rolling direction.

The values of maximum coefficients of planar anisotropy (see Table 4) were calculated according to the additional example:

$$\max PR_m = \frac{\max R_m - \min R_m}{\min R_m} \cdot 100 \quad (\%) \quad (3)$$

where $\max PR_m$ is the maximum coefficient of planar anisotropy of tensile strength, $\max R_m$ is maximal directional tensile strength, $\min R_m$ is minimum directional tensile strength.

Table 4 Coefficients of planar anisotropy of mechanical properties of tested steel strip

Coefficient of planar anisotropy	Storage time of strip from steel DC04					
	2 months	4 months	6 months	8 months	10 months	12 months
$PR_{p(45)}$ (%)	5.13	8.21	8.90	4.85	5.04	5.87
$PR_{p(90)}$ (%)	1.47	2.94	-5.27	3.22	1.93	3.82
$\max PR_p$ (%)	5.13	8.21	14.96	4.85	5.04	5.87
$PR_{m(45)}$ (%)	3.47	2.42	2.39	3.31	2.56	2.66
$PR_{m(90)}$ (%)	-0.58	-2.30	-2.01	-0.91	-2.25	-1.19
$\max PR_m$ (%)	4.07	4.83	4.49	4.26	4.92	3.89
$P(R_p/R_m)_{(45)}$ (%)	1.60	5.66	6.35	1.49	2.42	3.13
$P(R_p/R_m)_{(90)}$ (%)	2.06	5.36	-3.33	4.17	4.28	5.08
$\max P(R_p/R_m)$ (%)	2.06	5.66	10.01	4.17	4.28	5.08
$PA_{(45)}$ (%)	-12.83	-7.15	-9.24	-5.56	-6.47	-9.26
$PA_{(90)}$ (%)	-9.29	-2.22	-2.96	-4.33	-3.25	-2.59
$\max PA$ (%)	14.72	7.70	10.18	5.89	6.92	10.21

3.4 Evaluation of normal anisotropy

Normal anisotropy describes variations in properties between directions in the plane of the sheet and normal to it. Its practical importance turns on the fact that the resistance of sheet metal to thinning, which is advantageous for deep pressing operations, is a function of its normal anisotropic plasticity. The values of normal plastic anisotropy ratio, r , were determined from measurements according to ČSN ISO 10113.

3.5 Evaluation of strain-hardening exponent by method using maximum uniform elongation

The values of n_m , calculated by the method using maximum uniform elongation, are more strongly correlated with pure stretchability than are the values of n_m , calculated by the method



according to ČSN ISO 10275. That is why these values were used for evaluation of formability of tested sheet-metal.

Table 5 Values of normal plastic anisotropy ratio and its mean planar anisotropy at tested steel

Coefficient (-)	Storage time of strip from steel DC04					
	2 months	4 months	6 months	8 months	10 months	12 months
r_0	1.56	1.46	1.48	1.39	1.52	1.61
r_{45}	1.14	1.22	1.07	1.15	1.21	1.25
r_{90}	1.54	1.72	1.63	1.59	1.61	1.85
r_m	1.35	1.41	1.32	1.32	1.39	1.49
Δr	0.41	0.37	0.48	0.34	0.36	0.48

Table 6 Values of strain-hardening exponent and its mean planar anisotropy at tested steel

Coefficient (-)	Storage time of strip from steel DC04					
	2 months	4 months	6 months	8 months	10 months	12 months
n_0	0.255	0.254	0.256	0.246	0.246	0.247
n_{45}	0.229	0.227	0.236	0.233	0.229	0.227
n_{90}	0.233	0.240	0.248	0.231	0.240	0.235
n_m	0.236	0.237	0.244	0.236	0.236	0.234
Δn	0.015	0.020	0.016	0.006	0.014	0.014

3.6 Formability index

For reciprocal comparison of formability of tested steel strip stored 2, 4, 6, 8, 10 and 12 months after the date of its production the formability index, l , was calculated [1]:

$$l = r_{\alpha\min} \cdot n_m \cdot 1000 \quad (-) \quad (4)$$

where $r_{\alpha\min}$ is the minimal normal plastic anisotropy ratio from values of it in orientations 0° , 45° , 90° in relation to the direction of rolling, n_m is the mean strain-hardening exponent.

Table 7 Values of formability index at tested steel

Coefficient (-)	Storage time of strip from steel DC04					
	2 months	4 months	6 months	8 months	10 months	12 months
$r_{\alpha\min}$	1.14	1.22	1.07	1.15	1.21	1.25
n_m	0.236	0.237	0.244	0.236	0.236	0.234
l	269.04	289.14	261.08	271.40	285.56	292.50

4. CONCLUSIONS

The strip from steel DC04 did not present in any direction of 0° , 45° and 90° in relation to the direction of rolling outstanding yield point in tension R_e , which gives evidence about right carried out light re-rolling of these steel at its production.

Changes of separate properties of strip from steel DC04 during its storage are summarized in Tables 2 to 7. From mentioned tables is seen, that at strip from steel DC04 owing to storage only small modification of properties came about predominantly in direction to lower formability of sheet-metal. The changes of steel strip properties were small, because the steel is low-carbon, killed by aluminium, in which the nitrogen is bonded, which is specified in Czech State Standard 41 1305.



All measured values of deepening according to Erichsen, IE , of tested strip from steel DC04 fulfilled the demand of Czech State Standard 41 1305 for thickness 0.85 mm ($IE = \text{min. } 10.30 \text{ mm}$).

By storage of steel the mean value of strain-hardening exponent, n_m , which is crucial for stretchability, decreased about 1.8 % (see Table 6). According to lower n_m value the speed of strain-hardening at drawing is lower, the transposition of plastic deformations from places with great initial stress (biaxial tension zone) to places with lower initial stress is slower and that is why less uniform situation of deformations on stamping arises at drawing. The decreased value of n_m give evidence about the fact, that by storage the suitability of steel strip for the cases of deep drawing, where tension mechanical schemes of deformations predominate, decreased.

The exception is the mean value of plastic anisotropy ratio r_m , which by storage of steel increased about 10.4 % in direction to higher formability of sheet-metal. The value of $r_m = 1.49$ (see Table 5), found at strip from steel DC04 stored 12 months, gives evidence about increasing the resistance of sheet-metal to thinning at deep drawing and about increasing the suitability of this steel strip for the cases of deep drawing, where pressure-tension mechanical schemes of deformations predominate.

Thanks to high values of plastic anisotropy ratio in each of the directions of 0° , 45° and 90° in relation to the direction of rolling, which predominated upon the influence of decreased value of n_m , the higher value of formability index (see Table 7) was calculated at strip from steel DC04 stored 12 months. Thanks to higher formability index the strip from steel DC04 stored 12 months is more suitable for the cases of deep drawing, where together exists as pressure-tension as tension mechanical schemes of deformations.

At drawing of stampings from strip from steel DC04 stored 12 months the influence of high plastic anisotropy ratio appears mainly at non-hardened material, i. e. at initial stage of plastic deformation, while the influence of low value of n_m appears at certain stage of plastic deformation. Therefore the steel strip stored 12 months is suitable for the cases of drawing of flat stampings, where pressure-tension, eventually combined mechanical schemes of deformations occur.

5. REFERENCES

- [1] POLLÁK, L. Anizotropia a hĺbokot'ážnosť ocelových plechov. Bratislava: Alfa, 1978.
- [2] EVIN, E. Tvárniteľnosť vysokopevných ocelí a ich predikcia: habilitačná práca. Košice: SJF TU Košice, 1996, 83 p.
- [3] KEELER, S. Properties related to forming. Sheet Metal Industries, Vol. 48, 1971, No. 7, pp. 511-517. ISSN 0037-3435.
- [4] BUTLER, R. D., NORTH, D. and DAVIES, G. M. Metallurgical aspects of sheet steel for press shops. Sheet Metal Industries, Vol. 48, 1971, No. 11, pp. 842-854. ISSN 0037-3435.
- [5] EVIN, E., TOMÁŠ, M. and VÝBOCH, J. Prediction of local limit deformations of steel sheets depending on deformation scheme. Chemické listy, Vol. 106, 2012, No. S3, pp. 401-404. ISSN 0009-2770.



Acknowledgement

This paper was created within the project No. **CZ.1.07/2.3.00/20.0038** with the name "**Creation of an international scientific team and incorporation to scientific networks in the area of nanotechnologies and material unconventional forming**", which is financed by the European Social Fund and state budget of the Czech Republic. Results in the paper were achieved at solving of specific research project No. **SP2014/193** with the name "**Research and Optimization of Technologies for Higher Utility Properties of New Materials and Mechanical Engineering Products**" solved in year 2014 at the Faculty of Mechanical Engineering of VŠB – Technical University of Ostrava.





esf european
social fund in the
czech republic



EUROPEAN UNION



MINISTRY OF EDUCATION,
YOUTH AND SPORTS



OP Education
for Competitiveness

INVESTMENTS IN EDUCATION DEVELOPMENT

Development of Advanced Techniques for Incremental Bulk AlMg3 Nanostructure Alloy Forming

Tibor DONIČ^a, Milan MARTIKÁN^b

^a Department of Design and Mechanical Elements, University of Žilina, Univerzitná 1, 010 26 Žilina, Slovak Republic, tibor.donic@gmail.com

^b Research Centre of University of Žilina, Univerzitná 1, 010 26 Žilina, Slovak Republic, milan.martikan@rc.uniza.sk

Abstract

The most important parameters of Equal Channel Angular Extrusion (ECAE) as contact friction and tool design are discussed. Experimental material behaviour of AlMg3 plays very important role during severe plastic deformation and this experimental material was considered as an ideal plastic body. The rotary forging (RF) was used as following operation after ECAE. RF is an advanced precision and relatively new technology that combine forging (upsetting) and axial rolling. RF is incremental deformation process uses only small fraction of the force required for conventional forging. This process was applied on nanostructure AlMg3 obtained by ECAE process. The measure of crystal morphologies by using the scanning electron microscope (SEM) with electron backscattered diffraction (EBSD) after ECAE and RF is discussed.

Keywords

equal channel angular extrusion, incremental plastic deformation, nanostructure, alloy AlMg3, EBSD, SEM

1. INTRODUCTION

Ultrafine-grained (UFG) materials with a grain size in the submicrometer (100 – 1 nm) or nanometer (less than 100 nm) range possess much higher lengths of grain boundaries than usual coarse-grained counterparts, that is why the properties of UFG and nanomaterials depend considerably on destruction and behaviour of internal interfaces. The material for this study was commercial alloy AlMg3. The tensile tests at room temperature were carried out on samples by EU standards and at rate of extension 0.1388 s^{-1} . Modern manufacturing requirements demand short lead times and cost effective flexible production in this very origin technological procedure of preparing of nanostructured metal parts. This paper describes how the incremental deformation process known as a rotary forging is able to meet these needs. Fundamentally important process developments are presented and discussed. The nature of incremental deformation is introduced and types of rotary systems explained. Examples of some applications and processing characteristics are provided to assist process understanding and possible take up.



2. EQUAL CHANNEL ANGULAR EXTRUSION OF ALMG3 ALLOY

Methods of severe plastic deformation (SPD) have become very popular during the last years. The special SPD process is known as equal channel angular extrusion (ECAE) for homogeneously refining microstructure of bulk metallic materials at cold working condition. During ECAE a large uniform simple shear deformation is introduced into bulk billets without changing their cross section. The last published papers shown that a pre-ECAE solution heat treatment combined with post ECAE annealing is very effective to achieve a good combination of strength and ductility for precipitation hardening Al alloys.

The starting material for experimental works was a commercial AlMg3 alloy containing 2.92% Mg – 0.34% Mn – 0.06% Cu – 0.16% Si – 0.29% Fe – 0.02% Zn – 0.009% Ti – 96.16% Al. This experimental alloy AlMg3 belong into the aluminum alloys without ability of precipitation hardening. The static tensile test provided Hollomon's functions at rate of deformation $d\varphi/dt = 0.1388 \text{ s}^{-1}$. The equation for Hollomon's function is $\sigma = 295\varphi^{0.48}$. The initial dimensions of AlMg3 specimens for ECAE procedure were: length 50 mm, square profile of 6x6 mm. Figure 1 presents the basic ECAE scheme and real ECAE tool.

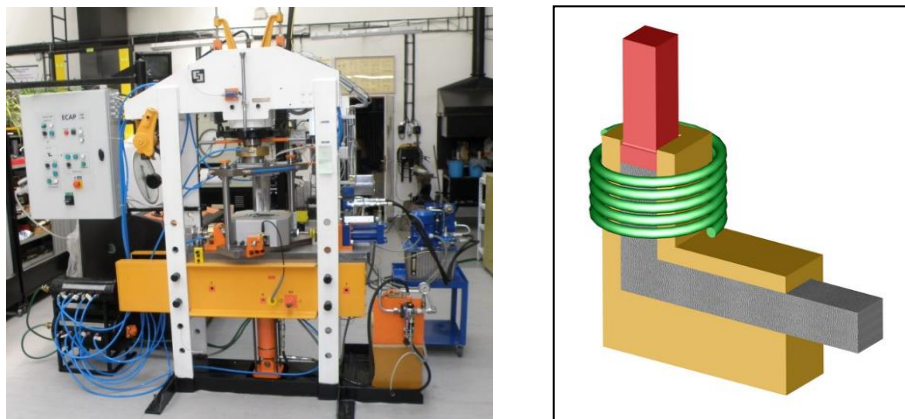


Fig. 1 Scheme and real ECAE tool

Multipass ECAE processing was performed in a heatable die-set with an intersection angle of 90° , resulting in an equivalent plastic strain of 1.15 per extrusion. The friction conditions inside the tooling are optimized by two moveable walls in the inlet channel and a moving bottom slider in the outlet channel. The ECA extrusions were performed at 25 mm per minute following road C. The specimens from ECAE process are presented in fig. 2.





Fig. 2 AIMg3 alloy specimen formed by ECAE technology

2.1 The scanning electron microscope and EBSD – AIMg3, ECAE, 1 passes

The crystal morphologies by using SEM with EBSD define a three dimensional nanostructure AIMg3 – one pass which satisfy the nanostructure orientation distribution.

The material for the analysis was prepared by electro polishing. The AIMg3 (1P) sample was electro polished in CH₃-CH₂-OH + HClO₄ solution. The electro-polishing conditions were as follows: T [°C] = +7°, I [mA] = 500, U [V] = 14, T [s] = 30-50.

Experimental Set-up	
Sample preparation:	Electrolytic polishing
SEM type	FEG Jeol 7000F
EBSD System Acquisition	Channel 5 – Flamenco Acquisition
EBSD System Data Processing	HKL Channel 5 – Tango, Mambo, Salsa
Acc. Voltage	17 kV
Probe Current	~70 μ A
EBSD description	
Total Grid Dimensions	256 x 192
Grid Spacing	0,55 μ m
Number of points	49 152



Scanning Speed	0,09 patterns/second
Noise filtering	Low

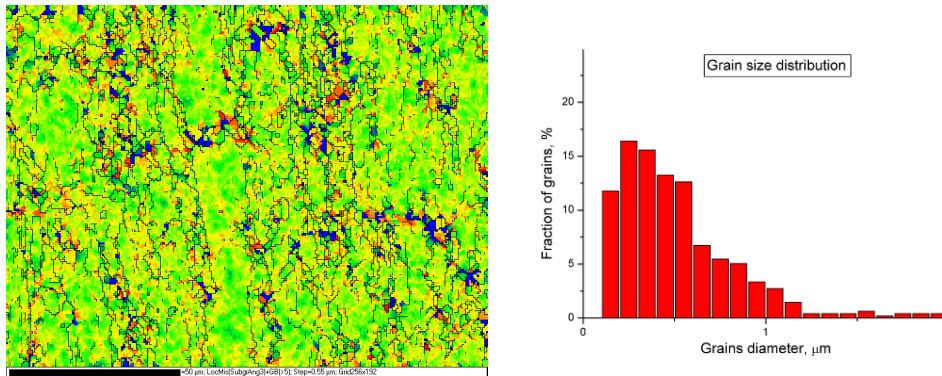


Fig. 3 Local disorientation map with appropriate key (grain boundaries with disorientation angle up to 3° were considered as sub-grain boundaries). Grain size distribution after ECAE process, 1 pass

3. INCREMENTAL BULK METAL FORMING – ROTARY FORGING

Rotary forging or orbital forging, is a two-die forging process that deforms only a small portion of the workpiece at a time in a continuous manner. In rotary forging (Fig. 4), the axis of the upper die is tilted at a slight angle with respect to the axis of the lower die, causing the forging force to be applied to only a small area of the workpiece. The orbital forming does not concern exclusively radial displacement of material by it concerns the combination of radial and transversal displacement of formable material. There is effort to realize the working movement under simple design and to secure a maximal eventually suitable radial component of formable material movement. The movement from the centre to the periphery is defined as a radial movement. The movement perpendicular to the diameter i.e. tangential to concentric circle, the of which is a centre of the co-ordinate is a transversal movement. At present three basic different characteristic methods of forming tool movement under orbital forming are known. It is obvious that each of them has a lot of modifications. Method 1: the simplest is a method of predominantly transversal displacement of formable material with a small radial component. The forming tool makes spherical movement, functional tool surface moves along concentric circles. The tool has a permanent contact with formed material – Fig. 5. Method 2: the next method of orbital forming is a method of radial – transversal displacement of formable material. The forming tool also makes spherical movement controled so that the functional surface – its point in projection on the horizontal plane carry out hypocycloids. The tool makes a complicated movement during which the tool functional surface deforms formed material so that radial component of forming is greater than transversal – Fig. 5. Method 3: this method of radial



forming is method DON where the formable material displacement is radial with a small transversal component. The tool makes a swinging movement in the direction of individual meridians, combined with rotational movement – Fig. 5.

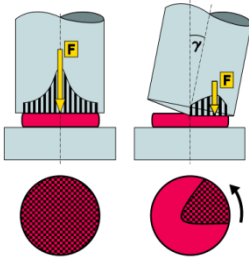


Fig. 4 The basic scheme of orbital forging process

In many cases during rotary forming, the material is according to the literature nodal points inevitably tend to move outward from the center of rotation if they are on a rotating body and their nodal velocities are assumed constant between two solution steps. In rotary forming, such a tendency causes excessive volume changes during the computer simulation. It is therefore important to resolve this problem. In this study, we decomposed the nodal velocity vector, defined as \mathbf{V}_N for the node N^t , into two components for deformation and rigid-body rotation. The deformation component, denoted as \mathbf{V}_D , was used directly to update the material node-by-node while the rigid-body rotation component, denoted as \mathbf{V}_R , was reflected by rotating the entire material with its given angular velocity around the central axis or the axis of rotation, as shown in Fig. 6. The deformation component \mathbf{V}_D of the nodal velocity \mathbf{V}_N was calculated from the following relationship $\mathbf{V}_D = \mathbf{V}_N - \mathbf{V}_R$,

where \mathbf{V}_R is calculated by $\mathbf{r} \times \boldsymbol{\omega}$, where $\boldsymbol{\omega}$ is the angular velocity and \mathbf{n} and r are the unit vector and the radius from the axis of rotation, respectively, as defined in Fig. 6. Thus, a new point $N^{t+\Delta t}$ due to time increment Δt can be obtained through moving by $\mathbf{D}_D = \mathbf{V}_D \Delta t$ after rigid-body rotation with respect to the axis of rotation by the degree $\boldsymbol{\omega} \Delta t$, as shown in Fig. 6. If the node N^t is moved to a new point N through simply updating by the vector $\mathbf{V}_N \Delta t$, as shown in Fig. 6, then excessive volume changes may take place.

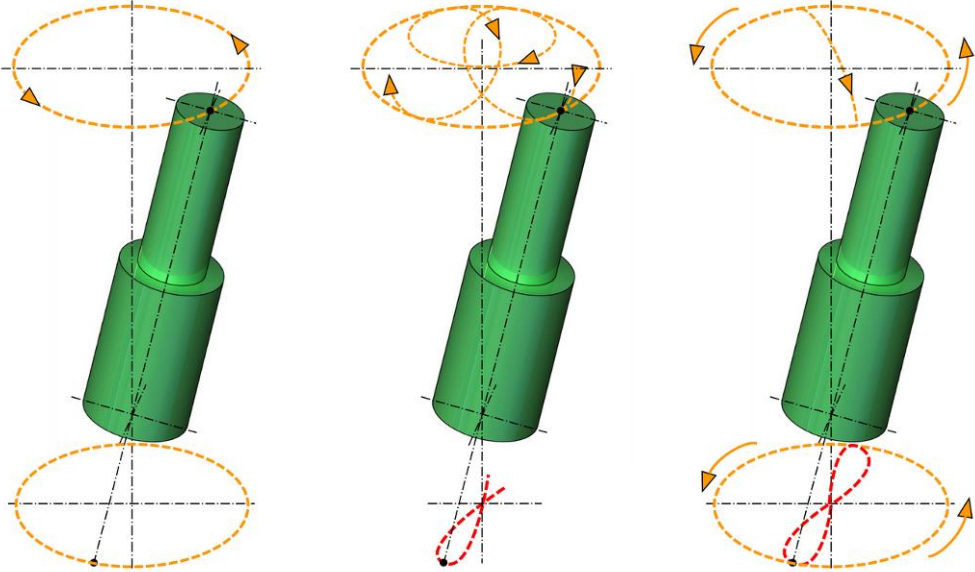


Fig. 5 The basic methods of orbital forming tool movement



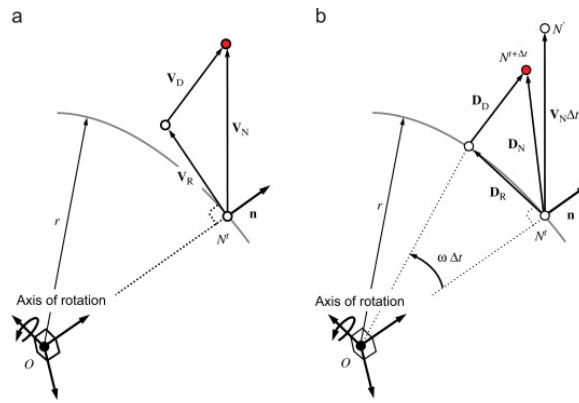


Fig. 6 New node updating scheme: (a) velocity and (b) displacement

The practical research was carried out on experimental specimen obtained by ECAE procedure. Formability tests have been made by rotary upsetting system which is situated in the Centre of Technological Plastometry, Faculty of Mechanical Engineering, Department of Applied Mechanics, by using different upper die movements (circular, spiral and planetary). Applied on a special cylinder specimen which was made from ECAE specimen by turning technology. The experimental specimen is presented on Fig. 7. Theoretical research is carried out by means of none – linear finite element analysis of the process phases, based on the proper material model. Experimental investigation methodology and theoretical research methodology of FEM simulation is presented on Fig. 8 and 9.



Fig. 7 Nanostructured specimen of ECAE process prepared for RF process



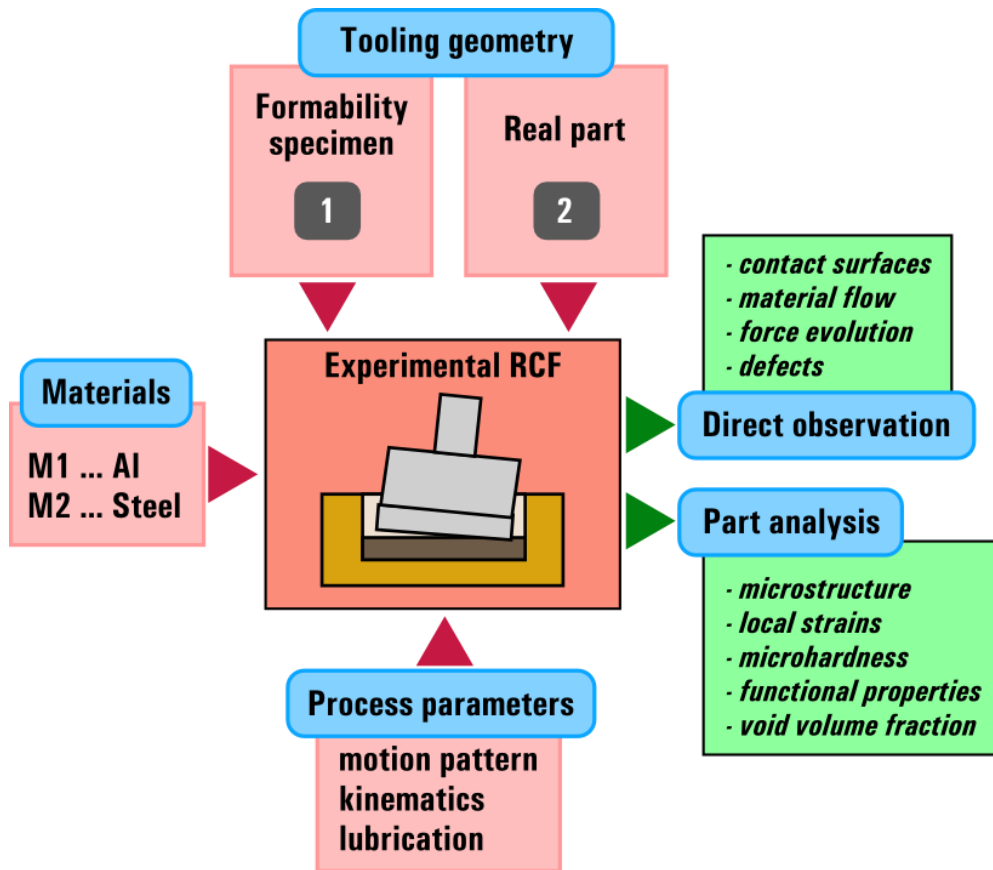


Fig. 8 Experimental investigation methodology

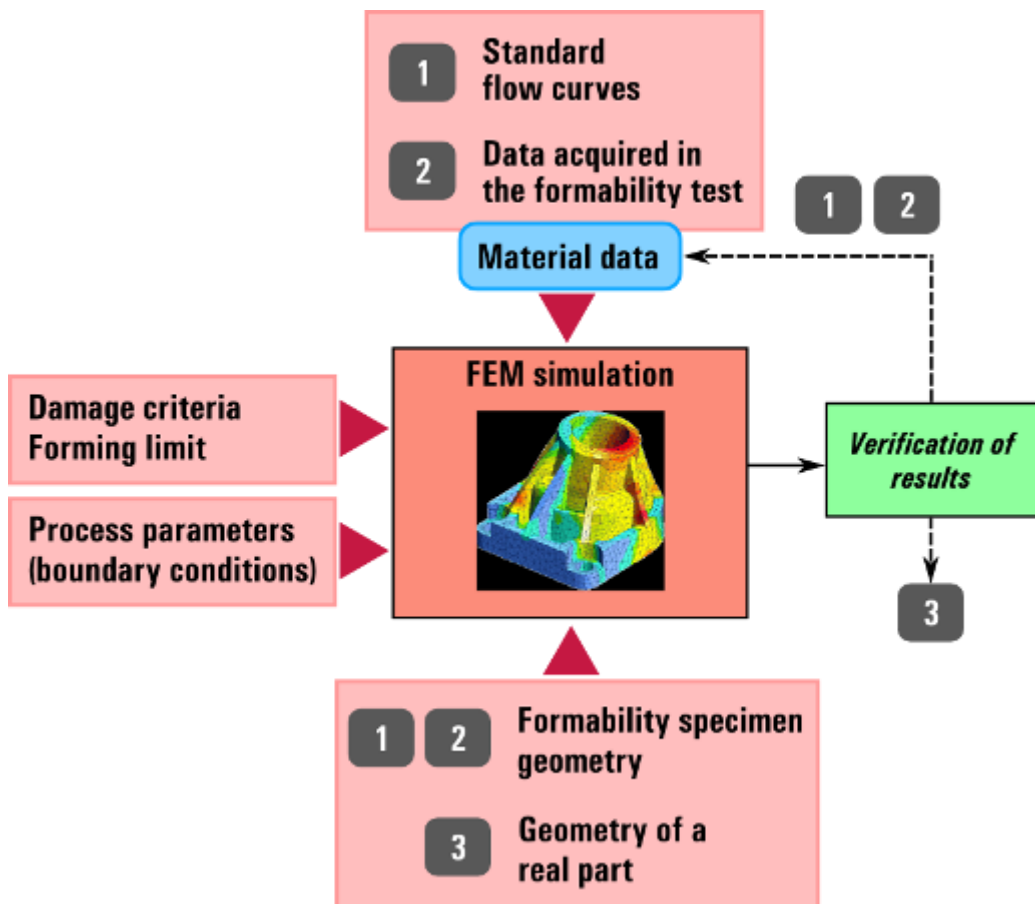


Fig. 9 Theoretical research methodology of FEM simulation

The phases - specimen of the RF upsetting process implicated on the nanostructured AlMg3 alloy is presented on the Fig. 10. The method number 3 of RF was used. The basic technology parameters are: n (number of revolution per minute) = 500, γ – instantaneous angle of the tool deviation proportional to the reversible generating amplitude = 3° , without lubrication.



Fig. 10 The phases of RF procedure – AlMg3 alloy – nanostructured

3.1 The scanning electron microscope and EBSD – AlMg3, Rotary Forging

The contact surface and grain size distribution of nanostructured AlMg3 specimen after orbital forging process is presented on fig.11. The comparison with fig.3 shows refinement of grain size distribution of AlMg3 alloy. The portion of grain diameter in the region 0 – 100 nm grows up to three times compare with volume of nanostructured grains after ECAE procedure.

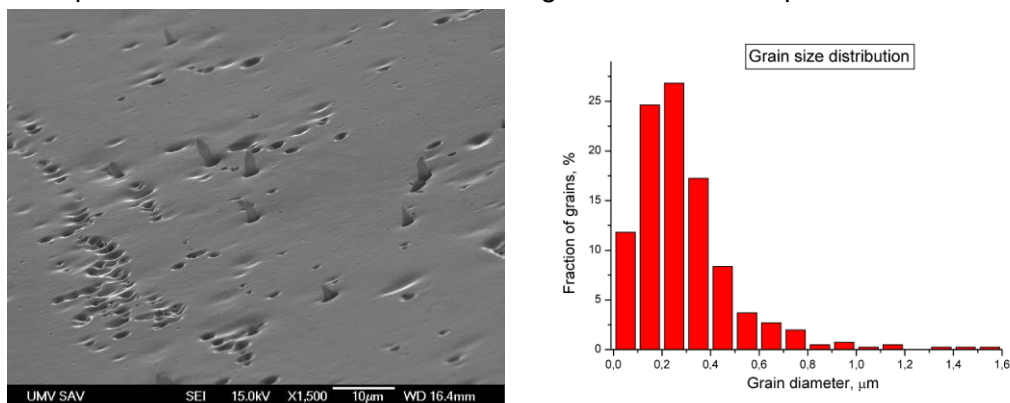


Fig. 11 Grain size distribution after rotary forging process

4. CONCLUSION

The following results have been achieved and the work on this very progressive technology prepared of metal nanostructure is under development:

- formability method for RF has been designed and applied on investigated AlMg3 alloy, formability data
- implementation of the inverse technique in identification of material law parameters resulted from experimentally determined flow curves
- FEM analysis of the formability test and process by mathematical and numerical implementation of constitutive equations by the inverse technique
- damage module has been developed based on fitting of experimental data by FEM simulation



- since non-linear multi-scale FE analysis requires large computation time, development of parallel computing technique is needed
- applying the domain partitioning technique to FE mesh of macro continuum, homogenized stresses based on micro or nanocrystal structures will be computed in parallel in the future without solving simultaneous linear equations. The parallel FEM code will be applied to simulate the limit dome height (LDH) test problem of incremental bulk metal forming nanostructure on the base AlMg3 alloy.

5. REFERENCES

- [1] RUSZ, S., DONIC, T.: *The Investigation of Orbital Forming Process*. International Conference Strojne Inzinierstvo 2000, STU Bratislava, pages 65 – 69.

Acknowledgement

This paper was created within the project "**Creation of an international scientific team and incorporation to scientific networks in the area of nanotechnology and unconventional forming material. CZ.1.07/2.3.00/20.0038**", which is financed by the European Social Fund and state budget of the Czech Republic.

The research is supported by European regional development fund and Slovak state budget by the project "Research centre of University of Žilina", ITMS 26220220183.



CZ.1.07/2.3.00/20.0038





euROPEAN
social fund in the
czech republic



EUROPEAN UNION



MINISTRY OF EDUCATION,
YOUTH AND SPORTS



OP Education
for Competitiveness

INVESTMENTS IN EDUCATION DEVELOPMENT

Structure and properties of ball milled and consolidated metal-ceramic and metal amorphous composites

Jan DUTKIEWICZ^a

Cooperation: W. Maziarz^a, A.Kukuła-Kurzyniec^a, C. Coddet^b, L. Dembinski^b

^a *Institute of Metallurgy and Materials Science of the Polish Academy of Sciences, ul. Reymonta 25 30-059 Kraków, Poland*

^b *Universite de Technologie de Belfort-Montbéliard, Site de Sevenans 90010 Belfort*

Abstract

Several types of metal matrix composites were prepared by ball milling and subsequent hot pressing in vacuum. The matrix was chosen either aluminum alloy for structural applications or silver for contact materials. As the strengthening phase were used either Al₂O₃ or ZrO₂ oxides or metallic amorphous powders prepared by spray forming. 40 hours ball milled powders of 7475 alloy with additions of 10 - 20% of ZrO₂ allowed obtaining powders of uniform distribution of ceramic particles and nanometric size (below 50 nm) of the grains of the aluminum solid solution. The microhardness of milled powders was in the range of 230-270 HV and the Young modulus near 140 GPa. The low porosity composites were obtained after hot pressing in vacuum under pressure of 600 MPa and temperature 380°C. Insignificant grain growth of aluminum solid solution grains was observed to be slightly above 100 nm. ZrO₂ and Zr particles reacted with magnesium from the aluminum solid solution forming the transition MgO rich layer around the ZrO₂ ceramic and Zr particles. The compression strength of composites with nano ZrO₂ particles additions was near 990 MPa, while those of larger particle additions was only slightly lower. All composites showed also a moderate plastic deformation in compression mode near 3 %. Another type of composites were prepared by hot pressing in vacuum of an aluminium powder with 20 and 40 wt. % addition of the amorphous Cu₄₃Zr₄₃Ag₇Al₇ (numbers indicate at. %) alloy obtained using gas atomisation method. The uniaxial hot pressing in vacuum allowed to obtain composites of hardness from 43 HV to 53 HV for both compositions of the amorphous phase and the compression strength of 150 MPa for 20 % of amorphous phase and 250 MPa for the higher content. The modest hardening effect was caused by crack initiation at the Al/amorphous interfaces. Application of the nanocrystalline aluminum powders obtained by high energy ball milling for the matrix of composites allowed to obtain nanocrystalline aluminum matrix composites strengthened with the amorphous powders, which compression strength near 550 MPa for the composite containing 40% of the amorphous phase.

Keywords

Al alloy base composites strengthened Al₂O₃, amorphous metal strengthened composites, strengthening effect



1. 7475 ALLOY BASE COMPOSITES

1.1 Introduction

Aluminum alloy matrix composites combine the metallic properties of ductility and toughness with the ceramic properties of high strength and high Young modulus [1-12]. The 7XXX series alloys are often applied as a matrix of composites, due to the advantages of high strength, low density and a good plasticity [1-9]. The composites possess superior wear resistance [1,4,6] and high temperature properties [1,8], however the room temperature strength is usually lower than that of common 7XXX alloys. Therefore attempts have been made to increase the strength of composites by application of ceramic nanoparticles [10], nanotube reinforcement of aluminum [11], spray forming of the matrix [2], which enables the improvement of strength in comparison to a basic alloy. The application of mechanical alloying to a mixture of 2014 aluminum alloy and VC carbides resulted in obtaining the powder with uniformly distributed ceramic particles leading to a significant hardening [12], similarly to the effect reported in aluminum strengthened with Al_2O_3 or SiC [15]. Ball milling was also used to introduce Al_2O_3 nanoparticles into the 6061 alloy, to produce a final composite by hot pressing, which increased wear resistance by 145% in comparison with a conventional aluminum alloy. High strength approaching 1000 MPa and some ductility was obtained in a composite consisting of 6061 aluminum alloy and 20 % of ZrO_2 prepared from the mechanically alloyed powder mixture [14]. The contribution to a high strength was not only due to the addition of nanoparticles, but also due to a grain refinement of aluminum solid solution during ball milling.

1.2 Experimental procedure

The powder of 7475 aluminum alloy enriched in zirconium of composition 5.7 % Zn, 2.2% Mg, 0.7% Fe, 1.6 % Cu, 0.1% Mn, 0.5% Zr- rest Al, was obtained by spray forming. The powders were mixed with nanosize ZrO_2 yttrium stabilized powder of spherical shape of average diameter near 20 nm supplied by TOSOH Company. Then, the powders were subjected to high energy ball milling in the planetary Fritsch mill Pulverisette 5 at 200 rpm for 40 hours in tool steel containers filled with argon, using 10 mm steel balls. The powders were compacted in VEB 40 hydraulic uniaxial press in the mould placed in vacuum, heated using high frequency generator. The temperature was controlled by a thermocouple. The powders were encapsulated in copper containers before placing in a mould. Discs 5mm thick of diameter 20 mm were obtained applying hot pressing in vacuum of 10^{-2} bar, at a pressure of 600 MPa and temperature of 380°C.

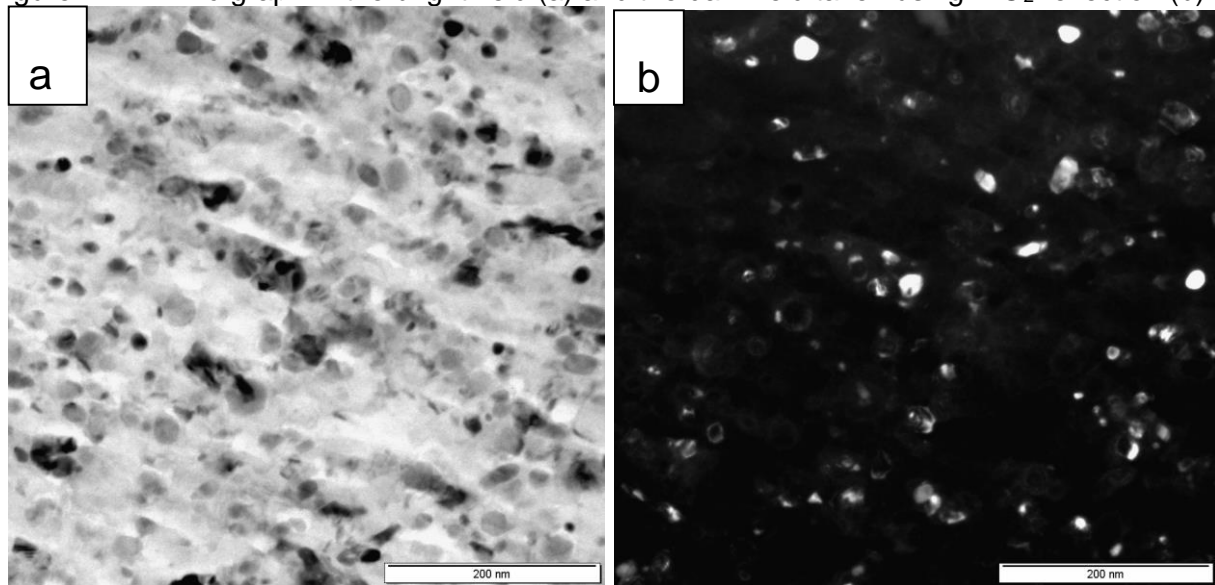
The morphology of milled powders and hot compacted composites was studied using Leica DM IRM optical microscope. The polished specimens were etched with 0.5 % HF solution. The microstructure was observed using Technai G² transmission electron microscopes (TEM) equipped with EDAX energy dispersive X-ray (EDX) detectors. Thin foils were cut out from powders immersed in epoxy using Leica microtome, while those from composites were obtained by mechanical thinning down to 0.1 mm and further electrolytic thinning using a „double-jet” technique in Tenupol-5 device using an electrolyte containing 30 % solution of HNO_3 in methyl alcohol. The thinning was carried out at the temperature of -30 °C and voltage 15 V. Vickers microhardness measurements were performed using a CSM-Instruments tester.



1.3 Results on composites based on 7475 alloy with additions ZrO_2

Fig. 1 shows a TEM micrographs taken of a 7475 alloy powder particle with 20 % of nano ZrO_2 milled 40 hours. In the bright field image one can see stripes within the aluminum solid solution resulting from the multiple joining of particles during ball milling and not caused by the preparation of thin samples. Within bands one can see grains of aluminum solid solution of size of several nanometers. In fact it is difficult to distinguish between the aluminum solid solution grains, intermetallic particles and ZrO_2 particles, all giving diffraction contrast, dependant on their orientation. In the dark field (taken using objective aperture placed on the part of a rings of Al and ZrO_2 reflections, marked in the diffraction pattern shown as an insert in Fig.2a) some aluminum grain can also be visible as the objective aperture might include some of the α -Al reflection.

Figure 1 TEM micrograph in the bright field (a) and the dark field taken using ZrO_2 reflection (b)



from a thin section of the ball milled 7475 alloy powders milled with 20 % of nano ZrO_2 for 40 hours.

The HAADF microstructure visible in Fig.2 was taken of the composite of 7475 alloy with 10 % of micro size addition ZrO_2 . The micrographs corresponding to elemental mapping from the area marked by a square in the HAADF micrograph, are based on intensities of Al- $K\alpha$, O- $K\alpha$, Zn- $K\alpha$, Zr- $K\alpha$, Mg- $K\alpha$ and Cu- $K\alpha$ and are presented on the right side of Fig.7. One can see that the brightest contrast particles are these with the ZrO_2 , while $MgZn_2$ precipitates and Cu rich ones show slightly weaker contrast. One can see also magnesium enrichment around ZrO_2 particles interfaces most probably due to reaction occurring during hot pressing between ZrO_2 and magnesium from the aluminum base solid solution. This reaction causes most probably formation of a new phase, like MgO, since no zirconium is present in rings surrounding ZrO_2 and for a different contrast observed at the interfaces of ZrO_2 particles. It can only be seen at higher magnification and it might cause some additional strengthening due to oxidation reactions of Zr, as suggested in AlMgZr amorphous/crystalline composites [16]. In fact, in Fig.2 most of particles are ZrO_2 , but some are Zr (like these visible at the bottom of the marked square). They show also MgO rings, like reported in [15]. The observation of the reaction at the ZrO_2 interface was confirmed also in the composite containing more i.e. 20% of the ceramic phase. Fig.8 shows the HAADF micrograph of such a composite and the elemental mapping of chemical composition of Al, Mg, Zr and O performed within a narrow area marked in Fig.8a. It can be seen that the enrichment in magnesium at the interface of a bright particle occurs as manifested by a clear increase of Mg pixels and drop of Zr content. The change of contrast at the interface toward a darker layer suggests also the formation of a new phase, most probably also MgO since no zirconium is present in the transition phase. The formation of this phase is slightly astonishing,



although some solution of magnesium in the ZrO_2 phase is possible as reported in X-ray Data International Tables. The attached particle on the left side of the micrograph, showing clearly a weaker contrast, is rich in zinc, copper and magnesium as results from the elemental mapping and is one of intermetallic phases forming in the 7475 alloy during ageing.

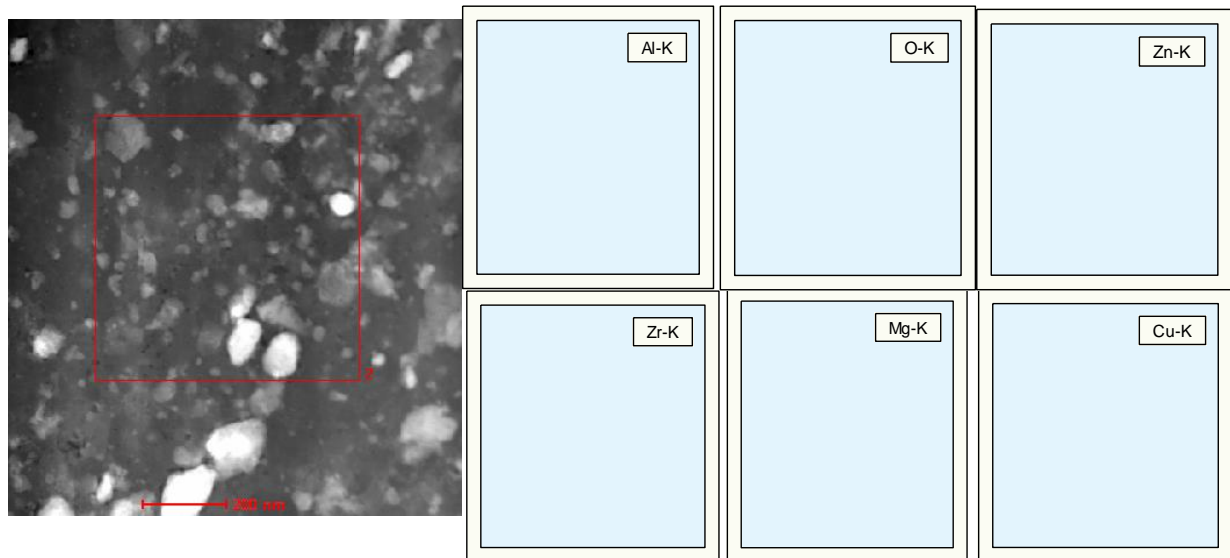


Figure 2 Vacuum hot pressed composite prepared from milled powders composed of 7475 alloy and 10 % of micro size addition ZrO_2 (a) HAADF micrograph and on the right elemental mapping of Al-K α , O - K α , Zn - K α , Zr - K α , Mg - K α and Cu - K α .

Fig.3 shows the stress-strain curves obtained from the compression test of the composite based on 7475 alloy with 10 % of ZrO_2 particles, but with various size of particles. One can see that maximum strength is 990 MPa for the composite with nano-particles addition, at the maximum of plastic deformation of 3 %. Measured Young modulus of both composites is equal near 55 GPa what is much smaller than that measured using the hardness measurements. However, due to a small size of the specimen used for the compression test, whose height was 5 mm, the value obtained from the hardness test seems to be more reliable. The strength of the sample with larger size of ZrO_2 additions is slightly lower, near 920 MPa as results from Fig.3 where the compression test of the composite with larger ZrO_2 particles addition can also be seen. The differences in strength are small between both types of composites with different size of the strengthening phase. It can be explained by the fact that the compression tests show high values of compression strength, not only due to the ceramic phase additions, but also due to the grain refinement of the 7475 alloy matrix, down to the nano range. The effect a high strength 7475 alloy matrix is not large, since composites based on the 6061 alloy matrix with nano ZrO_2 additions [14] have shown similar strength. It is most probably caused by a small strengthening effect of intermetallic phases rich in Mg, Zn and Cu formed in close to equilibrium state and noncoherent particles precipitation from the matrix.



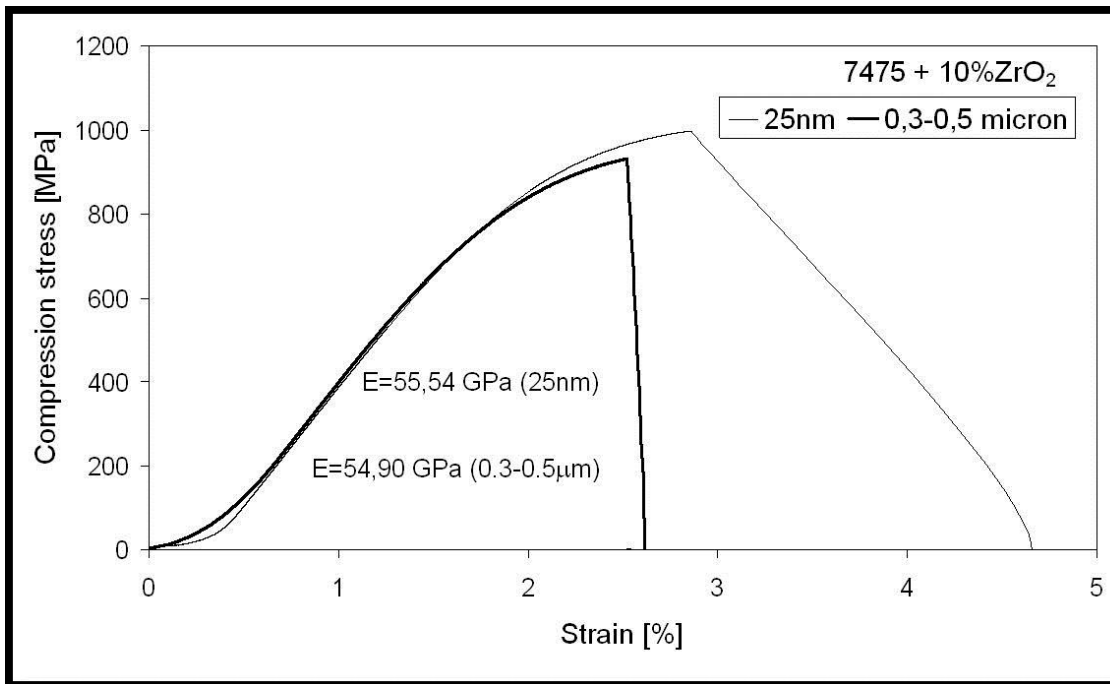


Figure 3 Compression stress/strain curves of the composite based on 7475 with 10 % of ZrO_2 nano particles and 10 % of larger ZrO_2 microparticles (0.3-0.5 μm)

1.3 Results on Al base composites strengthened with amorphous powder

Two types of composites with aluminium matrix were investigated – both with the addition of amorphous metallic powder of $Cu_{43}Zr_{43}Al_7Ag_7$ (at. %) alloy as a strengthening phase with a mean particle size below 60 μm . The aluminium powder supplied by Alfa Aesar of size 7-15 μm and purity 99,5%. The initial ingots were prepared melting using a high frequency in a purified argon atmosphere from high purity elements (99.9 wt. % and more) and then subjected to gas atomization process. The special atomizing unit using Nanoval Process, contain an autoclave head with insulated crucible is heated by an induction coil uses the Laval nozzle.

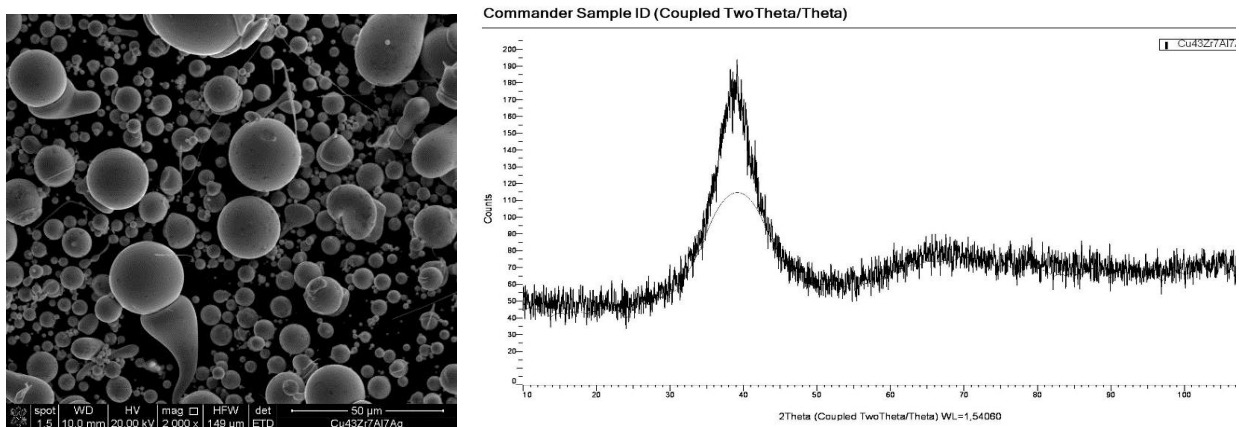


Fig. 4 SEM micrograph of the amorphous $CuZrAgAl$ powder and X-ray diffraction from the powder showing amorphous structure



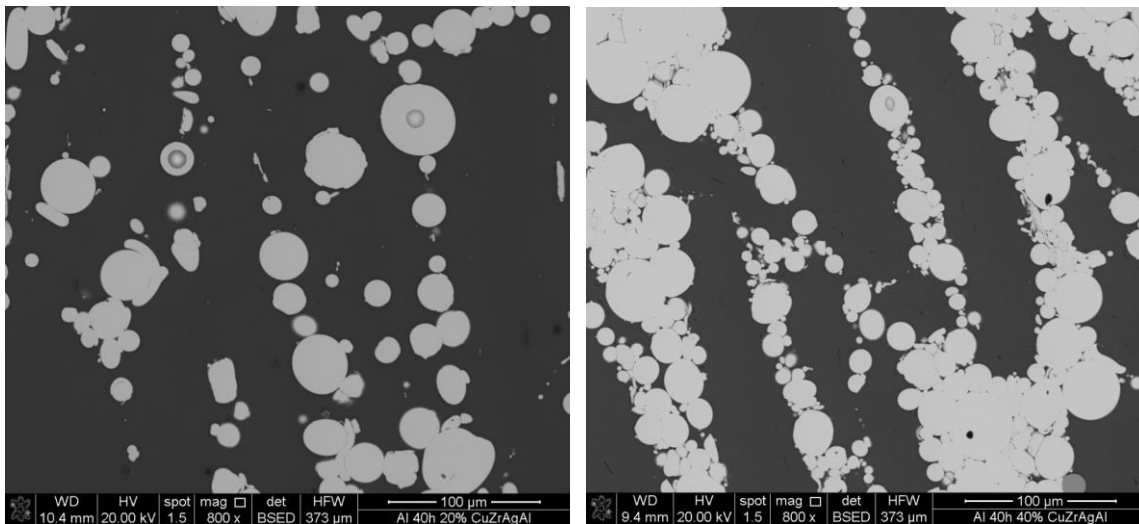


Fig. 5 SEM micrographs of the nanocrystalline aluminum matrix composites strengthened with (a) 20 % of the amorphous powder (sample) and (b) 40% of the amorphous powder (sample 2)

Fig.5 shows a SEM microstructures from the composites containing 20% and 40% of the amorphous powder. One can see a homogeneous distribution of the particles and no clear surface diffusion effects after hot pressing in vacuum can be seen, since the interface look rather not changed by a diffusion. The hardness of the composite containing 20 wt.% is near 45 HV and that containing 40 wt. % is 53 HV. Small hardness increase of the composites with increasing the amount of the strengthening amorphous phase similar as observed in [16]. The microhardness of the aluminum matrix was 46 HV_{0,01} and that of the amorphous part equal to 634 HV, slightly lower than 740 HV reported from the NiNbTa amorphous part of the Al matrix composite in [6]. It may be caused by a different composition of the amorphous phase and a different degree of crystallization during composite consolidation always involving a high temperature treatment.

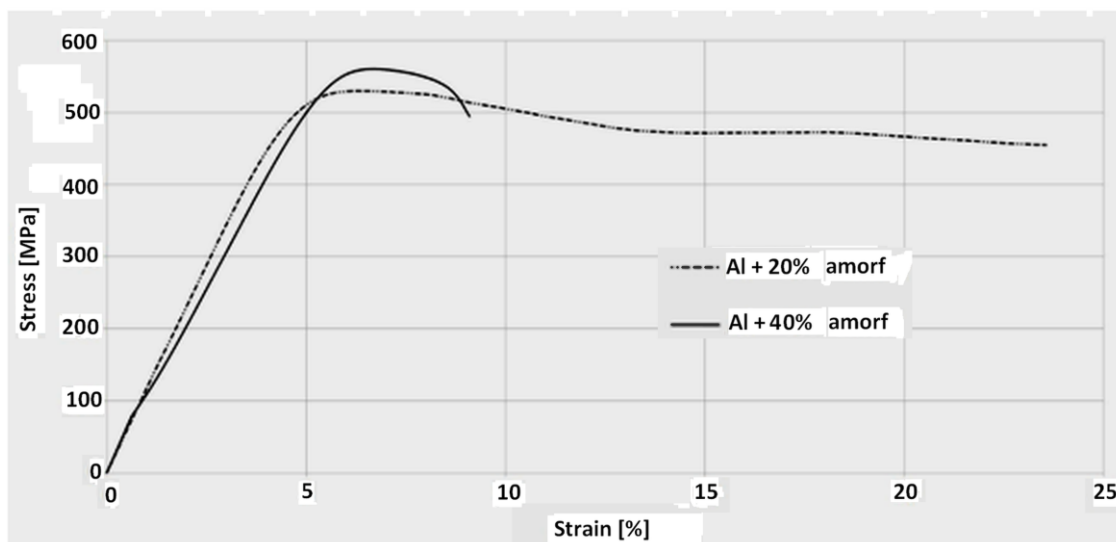


Fig.6 Compression curves of the nanocrystalline aluminum matrix composites strengthened with (a) 20 % of the amorphous powder and (b) 40% of the amorphous powder



Figure 6 shows compression curves of the aluminum matrix composites containing 20 and 40 wt. % of the amorphous powder. One can see that they are in accord with the hardness measurements where no hardness increase can be observed with the increase of the amount of the amorphous powder. The compression strength of the composite containing 40% of the strengthening phase is even lower (112 MPa) than that containing less amorphous powder (153 MPa). These are lower values than reported in [16] where higher compression strength was observed at 15% of the amorphous phase in aluminum, however the increase of strength with increasing amount of the strengthening phase was also rather small. The differences may result from a different type of the amorphous phase and shorter consolidation time what might help to avoid formation of the transition layer at the amorphous/aluminum interface and no clear particle/matrix debonding was observed. The latter one shows also much higher compression strain. Both show similar values of the yield stress near 90 MPa

2. CONCLUSIONS

1. 40 hours ball milled powders of 7475 alloy with additions of 10% or 20% of ZrO_2 of size near 25 nm or 0.2 μm allowed obtaining powders of uniform distribution of ceramic particles and nanometric size (below 50 nm) of the grains of the aluminum solid solution. The microhardness of milled powders was in the range of 230-270 HV and the Young modulus near 140 GPa.
2. The low porosity composites of uniform distribution of ZrO_2 particles with $MgZn_2$ and copper rich precipitates of size below 100 nm were obtained after hot pressing in vacuum under pressure of 600 MPa and temperature 380°C. Insignificant grain growth of aluminum solid solution was observed to be slightly above 100 nm. ZrO_2 and Zr particles reacted with magnesium from the aluminum solid solution forming the transition MgO rich layer around the ZrO_2 ceramic and Zr particles.
3. The compression strength of composites with nano ZrO_2 particles additions was near 990 MPa, while those of larger particle additions was only slightly lower. It means that contribution of nanosize grains of aluminum solid solution and the effect of $MgZn_2$ and Cu rich precipitates is also important. All composites showed also a moderate plastic deformation in compression mode near 3 %.
4. $Cu_{43}Zr_{43}Ag_{7}Al_7$ spray formed powder showing a large variation of particle size was sieved in order to obtain aluminum base composites strengthened with a particles below 60 nm. It allowed to obtain composites containing 20-40% of the amorphous phase with hardness increasing from 43 HV to 53 HV with increasing the amount of the amorphous powder. The compression strength 120 MPa. The cracks at the interface of the amorphous/aluminum matrix were observed what caused small hardening effect due to early crack formation there. The amorphous phase was partially crystallized in the hot pressed composites, however its hardness was near 640 HV not lower than the amorphous powder.
5. Application of the milled aluminum powders for matrix of composites allowed to harden the matrix of composites, which what resulted in growth of the compression strength up to 550 MPa for the composite containing 40% of the amorphous phase. The strength was however only insignificantly higher than that of composites strengthened with 20% of the amorphous, which have shown higher ductility. The strengthening particles formed bands where cracks nucleated during compression test.

3. LITERATURE

- [1] V.K. Lindroos and M.J. Talvitie, J. Mater. Proc. Technol., 53 (1995) 275-284
- [2] Wuhua Yuan, Jian Zhang, Chenchen Zhang, Zhenhua Chen, J. Mater. Proc. Technol., 209, (2009) 3251–3255
- [3] Rupa Dasgupta, Humaira Meenai, Materials Characterization, 54 (2005) 438– 445
- [4] Ali Kalkanlı, Sencer Yılmaz, Materials and Design 29 (2008) 775–780.
- [5] Kyung Ho Min, Baek-Hee Lee, Si-Young Chang, Young Do Kim, Materials Letters 61 (2007) 2544–2546
- [6] R.N. Rao, S. Das, D.P.Mondal, G.Dixit, Tribology International 43 (2010) 330–339



- [7] D.P. Mondal, S. Das, R.N. Rao, M. Singh, Mater. Sci Eng., A 402 (2005) 307–319
- [8] A. Bhaduri, V. Gopinathan, P. Ranakrishnan, A.P. Miodownik, Mater. Sci Eng., A 221 (1996) 94-101
- [9] Jer Horng-Hsieh, Chuen-Guang Chao, Mater. Sci Eng., A 214 (1996) 133-138
- [10] Z.Y. Ma, S.C. Tjong, Y.L. Li, Composites Science and Technology 59 (1999) 263±270
- [11] I. Sridhar, R.K. Narayanan, K.W. Seah, M.J. Tan: *Aluminium Alloys*, Ed. by J. Hirsch, B. Skrotzki and G. Gottstein, (WILEY-VCH, Weinheim, 2008) pp. 2263-2268.
- [12] E.M. Ruiz-Navas, J.B. Fogagnolo, F. Velasco, J.M. Ruiz-Prieto, L. Froyen, Composites: Part A 37 (2006) 2114–2120
- [13] A.M. Al-Qutub, I.M. Allam, T.W. Qureshi, J. Mater. Proc. Technol., 172 (2006) 327–331
- [14] J. Dutkiewicz, L. Lityńska-Dobrzyńska, W. Maziarz, K. Haberko, W. Pyda, A. Kanciruk, Crys. Res. Technol., 2009, No. 10, 1163-1169
- [15] I. Ozdemir, S. Ahrens, S. Muecklich, B. Wielage, J. Materials Proc. Technol., 205, (2008) 111–118
- [16] S. Jayalakshmi, Sujasha Gupta, S.Sankaranarayan, Shreyasi Sahu, M.Gupta, Mater. Sci. Eng. A581 (2013) 119–127

Acknowledgements

This paper was created within the project "**Creation of an international scientific team and incorporation to scientific networks in the area of nanotechnology and unconventional forming material. CZ.1.07/2.3.00/20.0038**", which is financed by the European Social Fund and state budget of the Czech Republic.





eu
esf
european
social fund in the
czech republic



EUROPEAN UNION



MINISTRY OF EDUCATION,
YOUTH AND SPORTS



OP Education
for Competitiveness

INVESTMENTS IN EDUCATION DEVELOPMENT

Application of SPD processes for manufacturing the applicable materials with nanometric structure on the base of magnesium and aluminium

Henryk DYJA ^a, Marcin KNAPINSKI ^a, Anna KAWALEK ^a,
Sebastian MROZ ^a, Szymon BERSKI ^a

*a Czestochowa University of Technology, Armii Krajowej av. 19,42-201 Czestochowa, Poland,
knap@wip.pcz.pl*

Abstract

The research concerning various SPD processes for obtaining materials with nanometric structure on the basis of magnesium and aluminium is proposed. Important rule is that for investigation will be chosen only processes which results the application in industry. The main goals of the proposed research are production of multilayer Mg-Al composite with aluminium outer layers and magnesium inner layers and also bimetal rod with magnesium sleeve and aluminium core. The composite of Mg-Al will be obtained by using modified ARB process where the flat rolls are replaced by box pass which eliminates the spread of the band. Moreover, an asymmetric rolling process will be used. The bimetal Mg-Al rod will be produced by ECAP process. It is assumed that during the ECAP process in optimal conditions the joining of the layers and refinement of the structure is possible. The third direction of the research is application of the multi-axial forging process to refinement structure of Mg-Al alloy. Such produced material will be the base material to compare the mechanical properties with properties of materials obtained in ARB and ECAP processes.

Keywords

SPD ECAP ARB processes, Mg-Al bimetal, Mg-Al alloys, multi-axial forging

1. INTRODUCTION

Ultrafine-grained and nano-crystalline structure materials exhibit very interesting properties and still not fully understood physicochemical properties, including, above all, very hard strength compared to materials obtained traditionally. The ultrafine-grained structure of metals can be obtained, among other methods, by applying processes with unconventionally high plastic deformations. Many methods and their variants of accomplishing large plastic deformations have been known: Equal-Channel Angular Pressing (ECAP), Multiaxial forming (MF), High-Pressure Torsion (HPT) method, Cyclic Extrusion Compression (CEC), Repetitive Corrugation and Straightening (RCS) and Accumulative Roll-Bonding (ARB).

The latter method has not yet been fully understood so far, and especially the production of bimetallic composites and their numerical modelling using advanced numerical methods is not



known. This is chiefly caused by the fact that such processes are conducted with very large deformations, which are not achievable during carrying out of traditional plastometric tests. Moreover, the distribution of local strains in the rolled strip is characterized by high diversity and is not monotonic during the time of metal residence in the roll gap. The use of accumulative roll-bonding for producing ultrafine-grained structures is also the only method that can be applied to a commercial process [1].

In recent years, the ARB process has been successfully applied to the manufacture of different types of plates and strips exhibiting an ultrafine-grained structure. The investigations concerning the application of the ARB process to the production of multi-layered composites, carried out so far, have determined the microstructure development and mechanical properties of the composites [2-8]. However, the corrosion resistance of the produced composites was not investigated.

Magnesium is characterized by low density and excellent ability to dampen vibrations. However, it exhibits poor strength and low deformability due to the fact that its crystal lattice has a limited number of slip systems at ambient temperature [6]. Reducing the grain size until the ultrafine ($100 \text{ nm} < d < 500 \text{ nm}$) or the nanoscales would thus make these alloys competitive in terms of strength with respect to other heavier materials, such as aluminium alloys. Additionally, small grain sizes often allow superplasticity at the appropriate temperatures and strain rates. Thus, fine-grained Mg alloys would be susceptible to be formed into complex parts in one single operation by superplastic forming. Another obstacle to its broader use in technology is also the fact of its relatively poor corrosion resistance and considerable abrasive wear. Hence, a prospective solution is to produce an Al/Mg composite that will provide increased corrosion resistance compared to magnesium sheets and strips produced by the ARB method. For this purpose, it is necessary to produce an Al/Mg composite, in which the outer layer will be aluminium or aluminium alloys, with the individual layers being diffusion bonded together.

Aluminium and its alloys exhibit higher strength and better deformability compared to Mg [9, 10]. Therefore, it can be foreseen that an Al/Mg layered composite produced in the ARB system would combine the advantages of the both materials, Al and Mg. Works [3,4] have investigated the microstructure of an Al/Mg composite produced in the ARB process and identified an intermetallic mixture at the interface between the Mg and Al layers. The ultrafine-grained structure of the Al/Mg composite was obtained in three passes, after which the Al grain size was 875 nm, and the Mg grain size was 656 nm. As a result of the ARB process applied, also the hardness of individual composite layers increased.

From the obtained testing results [11] it was found that the strength of the Al/Mg composite, as determined in both directions, i.e. in the rolling direction and the transverse direction, had considerably improved up to the second pass. Whereas, after the third pass, the strength in the rolling direction dramatically decreased, with the unchanged level of strength in the transverse direction. After the third pass, neckings and cracks of the Al layer were also observed, which were due to the difference in plastic flow resistance between particular composite layers.

2. ANALYSED PROCESSES OF SPD

In order to ensure a rolling process to take place under ARB conditions, a package of two sheets needs to be deformed with a reduction of 50%. To ensure the proper metal flow in the roll gap and the uniform strip deformation across the entire strip width, a special box pass was employed [12, 13]. A schematic this box pass is shown in Figure 1.



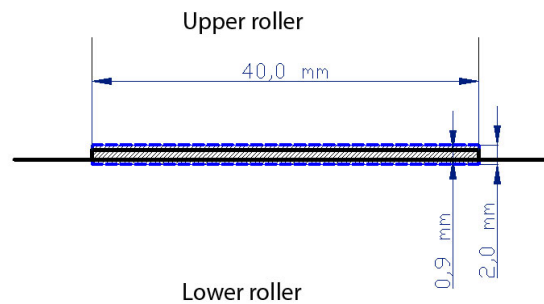


Fig. 1 Schematic of the box pass [12]

Owing to the use of rectangular passes for the tests, a stable strip flow was achieved during the rolling process. Moreover, the twisting of the strip in the horizontal plane upon strip exit from the roll gap was eliminated, which reduced the possibility of cracking at the sample edge. Thanks to the groove-rolling of sheet packages, more than ten passes could be preset for a single multi-layered strip [12, 13].

Figure 2a shows a photograph of a metallographic section made along the rolling direction for the specimen after the 4th pass (16 layers of the starting material). Successive strips and an unstable bond in the middle are clearly seen. Successive passes result in an enhancement in bonding of layers. Figure 2b shows a photograph of a metallographic section for the specimen after the 6th pass of the ARB process; considerable refinement of the microstructure is visible.

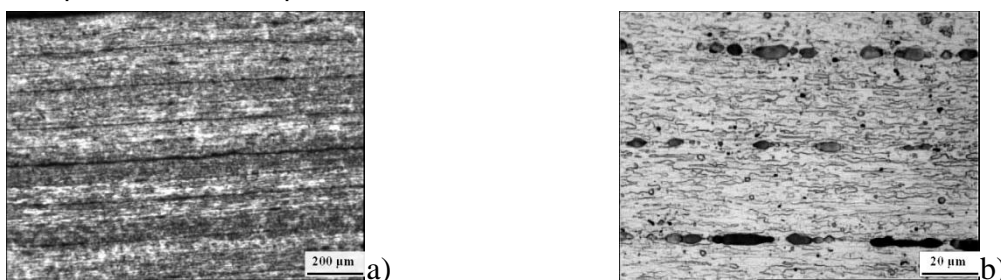


Fig. 2 A photograph of the metallographic section made along the rolling direction: a) for the specimen after the 4th pass, b) for the specimen after the 6th pass.

The second method of accomplishing large plastic deformations which will be investigated in the research is equal channel angular extrusion (ECAE) process. In the literature some research concerning simultaneous deformation of aluminium-magnesium bimetal in the extrusion process has been appeared [14]. During the deformation of bimetal material, especially in extrusion process, very important thing is knowledge how particle layers of bimetal are flowing through the die. The character depends on many parameters e.g. properties of bimetal components, type of flow, composition and thickness of bimetal layers, geometrical parameters of die, extrusion ratio. ECAE was used in many fields among others to manufacturing nanostructural materials, in powder metallurgy, for evolution of texture and microstructure and last time some investigations concerning the application of the method in joining metals were done [15]. The method also is characterised by getting a possibility of several deformations with different configurations. Authors of the paper [15] were stated that it is possible to obtain the strength joint better than after traditional extrusion process. There are many hypotheses which try explaining the joining metals in solid state metal during forming processes. The diffusive one explains that the joining process is connected with the fact that putting the metals in the distance of influence of atomic forces creates the bridges of joining in the slip planes. Into the



bridges the metal is heating until the melting point is attained and the great plastic deformation causes the multiplying the amount of joint bridges. In adhesive hypothesis the condition of creation the joint is activating the adhesion forces in contacted metals, and microroughnesses of the surface of metals are deformed which causes the increase of temperature in whole volume of the metals thus the increase of adhesion coefficient and for example for the magnesium is very significant for the range of temperatures: 20°C do 350°C [16]. From the analysis of the various hypotheses a few practical conclusions it could be stated which were taken into consideration during designing ECAE process of Al-Mg bimetal:

- to get the joint with proper strength it is necessary to contact pure surfaces of metals without oxide layer,
- during joining process should be assured the specific load conditions to create a new single bridge of joint and next the whole joint,
- for deformation in higher temperatures the smaller load should be used,
- the tolls for deformation should enables free displacement of joined layers (the initial investigations were presented in paper [17]).

Using of ECAP process to joint of aluminium and magnesium components in solid state was chosen because of advantageous state of deformation with the general state of compressive stress with one elongated strain, which causes higher plasticity of the deformed metals and enables the partial displacement of bimetal layers.

Magnesium alloys are characterized by low corrosion resistance and it is very important to create new alloys or to join most popular alloys with metals with higher resistance to corrosion and similar properties of plastic deformation. There are various compositions of such bimetals and the example application of bimetal rod Al-Mg could be for round rods with magnesium alloy core and sleeve represented by aluminium alloy with good resistance to water corrosion (6000 series Al-Mg-Si). On first stage of the investigations the typical magnesium alloys for extrusion could be analysed i.e. AZ31, AZ61 (Mg-Al-Zn) and ZM21 (Mg-Zn-Mn). The extrusion process will be done in cold conditions and also in temperatures of the billet which are characteristic for hot extrusion of such materials.

The third method of accomplishing large plastic deformations which will be investigated in this project is multiaxial forming (MF). One of the MF scheme is 2-D forming. The square specimen rotates to 90° back and force and is hit by two flat anvils at certain temperature per each rotation.

In this study the possibilities of all structure formation mechanisms in Al-Mg alloys during MF will be researched. The influence of different structure formation on the mechanical properties will be found out. The control of temperature during deformation in accordance with speed and rate of deformation, cumulative deformation allows to control structure and receive ultrafine and nanostructure in materials.

Previous science researches made with the help of thermo-mechanical simulator Gleeble 3800 and mobile convert unit (MCU) MaxStrain showed the possibility of nanostructure receiving by multiple deformations during certain conditions such as temperature, speed and rate of deformation [18]. MaxStrain is designed to provide precise control of temperature and the final strain value during high speed multi-hit, multi-axis compressions. Applications include the development of ultra fine grained steels, aluminium, titanium and other research in multi pass



Severe Plastic Deformation. The MAXStrain technology provides a research tool for well instrumented study of Severe Plastic Deformation processes on a variety of materials. The system offers the ability to control strain, strain rates, temperature, interpass time and both pre and post deformation heat treatments on materials.

3. SUMMARY

The expected results of the research is production of new functional materials which will be characterized by low weight and relatively high strength and plasticity, good corrosion resistance and also can be produced in industry processes.

4. LITERATURE

- [1] N.Tsuji, Y.Ito, Y.Saito, Y. Minamino. *Scripta Materiala*. 47 (2002), p. 893-899.
- [2] G.H. Min, J.M. Lee, S.B. Kang, H.W. Kim. *Mater. Lett.* 60 (2006), p.3255–3259.
- [3] M.C. Chen, H.C. Hsieh, W. Wu. *J. Alloy. Compd.* 416 (2006), p. 169–172.
- [4] M.C. Chen, C.W. Kuo, C.M. Chang, C.C. Hsieh, Y.Y. Chang, W. Wu. *Mater. Trans.* 48 (2007), p. 2595–2598.
- [5] S. Ohaski, S. Kato, N. Tsuji, T. Ohkubo, K. Hono. *Acta Mater.* 55, (2007), 2885–2895.
- [6] M. Eizadjou, A. Kazemi Talachi, H. Danesh Manesh, H. Shakur Shahabi, K. Janghorban. *Comp. Sci. Tech.* 68 (2008), p. 2003–2009.
- [7] Ö. Yazar, T. Ediz, T. Öztürk. *Acta Mater.* 53 (2005), p. 375–381.
- [8] J.M. Lee, B.P. Lee, S.B. Kang. *Mater. Sci. Eng. A* 406 (2005), p. 95–101.
- [9] X.S. Hu, K. Wu, M.Y. Zheng, W.M. Gan, X.J. Wang. *Mater. Sci. Eng. A* 452–453 (2007), p. 374–379.
- [10] J. Koike, R. Ohyama. *Acta Mater.* 53 (2005), p. 1963–1972.
- [11] K. Wu, H. Chang, E. Maawad, W.M. Gan, H.G. Brokmeier, M.Y. Zheng. *Materials Science and Engineering A* 527 (2010), p. 3073–3078.
- [12] M. Kwapisz. The study of the aluminium accumulative roll-bonding process and working out of the microstructure and mechanical property development model. Doctoral thesis, Czestochowa 2007 (in Polish). Non published.
- [13] A. Milenin, S. Mróz, M. Kwapisz. Mathematical modelling of the aluminium accumulative roll-bonding process. Transactions of the XIII Conference on Computer Science in Metals Technology, KomPlasTech2006, pp. 177÷183, Szczawnica 2006 (in Polish).
- [14] K. Kittner, C. Binotsch, B. Awiszus. Models for determination of interface strength and quality of aluminum-magnesium compounds. *Metal Forming 2010*, 19.-22. September 2010, Toyohashi, Japan, p. 454-457, ISBN 978-3-514-00774-1
- [15] A.R. Eivani, A. Karimi Taheri. A New method for producing bimetallic rods. *Materials Letters*, vol 61, January 2007, pp. 4110-4113.
- [16] L. Kowalczyk. Łączenie metali w stanie stałym w procesach obróbki plastycznej. WNT, Warszawa 1988, (in Polish).
- [17] S. Berski, H. Dyja, Analiza naprężeń i odkształceń podczas wyciskania bimetalu Al-Cu w procesie ECAE, *Hutnik Wiadomości hutnicze*, No. 5, 2011, pp. 360-364, (in Polish).
- [18] N.G. Kolbasnikov, O.G. Zotov, V.V. Duranichev, A.A. Naumov, V.V. Mishin, D.A. Ringinen. Influence of severe deformations in hot state on lowcarbon steel structure and properties. *SPb. Metal treatment*,. No 52, 2009, pp. 25-31.



Acknowledgements

This paper was created within the project "**Creation of an international scientific team and incorporation to scientific networks in the area of nanotechnology and unconventional forming material. CZ.1.07/2.3.00/20.0038**", which is financed by the European Social Fund and state budget of the Czech Republic.





esf european
social fund in the
czech republic



EUROPEAN UNION



MINISTRY OF EDUCATION,
YOUTH AND SPORTS



OP Education
for Competitiveness

INVESTMENTS IN EDUCATION DEVELOPMENT

Processing and mechanical behavior of fine grained metals.

Yannick Champion and Loïc Perrière

Institut de Chimie et des Matériaux Paris-Est – CNRS-UPEC,

2 rue Henri Dunant 94320 Thiais, Cedex France.

Abstract

Great interest in particular for mechanical properties (unusual high strength and rheology) focused our research towards fabrication of ultra fine grained metals (UFG) from nanopowder following a powder metallurgy processing. Today developments have been turned towards the fabrication of bulk ultrafine metals (UFG) using the spark plasma sintering technique (SPS). In this research our main interest is on the control of the UFG structure and the mechanical properties related to SPS processing. This opens interesting perspectives for fabrication of UFG complexe structure and composites.

Keywords

metal, nanopowder, ultrafined grain, spark plasma sintering, mechanical behavior

1. INTRODUCTION

Metallic nanopowders have been the subject of intensive research since the 80's for their very attractive size effect related properties. Particles with size below 100 nm exhibit high chemical reactivity, unusual magnetic properties (single domain and superparamagnetism), extreme strength. The nanopowders may find interesting use as fillers in composites with various matrices (polymers, metal, ceramic). The nanopowders are also precursors for the preparation with much precise control, of ultrafine grained metals, alloys and dual nanophases materials by compaction and sintering. Study of the synthesis of metallic nanopowders has been intensive in our laboratory since de early 80's. Objective has been manifold. First, one aimed at understanding the formation of nanoparticles from the evaporation and condensation of a metallic vapour within a cryogenic medium. Second, the nanopowders were investigated regarding their magnetic properties and their reactivity. Third, the compaction and sintering of the nanopowders leading to the development of a nano-powder metallurgy produced large size ultrafine grained metals for the investigation of the mechanical properties of the new type of materials. Today, the laboratory is no longer involved in a research on condensation of nanopowders. This will demand drastic conditions for experiments according to the REACH directive, due to the recognised high degree of potential toxicity of nanosized metallic materials. Then, for few years, we have focused our activity on the fabrication of ultrafined metals and alloys using the spark plasma sintering technique (SPS).



2. INSTITUT OF CHEMISTRY AND MATERIALS OF EAST-PARIS

2.1 Research topics and equipments

ICMPE (Instiut de chimie et des matériaux Paris-Est) is a joint laboratory CNRS and UPEC (University Paris East Créteil) composed of five research groups and six technical departments. About 100 permanents staff (CNRS and faculty members) and 50 non permanents (PhD, post doc invited researchers and trainees).

The researches are focused on 4 mains transversal topics including energy, ecology, health science and advanced materials in the fields of metallurgy, solid state chemistry, polymer science and organic chemistry. The institute in the framework of its technical departments possesses high standard means for metallurgical processing in particular r.f. induction melting and various solidification techniques (melt spinning, levitation, suction casting), powder processing among which the spark plasma sintering (Dr Sinter. 515S Syntex). With usual characterization techniques (RX, DSC ...) the institute has high standard transmission electron microscopes (TEM-STEM) equipped with HAADF, EELS, EDX mapping, orientation mapping (ASTAR) and new SEM with EBSD. Metallurgical researches are also supported by mechanical testing machine (MTS 150 KN) equipped with a high temperature furnace and new nano-indenter (HYSITRON TI950 Triboindente) with scratch test, DMA and temperature (600°C) stage.

2.2 Staff involved in UFG

Currently the activities on UFG metals are focused on nano-copper powder sintering using the SPS technique.

Dr Loïc Pèrière is a CNRS research Engineer and head of the department for metallurgical processing. The Spark plasma sintering is a platform of the Ile-de-France district and shared between different laboratories around Paris. The equipment is localised at ICMPE and Dr Judith Monnier (associate professor at UPEC) is the scientific responsible for the equipment. Dr Yannick Champion is CNRS research director.

L. Perrière and Y. Champion and member of the group MCMC (metals and ceramics with controlled microstructures) and J. Monnier is a member of the group CMTR (metallurgy of rare earth).

2.3 Teaching activities

Expertise of staff involved in the UFG activities is in particular chemical metallurgy including metal processing, structural characterisation and mechanical behavior. Teachings then contain bases on thermodynamics (phase diagram, solidification,) transport properties, physical metallurgy for plasticity. Teaching at master degree level and school of engineer for industry is then focused on metal processing and powder techniques.

3. ULTRA FINE GRAINED BY SPARK PLASMA SINTERING

Ultrafine grained mechanical properties and rheology has been intensively studied in our group (MCMC). Originally, nanopowders [1] were sintered in H₂ atmosphere and densified using extrusion technique [2-3]. YC has studied the unusual properties, high strength and strain rate sensitivity by mechanical testing at various temperature [4-6] and analytical model was proposed to analyse the behavior and bring perspective for potential improvements. The



processing was complex and tedious non adapted for applications. SPS has opened new perspectives for these materials.

So far, increasing strength of metals is obtained by either solution or precipitation hardening, leading in both cases to a severe decrease in other properties. An alternative to conventional alloying would be an appropriate copper grains refinement (and/or addition of nanodispersion) well suited in particular for small devices (active connections, micro coils...). We have studied the sintering of copper ultrafine powders using the spark plasma sintering technique (SPS). The process consists in heating a powder by Joule effect, produced by electric current pulses going through it. It is generally assisted by uniaxial compression, which leads eventually to reasonable high powder densification. The SPS tends to be intensively used for its short time processing, limiting grain growth in particular in fine and nano powders. In our approach, the powder technique is used since it allows inserting easily additional particles (of different nature) with control content that may improve strength with limited loss in electrical conductivity. We have focused initially on the analysis of the microstructure evolutions at various stages of the SPS processing of an ultrafine copper powder with particles size of about 50 nm. We have paid a particular attention to the effect of the natural oxide layer coating the particles to materials behavior, and have proposed a pre-annealing treatment under H_2 to improve the quality of the produced ultrafine copper material.

Currently our main results are the formation of pure UFG with nearly full densification and no grain coarsening during sintering. Oxide which passivates the powder much favourable for handling in the on-going processing is fully removed by pre annealing under H_2 .

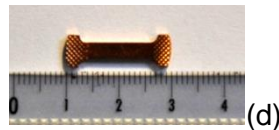


Fig. 1 Flat specimen prepared by hydrogen reduction and spark plasma (SPS) flash sintering for mechanical testing in traction

The processing demands further optimization for improving the mechanical properties.

4. CONCLUDING REMARK AND OBJECTIVES

Our work on UFG metals is focused today on the powder processing using the spark plasma sintering technique. The SPS has proved to form parts with absence of grain growth and potentially interesting mechanical properties. The most interesting perspectives are seemingly on the possibility to form controlled architectures and nano composites with improved and relevant properties.

5. REFERENCES

- [1] Y. Champion, Gas phase synthesis of nanopowders in Nanomaterials and nanochemistry. (Ed. C. Bréchnignac, Ph Houdy, M. Lahmani) Springer Berlin (2007) 396-426.
- [2] Y. Champion, F. Bernard, N. Guigue-Millot et P. Perriat, Sintering of copper nanopowders under hydrogen: an in situ X-ray diffraction. Materials Science and Engineering, A360 (2003) 258-263.
- [3] C. Langlois, M.J. Hÿtch, P. Langlois S. Lartigue-Korinek and Y. Champion, Synthesis and microstructure of bulk nanocrystalline copper. Metal. Mater. Trans. A 36A (2005) 3451-3460.



- [4] Y. Champion, C. Langlois, S. Guérin-Mailly, P. Langlois, J-L Bonnetien and M. J. Hytch, Near-perfect elasto-plasticity in pure nanocrystalline copper. *Science* 300 (2003) 310-311.
- [5] C. Duhamel, Y. Bréchet and Y. Champion, Activation volume and deviation from Cottrell-Stokes law at small grain size. *International Journal of Plasticity*, 26 (2010) 747-757.
- [6] Y. Champion, Competing regime of rate dependant plastic flow in ultrafine grained copper. *Mater. Sci. Eng. A*, 560 (2013) 315-320.

6. STRATEGY AND CONTENT OF POSSIBLE COLLABORATION WITHIN THE CONSORCIUM

The field of metallurgy (chemistry, physics, mechanics and engineering) is the subject of intense discussions for development of projects in the domains of research and education since it appears as much necessary for industrial development in Europe. Our group is involved in these metallurgy initiatives and strengthen its activities on chemical metallurgy with melting, solidification, processing and mechanical properties of complex alloys. UFG are among the materials of interest.

We are willing keeping connexions on this framework in particular organising joint scientific meetings, laboratory visits and welcoming visiting researchers (University has a visiting researcher program fundings). Collaborations can be organised in the framework of CNRS cooperative programs and we are looking for collaborations with co-supervising PhD students on EU programs or industry financial supports.

Acknowledgement

The authors would like to acknowledge gratefully the Ministry of Education, Youth and sports of Czech Republic for its support to the project "Creation of an international team of scientist and participation in scientific networks in the sphere of nanotechnology and unconventional forming metal", CZ.1.07/2.3.00/20.0038.

Social Fund and state budget of the Czech Republic.





eu
esf
european
social fund in the
czech republic



EUROPEAN UNION



MINISTRY OF EDUCATION,
YOUTH AND SPORTS



OP Education
for Competitiveness

INVESTMENTS IN EDUCATION DEVELOPMENT

Non-Traditional Use of Torsion Plastometer in Physical Simulation of Deformation Processes

Tomáš Kubina ^a, Josef Bořuta ^b

^a COMTES FHT a.s., Prumyslova 995, CZ 334 41 Dobruška, Czech Republic, tomas.kubina@comtesfht.cz

^b VSB – Technical university of Ostrava, 17. Listopadu 15, CZ 708 33 Ostrava – Poruba, Czech Republic, josef.boruta@seznam.cz

Abstract

The present paper provides a picture of metallographic and plastometric research in the border areas of steel production and forming. The focus of the paper is simulation conducted in SETARAM plastometer. The SETARAM plastometer used in the experiments has been modified recently. The changes concerned predominantly its temperature measurement and control devices. The lower limit of its operating temperatures was reduced to approximately 400 °C. The purpose of the most recent upgrade was to allow investigation in the region of steel brittleness related to loading in their freezing range. It will be possible to explore the behaviour of steels under the conditions of continuous casting processes, solidification in crystallizers and deformation during solidification. Microstructures of various types of steels are presented upon small continuous deformation applied at high temperature, which lead to partial melting and resolidification of test bars.

Various types of sheet rolling simulations with reduced finish temperatures conducted in the plastometer are described. Approaches to evaluating continuous torsion tests to fracture in the field of basic research into materials plasticity are presented as well. In terms of interrupted tests, the importance of the anisotropic interrupted test as a source of information for research is touched upon. In particular, demonstration is given of the potential for finding transformation temperatures governed by deformation in the 1.0583 steel grade. A physical simulation procedure involving strain-induced ferritic transformation has been developed on the basis of results of tests. Mechanical properties were measured on specimens processed in the simulation. Microstructures resulting from the thermomechanical simulation are discussed.

Keywords

Torsion test, large deformations, microstructure, plasticity, steels

1. INTRODUCTION

The paper discusses two areas of plastometric research. The first one concerns plastic properties of materials in the brittle failure region I, i.e. the deformation behavior of materials under load in the temperature region just below the solidus temperature. The other involves semi-hot forming, a process which leads to grain refinement [1].



Micro alloyed and thermo-mechanically rolled steel grades are already standardized according to EN10149-2 with minimum yield strength values from 315 to 700 MPa. However, further intensive research is underway.

According to [2] it is generally accepted that at currently used technologies of thermo-mechanical forming the achieved grain size of 4 - 5 micrometers is optimal for requirement of certain minimum plastic properties. The following physical-metallurgical principles are currently used in order to develop very fine-grain microstructure:

- Dynamic re-crystallization of austenite during hot-forming with subsequent transformation of austenite to ferrite.
 - Deformation-induced ferrite transformation (i.e. transformation to ferrite occurs during forming, not afterwards).
 - Rot rolling in inter-critical area – i.e. dual-phase area austenite-ferrite.
 - Hot rolling in ferritic area using dynamic re-crystallization in ferrite
 - Hot rolling in ferritic area using ferrite healing.
 - Cold-rolling and annealing of martensitic structure
- The text should be divided into separate chapters and sub-chapters. In exceptional cases third-level classification may be used.

2. PLASTOMETRIC TEST WITH SPECIMEN MELTING

Based on empirical findings related to the control of the torsion plastometer, a special test was developed, wherein part of the specimen melts and resolidifies. Both phenomena take place during twisting. The specimen is placed within a quartz glass tube. At the melting stage, the molten part of the material will be held by the quartz tube. The diameter of the tube is such that it compensates the resulting volume changes. Test bar diameter is 7.6 mm and its length is 100 mm.

The chemical composition of tested IF steel is given in Table 1. The torque curve recorded during a test of an IF steel [3] is shown in Fig. 1. Preheating at 1200 °C took one minute. It was followed by twisting of the specimen at the rate of 2 revolutions per minute. In the course of the twisting action, temperature was raised to 1450 °C. The temperature curve is plotted in Fig. 1. It is apparent that after reaching 1380 °C, the torque drops, owing to partial melting of the specimen. At the solidification stage, the torque begins to rise again, approximately beyond 1290 °C. Hence, this temperature can be considered the temperature of full solidification.

Table 1 Chemical composition of IF tested steel (wt. %)

Element	C	Mn	Si	V	Nb	Ti	Al
TiNb IF steel	0.0039	0.42	0.007	0.001	0.044	0.034	0.038



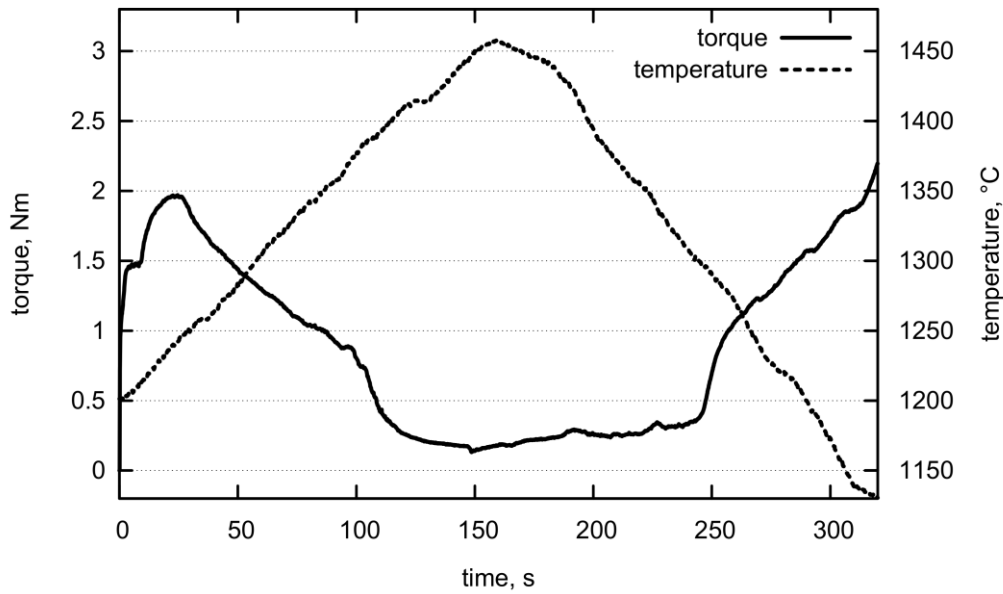


Fig. 1 Torque and temperature plots recorded during test with specimen melting.

Fig. 2 shows the specimen microstructure upon testing and air cooling from 1100 °C. Fine-grained areas are clearly visible between the overheated region and the area with cavities and cracks formed during twisting in the solidification region. The regions of twisting with aligned cracks are plain to see as well. The specimen prepared in this manner is suitable for fractographic observation.

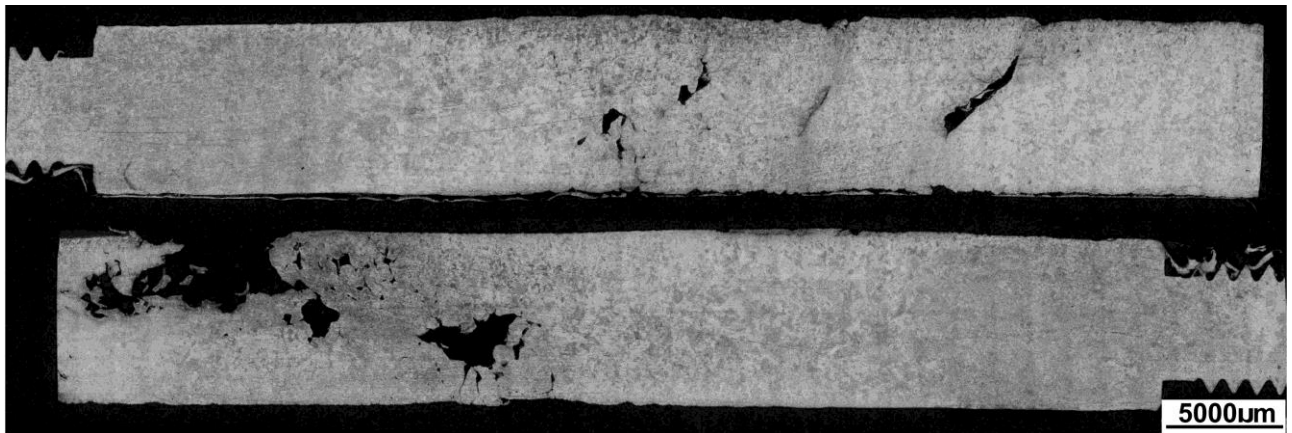


Fig. 2 Micrograph of specimen upon testing.

3. USE OF ANISOTHERMAL INTERRUPTION TORSION TEST TO PREPARE PHYSICAL SIMULATION

For our example of physical plastometric simulation using plastometer SETARAM-MMV, we used inspiration [2] from deformation-induced ferrite transformation (DIFT). The trials were performed on the material for shipbuilding sheet, grade 1.0583; the heat chemistry of tested samples is given in Table 2.

In case of the steel tested, we first needed to specify optimum temperature for DIFT, since the steel that we had investigated earlier had a higher carbon content. That is why we first used the



earlier-developed procedures of the anisothermal interruption test (AIT) in order to determine characteristic points of the austenite to ferrite transformation, co-effected by previous forming (Fig. 3).

Table 2 Chemical composition of tested steel grade 1.0583 (wt. %)

Element	C	Mn	Si	V	Nb	Ti	Al
grade 1.0583	0.159	1.16	0.256	0.069	0.031	0.0022	0.033

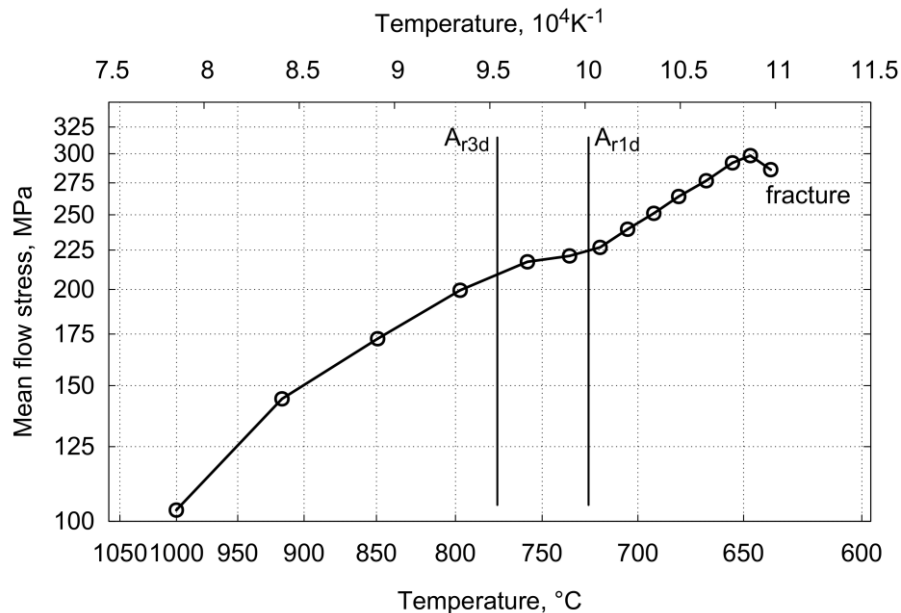


Fig. 3 Evaluation of AIT shown in the previous picture; deformation-affected transformation points are marked.

The test was performed after reheating with a holding time of 5' at the temperature of 1200 °C, then cooling down to the first deformation temperature of 1000°C with one minute holding time. After the first deformation, the AIT was performed without reheating regulation, i.e. the temperature evolution was governed mainly by the state of the microstructure and by thermal-mechanical testing parameters. These however, were maintained at constant levels: deformation of 0.2 and deformation speed of 0.5 s⁻¹, pauses of 5 s – air cooling. The trial ends when samples' formability under current conditions is exhausted, i.e. at the moment of fracture, or an interruption can be scheduled to analyze the instant structural state.

4. PHYSICAL SIMULATION IN AREA OF DUAL-PHASE STRUCTURE STATES

For our next example of plastometric simulation using plastometer SETARAM-MMV we have also drew inspiration [2] from deformation-induced ferrite transformation (DIFT). In order to dissolve microalloying elements, the steel with chemical composition given in Table 2 was first heated to 1200 °C with a holding time of 5 minutes. The purpose of the first reduction at approximately 1000 °C is to refine austenite grains by re-crystallization. This should have a positive impact on DIFT. The purpose of the second reduction at temperatures of 950 – 930 °C is to utilize the fastest available course of precipitation (Nb, V)(C, N), that should, at the same time, accelerate the kinetics of DIFT. Finally, three reductions at 820 °C are considered [2] as DIFT rolling. However, from Fig. 3 it is clear that the temperature for DIFT has to be reduced to approximately 780 °C. At the same time, the impact of the length of delay between deformations



at this temperature was explored. Two delay times representing different rolling processes were applied. The delay time of one second was used for the HSM-type continuous mill, whereas the ten-second delay time was to represent processing in the reversible Steckel mill. Detail comparison of flow stress is on Fig. 4.

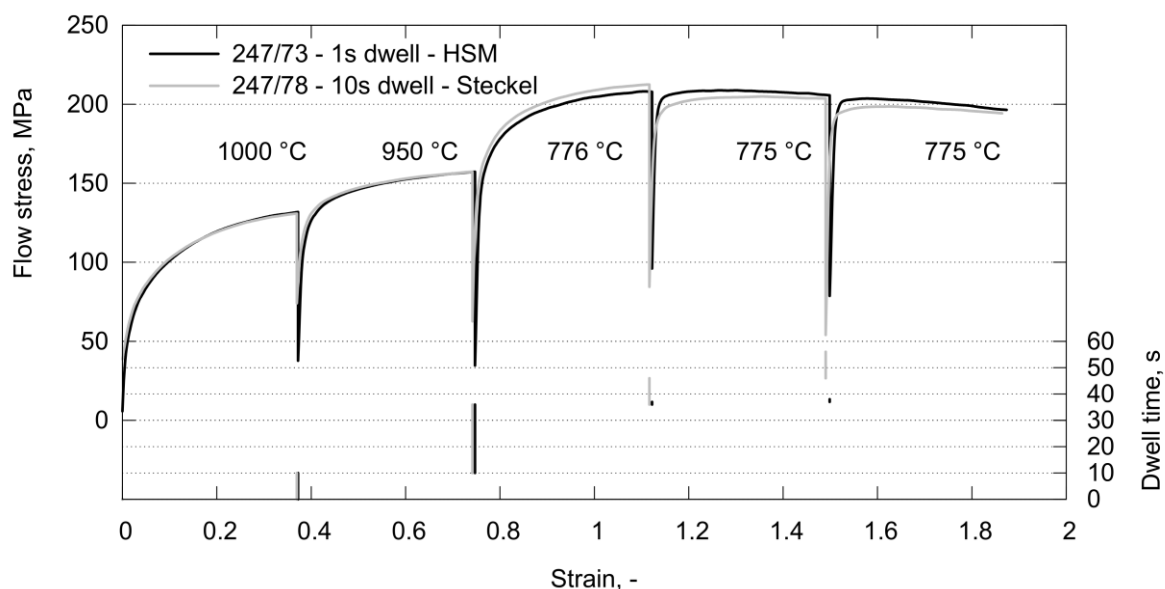


Fig. 4 Detailed comparison of physical simulation plots of DIFT for HSM and STECKEL.

As the test specimens did not fail, they were used for measuring mechanical properties by a tension test. An overview of mechanical properties is given in Table 3. The table includes information on the particular cooling method, as it has impact on the resulting ferrite grain size. The microstructure upon HSM rolling simulation is shown in Fig. 5. It is evident that the resulting ferrite grain size is non-uniform. This is why the mean ferrite grain size was determined separately for the coarse-grained and for the fine-grained regions. These results are given in Table 3 as well. Microstructures of specimens upon rolling in the Steckel mill were evaluated in the same manner (Fig. 6). Their ferrite grain size showed no substantial differences.

Table 3 Mechanical properties of samples upon plastometric simulation

Marking	Re _H	Re _L	Rp _{0.2}	Rm	Z	d _c	d _f	Note
	[MPa]	[MPa]	[MPa]	[MPa]	[%]	[μm]	[μm]	
247/73	543	510		601	35.4	8.9	2.6	HSM CC
247/74			531	635	21	5.6	1.9	HSM Q 640°C
247/75			688	820	5	-	1.8	HSM Q Td
247/77			653	938	6	-	1.7	HSM Q Td
247/78			662	949	9.8	-	2.2	STECKEL Q Td
247/79	534	519		594	18.5	7.9	2.6	STECKEL CC

Note: Q – water quenched with value of start temperature, CC- controlled cooling, Td – finishing deformation temperature, STECKEL – reversible rolling with large delay time, HSM – continuous rolling with short delay time.



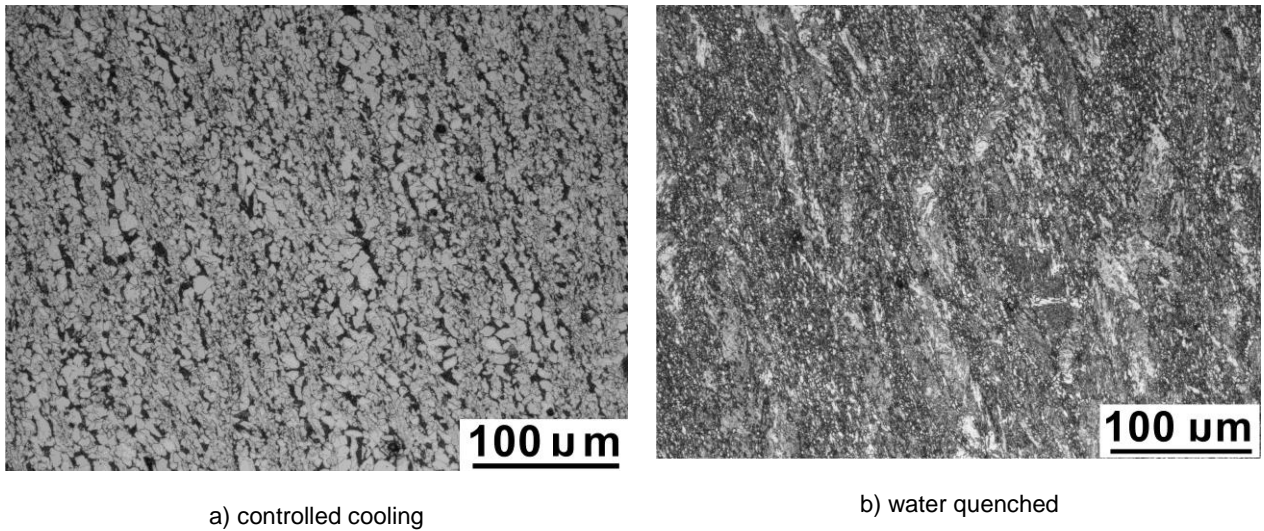


Fig. 5 The microstructure upon HSM rolling simulation with different cooling

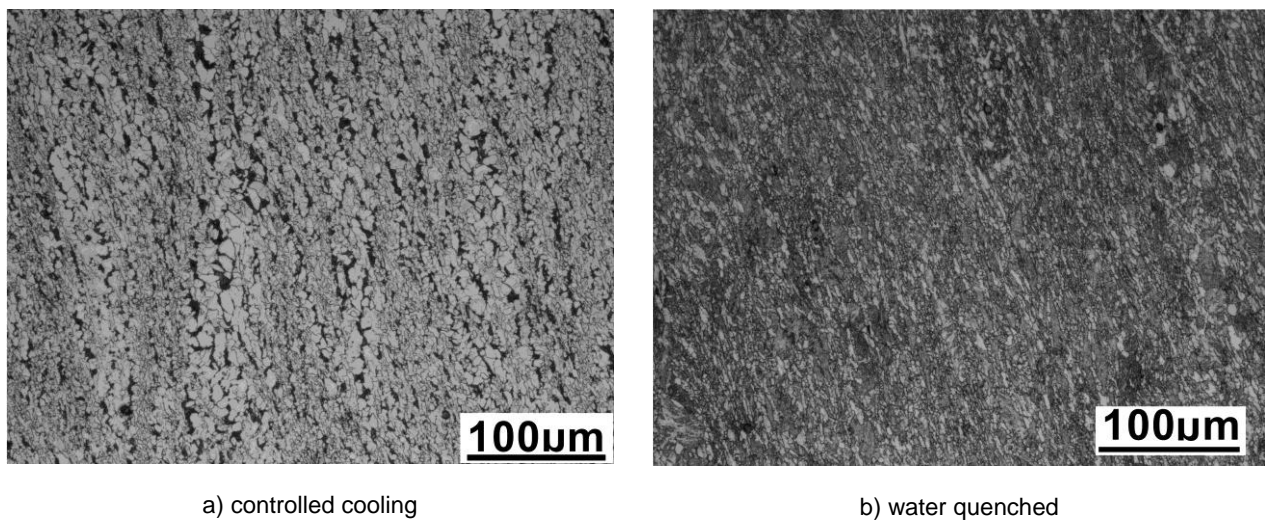


Fig. 6 The microstructure upon Steckel mill rolling simulation with different cooling.

5. CONCLUSION

The forty years of operation of the SETARAM-VÍTKOVICE-MMV torsion plastometer have yielded a number of inspirational findings in physical metallurgy-oriented research on hot-formed metals and, most notably, steels [4-6].

The traditional domain of plastometric exploration of deformation behavior of steels during hot forming processes, namely rolling and forging, has gradually expanded to encompass forming of other metals, such as non-ferrous and light metals [7-9].

Equally, the temperature range studied has been recently widened to include still little experimentally explored temperature intervals. This concerns both the high-temperature forming range bordering on the region for continuous casting and the forming interval at lower temperatures, which is the focus of the currently expanding study of controlled forming and cooling. For the purposes of research, mainly research into thermal-mechanical processing and optimization of thermal treatment that follows after hot forming, it was necessary to provide proper cooling in the region of phase transformation of austenite into ferrite and/or pearlite and



bainite, and all the way down to temperatures close to 400 °C. In preparation of the plastometer for physical simulations in this temperature range, frequent modifications to the control software were performed in order to allow data acquisition for these temperature ranges as well.

Currently, using this methodology it is possible to monitor the behavior of Ø 6 mm test bars down to temperatures of 400 °C at the cooling speed of max. 4°C/s.

6. LITERATURE

- [1] J. Bořuta, P. Gembalová, A. Bořuta, T. Kubina, Plastometric research of deformation behaviour steel strips, In. 7. International Conference Steel Strip 2006 (2006) 319 - 326.
- [2] J. Zník, L. Kraus, T. Prnka, K. Šperlink, The European strategy of manufacturing processes (4) - Preparation of ultra-fine grained and nanocrystalline metallic materials by severe plastic deformation and their properties, Repronis, Ostrava, 2007 (in Czech).
- [3] M. Longauerová, M. Fedorová, J. Bořuta, A. Bořuta, Effect of cooling rate in the critical areas of temperature on the occurrence of reduced hot plasticity, Hutnické Listy, No. 2, LXIV (2011) 75-79 (in Czech).
- [4] I. Schindler, J. Bořuta, New methods of studying the plastic properties of steels using the automated torsion plastometer. Hutnické aktuality, No. 9, 33 (1992) 1-35 (in Czech).
- [5] I. Schindler, J. Bořuta, Utilization Potentialities of the Torsion Plastometer, Dept. of Mechanics and Metal Forming, Silesian Technical University, Katowice, 1998.
- [6] J. Bořuta et. al., Plastometric research of deformation behavior of controlled rolling materials [in czech], Hutnické Listy, No. 1, LXI (2008) 80-87.
- [7] T. Kubina, J. Bořuta, Processing of results of hot torsion plastometric tests using the new technique of smoothing the torque curves. Hutnické listy, No. 4, LXII (2010) 150-153.
- [8] T. Kubina et al., Determination of Energy Dissipation and Process Instability in Various Alloys on The Basis of Plastometric Tests, Metalurgija, 52 (2013) 325-328.
- [9] R. Pernis, J. Kasal, J. Boruta, High temperature plastic deformation of CuZn30 brass – calculation of the activation energy. Metallic Materials, 48 (2010) 41- 46.

Acknowledgements

This paper was created within the project "**Creation of an international scientific team and incorporation to scientific networks in the area of nanotechnology and unconventional forming material. CZ.1.07/2.3.00/20.0038**", which is financed by the European Social Fund and state budget of the Czech Republic.





eu
esf european
social fund in the
czech republic



EUROPEAN UNION



MINISTRY OF EDUCATION,
YOUTH AND SPORTS



OP Education
for Competitiveness

INVESTMENTS IN EDUCATION DEVELOPMENT

Magnesium - based Composites

Pavel LUKÁČ^a, Zuzanka TROJANOVÁ^a

^a Charles University, Faculty of Mathematics and Physics, Ke Karlovu 5, CZ 121 16 Praha 2,
Czech Republic,

lukac@met.mff.cuni.cz; ztrojan@met.mff.cuni.cz

Abstract

Magnesium alloys exhibit a high specific strength. Grain refinements, precipitation, solid solution hardening are often used in order to increase the strength of Mg alloys. An effective method is particle or fibre-reinforcement that is useful for improvement of strength of alloys at elevated temperatures. In this study, we will present examples showing how the addition of short fibres or particles influences the mechanical properties of pure magnesium and magnesium alloys. Tensile (compression) tests were performed at room temperature and over a wide temperature range. Reinforcements and matrix Mg alloys have different mechanical, chemical and physical properties. This causes changes in properties of the composite. Reinforcements have usually the coefficient of thermal expansion different from that of a matrix. The presence of reinforcements with different thermal expansion coefficients may increase the dislocation density. The density of the newly created dislocations depends on the reinforcement volume fraction, the reinforcement shape and the difference in the coefficients of thermal expansion of both of the composite components. Therefore strength, plastic deformation and physical properties are influenced. The yield stress of magnesium alloys increases strongly if a small volume fraction of nanoparticles is used as reinforcement.

Keywords

Magnesium composite; mechanical properties.

1. INTRODUCTION

Magnesium with a density of 1.8 g/cm³ as the lightest of all structural metals plays a significant role in development new alloys and composites suitable for applications. Magnesium alloys have low density, high specific strength (the ratio of the strength to density) and high stiffness. Grain refinement, solid solution hardening and precipitation hardening are effective ways of improving mechanical properties. Magnesium alloys can be strengthened by reinforcement – producing composites. Composites – materials containing two or more distinct phases – may be fabricated by different techniques. The liquid metallurgy methods (the reinforcing components are in contact with the molten metallic matrix) and the powder metallurgy routes (extrusion, forging, HIP/sintering) are often used as ways to fabricate the magnesium-base composites. Ceramic reinforcements are the most commonly used in magnesium-based composites. The mechanical and physical properties of the magnesium composites are influenced by processing



method, type of matrix alloy (or pure Mg), type, shape and volume fraction of reinforcement. Particulates and/or short fibres are very often used as the reinforcements. It is important to mention that the mechanical and physical properties of the reinforcements are different from those of the matrix. Among the reinforcement properties, the following ones are important: elastic modulus, yield strength, density, melting temperature, coefficient of thermal expansion, thermal conductivity. These properties greatly influence the end properties of the composite. Of course, cost of reinforcement plays an important role in its choice for the fabrication of a composite designated for applications. The present study gives some examples describing the strength of magnesium-based composites.

2. EXPERIMENTAL RESULTS

In this chapter we will give some examples illustrating the strength of composites prepared by two different processing techniques. We shall focus on composites prepared by the powder metallurgy technique and the squeeze casting technology. We want to show the influence of the addition of various reinforcements on the mechanical properties of the produced composites – particles SiC and short fibres of δ -Al₂O₃ (Saffil).

The first group are three different magnesium alloys – AZ91, Mg-8Li and WE54 – reinforced with SiC particles. Powders of AZ91 (Mg-9Al-1Zn), WE54 (Mg-5Y-4Nd) and Mg-8Li alloys were first mixed with SiC microparticles in an asymmetrically moved mixer and then in a ball mill. The powder was capsulated in magnesium container and extruded at 400 °C using a 400 t horizontal extrusion press. The SiC more or less uniaxial microparticles with a diameter of about 9 µm were not homogeneously distributed in the matrix. They formed small clusters in many cases. The volume fraction of SiC particles in the matrix was: AZ91+13 vol% SiC, WE54+13 vol% SiC and Mg-8Li+7 vol% SiC. Cylindrical specimens with a diameter of 8 mm and a length of 12 mm were deformed in compression using an INSTRON testing machine. The specimens were deformed with a constant crosshead speed giving an initial strain rate of $2.8 \times 10^{-4} \text{ s}^{-1}$ at various temperatures. Samples were deformed either to fracture or to a predetermined strain at higher temperatures. It should be noted that the stress-strain curves obtained at higher temperatures are flat. The strain hardening rate is close to zero, i.e. a dynamic balance between hardening and softening occurs. The compressive yield stress (CYS) and the compressive ultimate strength (CUS) were determined as the proof stress at a strain of 0.002 and the maximum stress, respectively. Both stresses are influenced by the test temperature. Both the yield stress and the ultimate compressive strength decrease with increasing temperature. The compressive yield stress decreases with increasing temperature slowly up to about 150 – 200 °C and about this temperature it decreases more rapidly. The value of this boundary temperature depends on the matrix [1 – 3]. The values of the compressive yield stress and compressive ultimate strength of the three above mentioned composites estimated at three different temperatures are given in Table 1.

Table 1 Values of the compressive yield stress and compressive ultimate strength

	RT	RT	150 °C	150 °C	200 °C	200 °C
	CYS(MPa)	UCS(MPa)	CYS(MPa)	UCS(MPa)	CYS(MPa)	UCS(MPa)
AZ91+13SiC	222	437	98	164	16	31
WE54+13SiC	246	370	220	327	65	82



Mg-8Li+7SiC	198	405	126	159	15	22
-------------	-----	-----	-----	-----	----	----

It can be seen that the testing temperature influences the values of both the compressive stress and the compressive ultimate strength. A decrease in CYS of AZ91+13SiC between 150 °C and room temperature (RT) is very extensive, whereas the CYS of WE54+13SiC in the same temperature range decreases insignificantly. It is interesting to note that the value of CYS of AZ91 at room temperature is about 148 MPa, whereas that of WE54 is about 175 MPa. The CYS of AZ91 magnesium alloy decreases with increasing test temperature more rapidly than that of WE54 magnesium alloy.

The second group are AZ91 and AS21 magnesium alloys reinforced with 20 vol.% short Saffil fibres. Specimens prepared by the squeeze casting technology were deformed in tension at different temperatures between room temperature and 300 °C at a constant cross-head speed giving an initial strain rate of about $2 \times 10^{-4} \text{ s}^{-1}$ [4, 5]. The values of the yield strength of AZ+20 vol.% Saffil fibres and AS21+20 vol.% Saffil fibres obtained are given in Table 2.

Table 2 Values of the tensile yield stress at room temperature

	AZ91	AS21
Unreinforced	116 MPa	112 MPa
Reinforced	324 MPa	432 MPa

It can be seen that the addition of short Saffil fibres as reinforcements increases the yield stress of the matrix. The effect of the testing temperature on the tensile yield stress and ultimate tensile strength of the AZ91 and AS21 alloys reinforced with the Saffil fibres is similar [4, 5] to that in the case of magnesium alloys reinforced with particles.

3. DISCUSSION

The differences between the yield stress of a composite and that of an unreinforced alloy is caused by reinforcement. Several strengthening mechanisms contributing to the increase of the composite should be considered. The load transfer from the matrix to the mechanically stronger particles can be calculated according to [6]

$$\sigma_{LT} = \sigma_m 0.5f \quad (1)$$

where σ_m is the stress for the unreinforced alloy and f is the volume fraction of particles. There is a great difference between the coefficients of thermal expansion (CTE) of the matrix and the reinforcement. Thermal stresses may be induced. They depend on the difference in the coefficients $\Delta\alpha = \alpha_M - \alpha_f$, (α_M is the CTE of the matrix α_f is the CTE of the reinforcement) according to the following relationship [7]

$$\sigma_{TS} = E_f E_M f \Delta\alpha \Delta T / [E_f + E_M(1-f)] \quad (2)$$

where E_f and E_M are Young's moduli of the reinforcing phase and the matrix, respectively and ΔT is the temperature difference. The thermal stresses may be sufficient to generate new dislocation at the interface between the matrix and the reinforcements. The density of the newly created dislocation at the matrix/reinforcement interfaces can be expressed as [8]

$$\rho = Bf\Delta\alpha\Delta T/b(1-f)d_f \quad (3)$$



where b is the Burgers vector and d_f is the diameter of particles; generally a minimum size of the reinforcing phase. Particles in the matrix are obstacles for motion of dislocation. Particles can be considered as incoherent and therefore we can take into account Orowan strengthening. The contribution due to Orowan strengthening can be written as [9]

$$\Delta\sigma = Gb/L_p + 5Gf\varepsilon_p/2\pi \quad (4)$$

where G is the shear modulus, L_p is the distance between particles in the slip plane and ε_p is the plastic strain. The second term in equation (4) has to be used if we consider an increase in stress during deformation of the composite. It is obvious that dislocations accumulate at the reinforcing phases. In many cases, the average grain sizes in composites are lower than in unreinforced alloys. A contribution to the composite strengthening due to the grain refinement can be calculated using the well-known Hall-Petch relationship.

Calculation of particular contributions shows that important are the density of the newly created dislocations and the load transfer (especially for fibres).

4. CONCLUSIONS

The examples mentioned above illustrate the effects of reinforcements. It should be noted that the interface plays an important role for mechanical and physical properties of a composite. It has been documented by Lukáč and Trojanová [10]. They investigated micromagnesium reinforced with 3 vol.% of Al_2O_3 (alumina) and 3 vol.% ZrO_2 (zirconia) nanoparticles, respectively. The nanoparticles had a mean diameter of 14 nm. The yield stress of Mg + alumina nanoparticles was higher than that of Mg + zirconia nanoparticles. This difference in the values of the yield stress may be explained by the bonding between the particles and the matrix.

In many applications of composites, especially at elevated temperatures, the thermal expansion and rate of the heat flow transfer are very important. The thermal conductivity of a composite depends on the matrix and reinforcement and it is influenced by temperature. The values of the thermal conductivity of a composite are lower than those of unreinforced alloy. Likewise the coefficient of thermal expansion is dependent on the combination of the reinforcement and the matrix.

5. LITERATURE

- [1] TROJANOVÁ, Z. et al. Mechanical and fracture properties of an AZ91 magnesium alloy reinforced by Si and SiC particles. *Composite Science and Technology*. 2009, 69, 2256-2264.
- [2] SZÁRAZ, Z., Z. TROJANOVÁ, M. CABBIBO, E. EVANGELISTA. Strengthening in a WE54 magnesium alloy containing SiC particles. *Materials Science and Engineering A*. 2007, 462, 225-229.
- [3] TROJANOVÁ, Z. et al. Strengthening in Mg-Li composites. *Composite Science and Technology*. 2007, 67, 1965-1973.
- [4] TROJANOVÁ, Z., V. GÄRTNEROVÁ, P. LUKÁČ, Z. DROZD. Mechanical properties of Mg alloys composites reinforced with short Saffil fibres. *Journal of Alloys and Compounds*, 2004, 378, 19-26.
- [5] TROJANOVÁ, Z., Z. SZÁRAZ, J. LÁBÁR, P. LUKÁČ. Deformation behavior of an AS21 alloy reinforced by short Saffil fibres and SiC particles. *Journal of Materials Processing Technology*, 2005, 162-163, 131-138.
- [6] AIKIN Jr, RM., L. CHRISTODOULOU. The role of equiaxed particles on the yield stress of



- composites. *Scripta Metallurgica et Materialia*. 1991, 25, 9-14.
- [7] CARRENO-MORELLI, E., SE. URRETO, R. SCHALLER. Micromechanisms of thermal stress relaxation in MMCs studied by mechanical spectroscopy. In: Proceedings of the international conference on fatigue of composites. Paris: Société Française de Métallurgie et de Matériaux, 1997, 112-119.
- [8] ARSENAULT, R.J., N. SHI. Dislocation generation due to differences between the coefficients of thermal expansion. *Materials Science and Engineering*. 1086, 81, 175-187.
- [9] LINHOLT, H. Aspects of deformation of metal matrix composites. *Materials Science and Engineering A*, 1991, 135, 161-171.
- [10] TROJANOVÁ, Z., P. LUKÁČ. Magnesium-based nanocomposites. *International Journal of Materials and Product Technology*, 2005, 23, 121-131.

Acknowledgements

This paper was created within the project "**Creation of an international scientific team and incorporation to scientific networks in the area of nanotechnology and unconventional forming material. CZ.1.07/2.3.00/20.0038**", which is financed by the European Social Fund and state budget of the Czech Republic.





esf european
social fund in the
czech republic



EUROPEAN UNION



MINISTRY OF EDUCATION,
YOUTH AND SPORTS



OP Education
for Competitiveness

INVESTMENTS IN EDUCATION DEVELOPMENT

EU R&D projects - experience with the proposal evaluation

Karel Malaník

VÚHŽ a.s., 739 51 Dobrá 240, CZ, malanik@vuhz.cz

Abstract

The paper deals with the evaluation of the international project proposals. The experience with procedures of evaluation procedures of the European Community R&D programmes is performed within the programme FP7. New programme Horizon 2020 is mentioned, too.

The particular steps of proposal evaluation are discussed in light of pilot and demonstration projects, their evaluation (justification of marking, resubmitted proposals, outcome of the individual evaluation, thresholds), consensus (consensus meeting, marking, outcome of the consensus meeting) and ranking.

The presentation is focused on the individual evaluation process of proposals, deals with the evaluation criteria – such as scientific and technical approach, innovative content, consistency of resources and quality of partnership, industrial interest and scientific/technical prospects, added value for the European Union and contribution to EU policies.

Keywords

EU funds, R&D projects, FP7, proposal, evaluation process, evaluation criteria, Horizon 2020

1. EVALUATION OF PROPOSALS – FP7

This paper gives information about the evaluation of the proposals in the R&D programme FP7. Knowledge of the appraisal process is very useful for increasing of success facility in selection procedure.

In general, eligible proposals are evaluated by the Commission with the assistance of independent external experts.

Two types of evaluation are usually used:

- single stage evaluation – e.g. Research Fund for Coal and Steel,
- two-stage evaluation – e.g. FP7, Horizon 2020 (for two-stage submission).

The first stage is usually performed in residence of the evaluator.

As regards the second stage the Commission invites independent experts to the Commission's premises in order to carry out the evaluation of proposals.

1.1 Objectives of NMP programmes

The example of evaluation procedure is presented on the FP7 programme - Cooperation, Theme 4 "Nanosciences, nanotechnologies, materials and new production technologies –



NMP”, FP7-NMP-1.4-3 "Tools and methodologies for imaging structures and composition at the nanometre scale”.

Evaluation period

Stage 1: usually November - December , working place - expert residence

Stage 2: next year (June), Brussels

Proposal had to fulfill the general objective of the NMP programme, the objective of the relevant NMP Area and the specific objective of the Call topic. The overall Objective of the NMP Theme in FP7 was to improve the competitiveness of EU industry (including SMEs) and ensure its transformation through:

- transition to knowledge-based industry,
- generation of applicable knowledge of radical potential,
- strengthening EU leadership in nano materials and production technologies ,
- validated integration of different technologies and disciplines that demonstrates industrial change.

The objectives of the Call Area - Activity 4.1 Nanosciences and Nanotechnologies consisted in:

- maximizing the contribution of nanotechnology on sustainable development,
- nanotechnology for benefiting Environment,
- energy and health,
- ensuring safety of nanotechnology,
- cross-cutting and enabling R&D.

Specific objective of the Call topic - NMP.2011.1.4-3 “Tools and methodologies for imaging structures and composition at the nanometre scale” dealt with development of integrated structural and chemical imaging and characterization tools. Technical content/scope was focused on:

- 3D imaging and spectroscopy tools and techniques,
- multimodal microscopy,
- sample preparation protocols and procedures,
- automation for tool control,
- integrated metrology to measure in situ structure, composition, and orientation of nanoparticles or low dimensional structures,
- proof of concept and application to industrially relevant samples.

1.2 Evaluation process

Reporting included three sequential steps - IER "individual evaluation report", CR "Consensus report" and ESR "Evaluation summary report". The individual evaluation demanded at least two/three detailed comments to every criterion with justifying and explaining the marks (strong points, weak points). The comments were used for feed-back to proposers.

Assessment was focused on soundness of the concept & quality of the objectives (including relevance to the call topic) including the progress beyond the current state-of-the-art, three guiding principles - objectivity, accuracy, consistency and contribution to the expected impacts mentioned in the Work Programme for this topic at European and international level.

Usually as many as 10 proposals is assessed by each expert within the first stage (Individual Evaluation Reports). Evaluation is performed via internet.



Evaluation criteria

1. Scientific and/or technological excellence (relevant to the topics addressed by the call)

Note: when a proposal only partially addresses the topics, this condition will be reflected in the scoring of this criterion.

- Soundness of concept, and quality of objectives
- Progress beyond the state-of-the-art
- *Quality and effectiveness of the S/T methodology and associated work plan (only stage 2)*

2. Quality and efficiency of the implementation and the management (only stage 2)

- *appropriateness of the management structure and procedures*
- *quality and relevant experience of the individual participants*
- *quality of the consortium as a whole (including complementarity, balance]*
- *appropriateness of the allocation and justification of the resources to be committed (budget, staff, equipment)*

3. Potential impact through the development, dissemination and use of project results

- contribution, at the European and/or international level, to the expected impacts listed in the work programme under relevant topic/activity
- *appropriateness of measures for the dissemination and/or exploitation of project results, and management of intellectual property (only stage 2).*

Proposal marking and thresholds

Stage 1: S&T excellence (4/5) + Impact (3/5) = Minimum 8/10

The evaluation is performed by means of internet. Only two criteria (S&T excellence and Impact) are considered at stage 1 (consortia/budget distribution is not required). The first stage evaluation is essentially about “**GO / NO GO**” decision, no ranking is needed - no pre-defined success rate but only the very best. It is necessary to keep the prescribed range of pages in particular parts of proposal, material submitted beyond the range is not taken into account.

Stage 2: S&T excellence (4/5) + Implementation (3/5) + Impact (3/5) = Minimum 10/15

Consensus

The aim of the consensus process is to achieve a consensus of experts and obtain consistent final evaluation, the comprehensive, concise and clear summary made in accordance with marking. The consensus proceedings are performed by means of internet, phone conferences, electronic forums, individual phone contacts.

Exceptionally, if no consensus is found, it is possible to continue with a majority decision “GO / NO GO”, but the differing views can be recorded in the consensus report.

Expectation of success - in the stage 1 were evaluated ca 30 proposals, to the stage 2 were selected ca 8 proposals.

2. HORIZON 2020

Horizon 2020 is the European Framework Programme supporting research and innovation projects and programmes in ground breaking basic research, strategic and applied research,



demonstration projects and close-to-market activities. Horizon 2020 is subsequent to FP7 and covers the period 2014-2020.

Proposal procedures are similar to FP7, everything will be done electronically via a web-based Participants Portal. The process of evaluation will be also as in FP7 - all eligible proposals will be evaluated independently by at least three experts against the pre-determined evaluation criteria.

The evaluation criteria for proposals are the same as in FP7 - Scientific/Technology Quality, Impact and Implementation.

- 1) S/T Quality: "Scientific and/or technological excellence (relevant to the topics addressed by the call)"
 - soundness of concept, and quality of objectives
 - progress beyond the state-of-the-art
 - quality and effectiveness of the S/T methodology and associated work plan
- 2) Impact: "Potential impact through the development, dissemination and use of project results"
 - contribution, at the European (and/or international] level, to the expected impacts listed in the Work Programme under the relevant topic/activity)
 - appropriateness of measures for the dissemination and/or exploitation of project results and management of intellectual property
- 3) Implementation
 - appropriateness of the management structure and procedures
 - quality and relevant experience of the individual participants
 - quality of the consortium as a whole (including complementarity, balance)
 - appropriateness of the allocation and justification of the resources to be committed (staff, equipment ...)

3. CONCLUSIONS

Knowledge of the evaluated criteria and assessment procedures is very important. Cognition in this field may significantly increase the probability chances to obtain the financial support from the EU funds.

Acknowledgements

This paper was created within the project "**Creation of an international scientific team and incorporation to scientific networks in the area of nanotechnology and unconventional forming material. CZ.1.07/2.3.00/20.0038**", which is financed by the European Social Fund and state budget of the Czech Republic.





esf european
social fund in the
czech republic



EUROPEAN UNION



MINISTRY OF EDUCATION,
YOUTH AND SPORTS



OP Education
for Competitiveness

INVESTMENTS IN EDUCATION DEVELOPMENT

UFG shape memory and magnetic shape memory materials

Wojciech MAZIARZ, Paweł CZAJA, Jan DUTKIEWICZ

*Institute of Metallurgy and Materials Science, Polish Academy of Sciences, 25 Reymonta Str. 30-059
Kraków, Poland*

w.maziaz@imim.pl

Abstract

The paper presents recent results concerning the magnetic shape memory materials based on the Heusler Ni_2MnX structure. Ternary Ni-Mn-Sn and quaternary Ni-Mn-Sn-Al and Ni-Mn-Fe-Sn melt spun ribbons with ultra fine grain are presented. In ternary $\text{Ni}_{50-x}\text{Mn}_{37+x}\text{Sn}_{12.5}$ alloys the effect of Ni/Mn concentration ratio on microstructure and martensitic transformation in the composition range between $0 \leq x \leq 6$ has been investigated. In the quaternary $\text{Ni}_{48}\text{Mn}_{39.5}\text{Sn}_{12.5}\text{Al}_x$ ($x=0, 1, 2, 3$) Heusler alloys ribbons the room temperature magneto-structural transitions were examined as well as effect of Mn substitution for Fe on magnetic and martensitic transformations in $\text{Ni}_{46}\text{Mn}_{41.5-x}\text{Fe}_x\text{Sn}_{12.5}$ ribbons. The several techniques and apparatus like X-Ray diffraction, transmission and scanning electron microscopy (SEM, TEM), differential scanning calorimeter (DSC) and vibrating sample magnetometer (VSM) were applied for this investigations.

Keywords

Magneto-caloric effect, Heusler alloys, rapid solidification, ultra fine grain materials, martensitic transformation, magnetic transformation, microstructure

1. INTRODUCTION

The ferromagnetic Ni-Mn-X ($X = \text{Sn, In, Sb}$) shape memory alloys have attracted attention due to their unique properties resulting from the coupling between magnetic and structural degrees of freedom [1]. With the decreasing temperature these alloys undergo a reversible first order martensitic transformation (MT) from a high symmetry ferromagnetic austenite to a low symmetry and weakly magnetic martensite [2]. In addition the reverse martensitic transformation in these alloys, apart from the temperature, may be induced by magnetic field and hence these alloys are named metamagnetic shape memory alloys [3,4]. These interesting phenomena give rise to several attractive properties such as the shape memory effect, large magnetoresistance and the magnetocaloric effect [5,6]. It has been demonstrated that the high symmetry parent austenite phase typically features the $L2_1$ Heusler structure, whereas the martensite phase may display modulated $10M$, $14M$, $4O$ or non modulated $L1_0$ structure, which is dependent on alloy composition [7,8]. It is established that by changing the composition it is also possible to tune the MT temperature. This is done by changing the amounts of ingredients of alloys or by substituting one element for another [9]. This is ascribed to the fact that MT temperatures are reported to be sensitive to the electron to atom ratio (e/a), which changes with composition, and



is calculated for Ni–Mn–X (X = Sn, In, Sb) alloys as the number of 3d and 4s electrons of transitional metals and the 4s and 4p electrons of the third element [10]. Recently high magnetic entropy changes (DSM) at room temperature and at low field of 2T have been reported in the $\text{Ni}_{50-x}\text{Mn}_{37+x}\text{In}_{13}$ alloy tuned by varying Ni/Mn ratio [11]. It is essentially associated with the occupation of excess Mn atoms at Ni and In sites, which modifies the Mn–Mn exchange interactions and leads to ferromagnetic and antiferromagnetic coupling (FM-AFM). This is of paramount importance from the practical applications point of view, since it advances the search for efficient magnetocaloric materials operating at ambient temperatures [12]. The researches has focused on bulk polycrystalline as well as melt spun ribbons prepared from these materials. The latter have the advantage of faster heat exchange between the working body and the exchange fluid and thus may improve the technical characteristics of a refrigeration unit. This paper provides an overview of the recent achievements in research of the magnetic shape memory materials based on the Heusler Ni_2MnX structure prepared as ultra fine grain materials in the melt spun ribbon form.

2. EXPERIMENTAL PROCEDURE

The alloys with the chemical composition as follow: ternary $\text{Ni}_{50-x}\text{Mn}_{37+x}\text{Sn}_{12.5}$ ($0 \leq x \leq 6$) and quaternary $\text{Ni}_{48}\text{Mn}_{39.5}\text{Sn}_{12.5-x}\text{Al}_x$ ($x=0, 1, 2, 3$) and $\text{Ni}_{46}\text{Mn}_{41.5-x}\text{Fe}_x\text{Sn}_{12.5}$ were cast by induction melting of elements with purity better then 99.9%. Then ingot were homogenized at 1000°C for 6 hours in a vacuum. The rapid solidification trough the melt spinning onto copper wheel rotating at a surface speed of 25 m s⁻¹ was used for production of ribbons. The investigations of microstructure were performed by light (LM), scanning (SEM) and transmission electron microscopy (TEM). The crystallographic structure of samples were examined by X-ray diffraction (XRD) and characteristic temperature of martensitic transformation by differential scanning calorimeter (DSC). Magnetic properties were characterized by use the vibrating sample magnetometer (VSM).

3. RESULTS AND DISSCUSION

3.1 $\text{Ni}_{50-x}\text{Mn}_{37+x}\text{Sn}_{12.5}$ ($0 \leq x \leq 6$) ribbons

Four alloys with varying Ni/Mn ratio have been studied. It has been shown that melt spun ribbons regardless of composition feature heterogeneous microstructure. It consists of a zone of small, equiaxed grains formed on the ribbon side in contact with the rotating wheel. Above this zone another layer of columnar grains is observed.

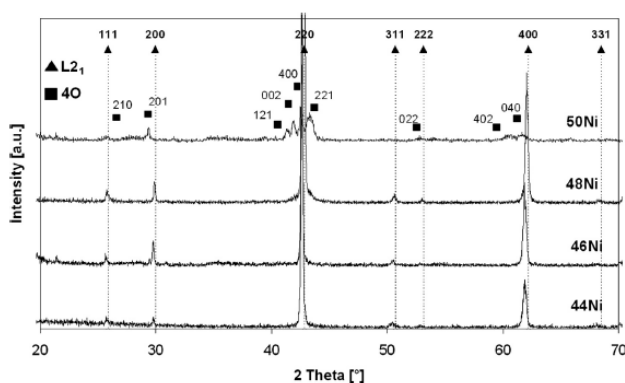


Fig. 1 Set of the XRD patterns of melt spun ribbons recorded at room temperature.



The formation of such a heterogeneous microstructure is related to the heat transfer upon rapid quenching. With respect to structural properties at room temperature the 44Ni and 46Ni ribbons have been shown to contain a single phase, parent L2₁ structure, whereas the 48Ni and 50 Ni ribbons have been demonstrated to be a mixture of austenite, with a typical L2₁ Heusler structure, and martensite whose structure changed in accordance with varying Ni/Mn ratio (Fig. 1). This has been ascribed primarily to the varying e/a ratio, since it is well known that martensite structure is sensitive to composition. The martensite structures have been determined as: five (10M) and four (4O) layered modulated martensites (Fig. 2). Both belong to the orthorhombic symmetry for alloys with the Ni/Mn ratios 1.333 and 1.215 respectively.

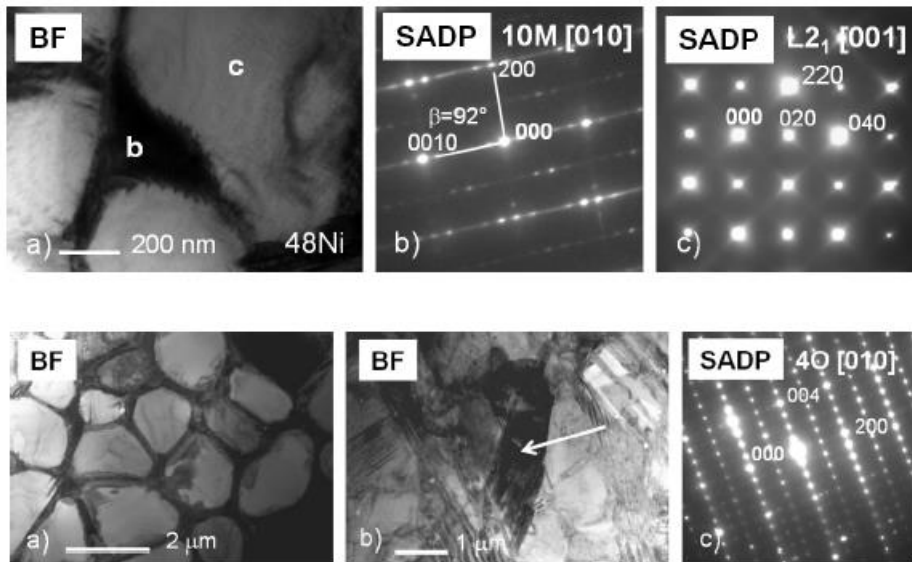


Fig. 2 BF microstructure of 48Ni ribbon (upper) and 50Ni ribbon (bottom) showing two types of martensite at the grain boundaries of L2₁ grains.

It has to be remarked that preferential martensite formation was observed at the grains boundaries and it is related to chemical micro-segregation occurring upon rapid cooling and affecting the composition. Another factor which may contribute to this behaviour is the relaxation of internal stresses. The average grain size of the ribbons as determined by TEM has been estimated at $1.5 \pm 0.5 \mu\text{m}$. It has been also shown that with increasing Ni content the temperatures of martensitic and magnetic transformations, as demonstrated by DSC results (Fig. 3), increase and in the case of Ni50 alloy approach room temperature being close to coincidence. This again is associated with the varying e/a ratio. The transformation temperature increase was coupled with the increase of enthalpy of transformation.

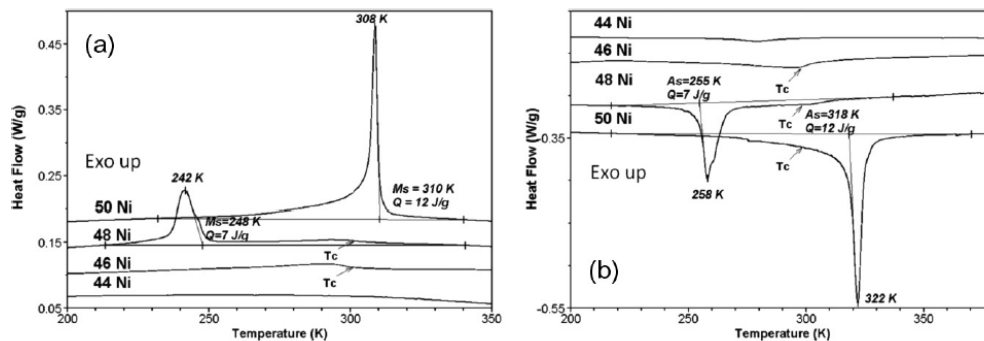


Fig. 3 DSC curves recorded for investigated ribbons during (a) cooling and (b) heating cycles.



3.2 Ni₄₈Mn_{39.5}Sn_{12.5-x}Al_x (x=0, 1, 2, 3) ribbons

The Heusler Ni₄₈Mn_{39.5}Sn_{12.5-x}Al_x (x=0, 1, 2, 3) melt spun ribbons undergo martensitic and reverse transformation between the ferromagnetic austenite phase and the weakly magnetic martensite phase already at room temperature (Table 1).

Table 1 The martensitic transformation temperature (T_{A-M}), the reverse martensitic transformation temperature (T_{M-A}), the width of the ΔT hysteresis ($T_{M-A}-T_{A-M}$), the Curie temperature of martensite T_C^M and the Curie temperature of austenite T_C^A of the studied Ni₄₈Mn_{39.5}Sn_{12.5-x}Al_x ribbons determined by the magnetic measurements at 50 Oe.

x (at%)	T_{A-M} [K]	T_{M-A} [K]	ΔT [K]	T_C^M [K]	T_C^A [K]
0	242	258	16	229	300
1	271	281	10	215	298
2	283	291	8	205	297
3	291	299	8	193	296

The martensitic phase persists at this temperature. The structure of austenite has been determined as the L21 type Heusler structure, which persisted in all the studied samples regardless of Al concentration. The structure of martensite on contrary has been shown to depend on the alloys composition and it was determined as the 10 M martensite with a monoclinic unit cell and with the $(3\bar{2})$ stacking sequence of planes according to the Zhdanov notation in the Al free sample (Fig. 4) and the 4O martensite with the $(3\bar{1})$ periodic stacking of planes in the Al containing samples (Fig. 4). It was confirmed that with increasing Al concentration, despite the decrease in e/a resulting from Al substitution for Sn, the martensite start and the austenite start transformation temperatures increase.

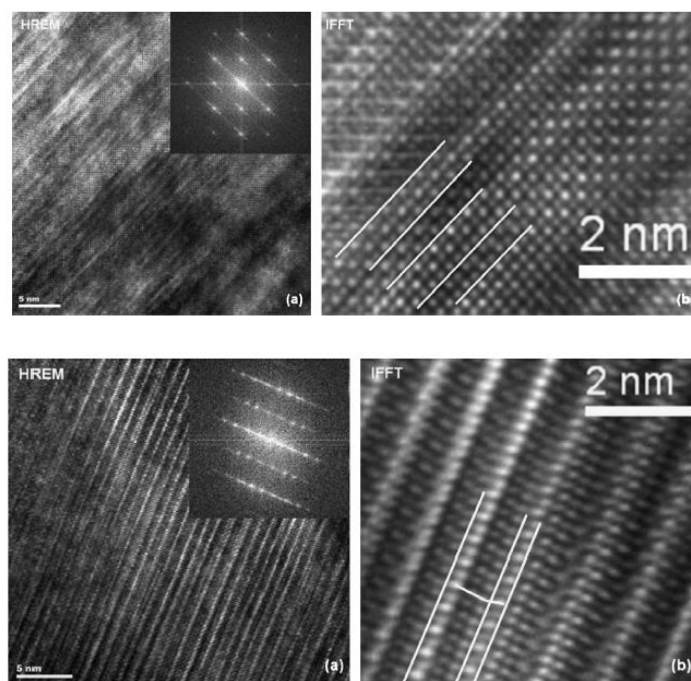


Fig. 4 (upper) Experimental HRTEM image (a) of the 10 M martensite and its corresponding FFT (inset) and IFFT (b) taken at RT from the 0Al Heusler alloy ribbon and (bottom)



experimental HRTEM image (a) of the 4O layered martensite and its corresponding FFT (inset), and IFFT (b) taken at RT from 2Al Heusler alloy ribbon.

This has been primarily attributed to the unit cell volume reduction, since Al has a smaller atomic radii than Sn. Furthermore multistage martensitic transformations were observed; their magnitude depended on Al concentration. These transitions appeared below M_s corresponding to intermartensitic transitions. Simultaneously the Curie temperature of martensite decreases and the Curie temperature of austenite remains practically unaffected by Al substitution. The magnetization difference ΔM across the structural transition decreases with Al incorporation because the magnetization of austenite considerably weakens while the magnetization of martensite does not change much. The effect of Al substitution permits to tune the martensite start temperature, however at the cost of magnetization loss, to the Curie temperature of austenite leading to the coupling between magnetism and structure and making these alloys promising for magnetic refrigeration.

3.3 $\text{Ni}_{46}\text{Mn}_{41.5-x}\text{Fe}_x\text{Sn}_{12.5}$ ($x=0, 2, 4, 6$) ribbons

$\text{Ni}_{46}\text{Mn}_{41.5-x}\text{Fe}_x\text{Sn}_{12.5}$ ($x=0, 2, 4, 6$ in at.%) melt spun ribbons have been studied. The ribbons featured the $L2_1$ Heusler type structure in the parent austenitic phase. With the amount of Fe increasing a formation martensite phase have been observed. The structure of the martensite has been determined as the 10M and its occurrence was due to the different melting points of the constituent elements. The ribbons containing Fe in the range 0-4 at. % displayed similar magnetic behaviour with a distinct hysteresis, whereas the sample denoted as Fe-6 showed the thermo-magnetic curve an initial increase of magnetization with increasing temperature suggesting the Curie transition of austenite and subsequently upon further cooling a sudden drop of magnetization just below the T_C^A was observed indicating the martensitic transition. This suggests that at this composition the Curie temperature and structural transformation temperature appear in close proximity. Marginal hysteretic splitting has been recorded for this alloy composition. Based on the literature data and on the obtained results e/a ranges have been determined for Fe, where it acts to increase or decrease M_s (Fig. 5). This will facilitate the selection of future alloys compositions.

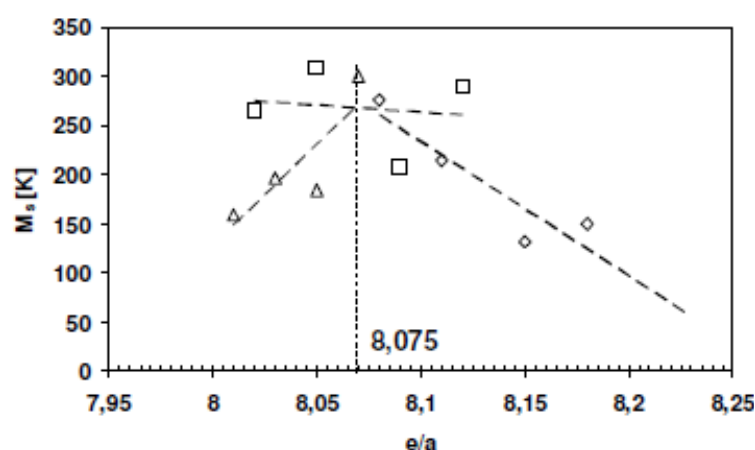


Fig. 5 Relationship of M_s temperature as a function of e/a for Ni-Mn-Sn alloys doped by Fe.

4. SUMMARY

The paper presents recent results concerning the magnetic shape memory materials based on the Heusler Ni_2MnX structure. Ternary Ni-Mn-Sn and quaternary Ni-Mn-Sn-Al and Ni-Mn-Fe-Sn



melt spun ribbons with ultra fine grain of size of about 1 μm are presented. In ternary $\text{Ni}_{50-x}\text{Mn}_{37+x}\text{Sn}_{12.5}$ alloys the effect of Ni/Mn concentration ratio on microstructure and martensitic transformation in the composition range between $0 \leq x \leq 6$ has been investigated. With respect to structural properties at room temperature the 44Ni and 46Ni ribbons have been shown to contain a single phase, parent L2_1 structure, whereas the 48Ni and 50Ni ribbons have been demonstrated to be a mixture of austenite and martensite whose structure changed in accordance with varying Ni/Mn ratio. In the quaternary $\text{Ni}_{48}\text{Mn}_{39.5}\text{Sn}_{12.5-x}\text{Al}_x$ ($x=0, 1, 2, 3$) Huesler alloys ribbons the room temperature magneto-structural transitions were examined as well as effect of Mn substitution for Fe on magnetic and martensitic transformations in $\text{Ni}_{46}\text{Mn}_{41.5-x}\text{Fe}_x\text{Sn}_{12.5}$ ribbons. It was confirmed that with increasing Al concentration, despite the decrease in e/a resulting from Al substitution for Sn, the martensite start and the austenite start transformation temperatures increase. With the amount of Fe increasing a formation martensite phase have been observed. The structure of the martensite has been determined as the 10M and its occurrence was due to the different melting points of the constituent elements. The ribbons containing Fe in the range 0-4 at. % displayed similar magnetic behavior with a distinct hysteresis, whereas the sample denoted as Fe-6 showed the thermomagnetic curve an initial increase of magnetization with increasing temperature suggesting the Curie transition of austenite and subsequently upon further cooling a sudden drop of magnetization just below the austenite Curie temperature was observed indicating the martensitic transition.

Literature

- [1] J. Liu, T. Gottschall, K.P. Skokov, J.D. Moore, O. Gutfleisch, *Nat. Mater* 11 (2012) 620–626.
- [2] Y. Sutou, Y. Imano, N. Koeda, T. Omori, R. Kainuma, K. Ishida, K. Oikawa, *Appl. Phys. Lett.* 85 (2004) 4358–4360.
- [3] V.A. Chernenko, J.M. Barandiaran, J. Rodriguez Fernandez, D.P. Rojas, J. Gutierrez, P. Lazpita, I. Orue, *J. Magn. Magn. Mater.* 324 (2012) 3519–3523.
- [4] R. Kainuma, Y. Imano, W. Ito, Y. Sutou, H. Morito, S. Okamoto, O. Kitakami, K. Oikawa, A. Fujita, T. Kanomata, K. Ishida, *Nature* 439 (2006) 957–960.
- [5] A. Planes, Ll. Manosa, X. Moya, T. Krenke, M. Acet, E.F. Wassermann, *J. Magn. Magn. Mater.* 310 (2007) 2767–2769.
- [6] K.A. Gschneidner Jr., *Acta Mater* 57 (2009) 18–28.
- [7] W. Maziarz, *Solid State Phenomena* 186 (2012) 251–254.
- [8] X. Moya, Ll. Manosa, A. Planes, T. Krenke, M. Acet, E.F. Wassermann, *Mater. Sci. Eng. A* 438–440 (2006) 911–915.
- [9] W. Maziarz, P. Czaja, M. Faryna, T. Czeppe, A. Góral, J. Dutkiewicz, *Solid State Phenomena* 203–204 (2013) 232–235.
- [10] R.L. Wang, J.B. Yan, H.B. Xiao, L.S. Xu, V.V. Marchenkov, L.F. Xu, C.P. Yang, *J. Alloys Comp.* 509 (2011) 6834–6837.
- [11] N.V. Rama Rao, V. Chandrasekaran, K.G. Suresh, *J. Appl. Phys.* 108 (2010) 043913.
- [12] E. Bruck, O. Tegus, D.T.C. Thanh, K.H.J. Buschow, *J. Magn. Magn. Mater.* 310 (2007) 2793–2799.

Acknowledgements

This paper was created within the project "**Creation of an international scientific team and incorporation to scientific networks in the area of nanotechnology and unconventional forming material. CZ.1.07/2.3.00/20.0038**", which is financed by the European Social Fund and state budget of the Czech Republic.





esf european
social fund in the
czech republic



EUROPEAN UNION



MINISTRY OF EDUCATION,
YOUTH AND SPORTS



OP Education
for Competitiveness

INVESTMENTS IN EDUCATION DEVELOPMENT

Influence of grain structure, texture and precipitation on properties of Aluminium heat treatable alloys after inhomogeneous plastic deformation

Vladivoj OČENÁŠEK

SVÚM a.s., Podnikatelská 565, 190 11 Prague 9 – Běchovice, Czech Republic, ocenasek@svum.cz

Abstract

Various types of structures differing in work-hardening state, recovery, recrystallization, and grain- and subgrain orientation and dimensions are formed during plastic deformation. These structures depend on deformation temperature, intensity and inhomogeneity. When precipitation occurs in these structures, mechanical and fatigue properties will be changed in dependence on the type of structure. In many cases, mechanical and fatigue properties become inhomogeneous, their values differ substantially in different directions i.e., on the orientation of test piece. These effects are typical for hardenable Al alloys and are not quite understood as yet. Inhomogeneity and anisotropy of structure and properties are relatively well described in industrial applications (extrusion, forging, rolling); on the other hand, in case of a severe plastic deformation, during which a quite specific wrought structure is formed, that information completely lack for the time being. „Interaction“ between grains- and subgrains structure (size, orientation, dislocation density) and precipitation of hardening phases seems to be an interesting topic that could contribute to a better understanding of these processes and their exploitation in obtaining the structures with extraordinary properties.

Keywords

Hot extrusion, inhomogeneity, precipitation, grain structure, properties, heat treatable aluminium alloys

1. INTRODUCTION

The inhomogeneity and especially the anisotropy of the properties of aluminium alloy products has been the subject of intensive interest. Usually the anisotropy of sheet materials is evaluated, whereas the inhomogeneity of properties is studied in forged and extruded products. The investigations usually concern the evaluation of the texture and its effect on properties [1, 2, 3 and 4]. Recrystallization textures and deformation textures are studied in sheets and in forgings and extrusions, respectively. The recently developed methods for local texture measurement are a great contribution for the actual studies of inhomogeneity and anisotropy [5, 6]. The heterogeneous and anisotropic properties of forgings and extrusions have not been studied with the same intensity as the inhomogeneity of rolled sheets. It is a generally known fact that the inhomogeneity and anisotropy of hot extruded or forged products is connected with the presence of certain textures. Depending on the nature of material flow during the hot



forming process, certain mixed textures form at different positions of extrusion cross-section and they affect both the anisotropy and the level and scatter of properties. Maximum yield stress and strength values and also their marked anisotropy are connected with the presence of the double fibre texture $\langle 111 \rangle + \langle 100 \rangle$. This texture is found in the centre of extruded circular sections. Minimum values are observed in connection with textures similar to rolling textures and their occurrence is typical for extrusions with flat parts such as L- or T-shape profiles [2, 7, and 8]. The rate of inhomogeneity and anisotropy are affected by several factors. The type of alloy, the forming method and the thermo-mechanical treatment are the most important among them [7-10]. This paper presents results which allow us to quantify the effect of critical factors on the inhomogeneity and anisotropy of properties of extrusions from 2xxx, 5xxx and 8xxx series aluminium alloys.

2. EXPERIMENTAL

Several alloys and extruded shape (Fig. 1) were used as experimental material. Extrusions from high strength hardenable alloys were of principal interest. The alloys used and their composition are in Tab.1.

The inhomogeneity and anisotropy of model extrusion were evaluated. The shape of model extrusions was chosen considering the results of properties study of industrial extrusions. The shape was designed to contain the textures which represent extreme cases from the point of view of their effect on the level of mechanical properties, i.e. the double fibre texture $\langle 111 \rangle + \langle 100 \rangle$ (circular part of cross-sections) and rolling texture (flat part). At the same time, the shape was chosen in such a way that it allowed the evaluation of both the inhomogeneity of longitudinal properties and their anisotropy. Both tensile and fatigue properties were studied. The shape, dimensions and characteristics of the individual products are given below together with the presentation of results.

Table 1 Composition of the alloys used (in wt. %).

Alloy / Element	Designation	Cu	Mg	Mn	Li	Si	Fe	Zr
AlCuLi	1450 (2090)	2.59	0.04	-	2.05	0.02	0.09	0.11
AlLiCuMg	1441 (8090)	1.71	0.99		1.81	0.03	0.08	0.06
AlCuMg	2124	4.02	1.36	0.71	-	0.19	0.21	-
AlMg2	5251	0.012	1.89	0.20	-	0.092	0.13	-

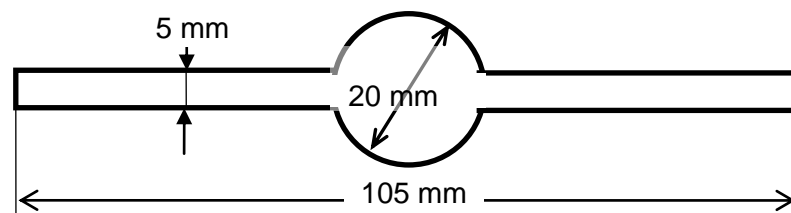


Fig. 1 Studied extruded experimental shape



3. RESULTS AND DISCUSSION

The factors affecting the inhomogeneity and anisotropy of properties of aluminium products are fairly diverse and numerous, so only the most important factors have been selected for this presentation. The evaluation and quantification of the effect of several technological factors cannot be done separately for every factor but their interaction must be taken into account.

Due to the complicated material flow in the die the systematic evaluation of heterogeneous and anisotropic structure and properties occurring in die forgings is difficult. In the case of sheets and extrusions the situation is simpler because the direction of deformation can be easily determined and thus the specimens can be oriented unambiguously. The results can then be related to different positions on product cross-section and the variation of properties along strip or extrusion length can be neglected.

The evaluation of the microstructure and properties of large extrusion indicated that property inhomogeneity increases with increasing complexity of extrusion cross-section [2, 8, 9, and 10]. It was also found that the longitudinal properties are significantly heterogeneous even in simple circular or rectangular cross-sections, and that these heterogeneities are characteristic of each cross-section type. The local differences of R_m can be up to 60 MPa. In extrusions of more complex shape these differences can be up to 120 MPa [9, 10]. The inhomogeneity of microstructure affects the values of yield stress $R_{p0,2}$ even more markedly and differences from 130 to 150 MPa can be observed (Fig. 2). The heterogeneities of longitudinal tensile properties described above were found in high strength hardenable alloys with non-recrystallized microstructure.

The level of property inhomogeneity and anisotropy depends also on alloy type - hardenable and non-hardenable alloys behave in a different way. As can be seen from Fig.2, in spite of the fact that the different hardenable alloys have a different strength level, their inhomogeneity has similar character through the cross section of the shape. This result indicates that in all studied alloys the nature of precipitation (size, shape and orientation of precipitates) in every position of the cross-section is similar. On the other hand, the non-hardenable alloy AlMg2 exhibits very low inhomogeneity, comparable with the overaged condition of 2124-O alloy. Therefore, the hardenable alloys in the overaged condition and the non-hardenable alloys have very similar (low) property inhomogeneity - the level, scatter and anisotropy of properties are determined by the structure of the aluminium matrix.

The assessment of property values in the two main directions L and T (parallel and perpendicular resp. to the direction of extrusion) is not sufficient for the characterization of material anisotropy. Fig. 3 presents the distribution of R_m values for several orientations to the direction of extrusion in the model shape from the alloy 2124 (see Fig.2). The largest difference is found between the orientations 45° and 0° (L) with a value of 160 MPa. The microstructure of the material was unrecrystallized.



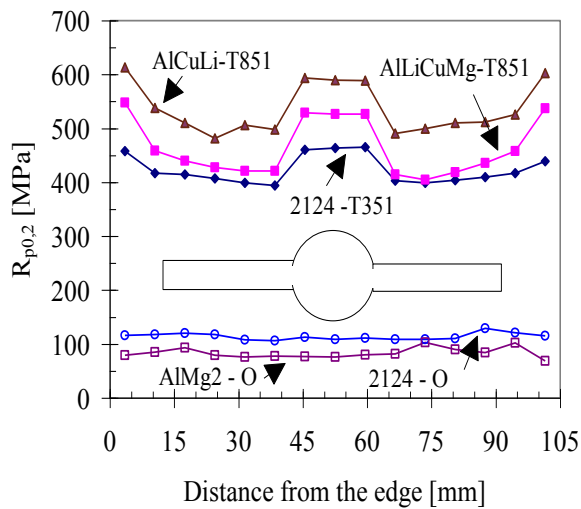


Fig. 2 Influence of alloy type and temper on $R_{p0,2}$ inhomogeneity for a model shape

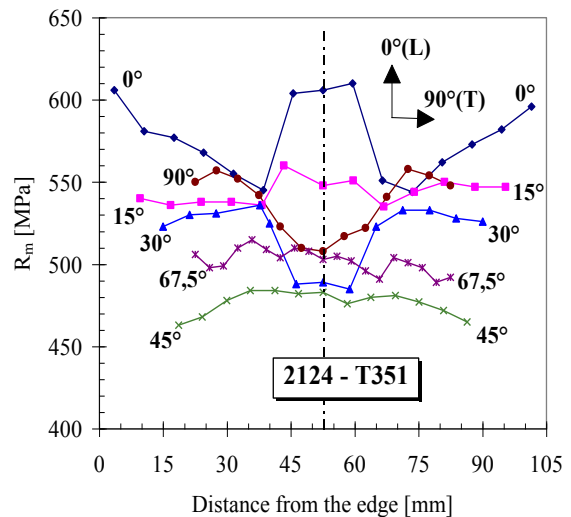


Fig. 3 Properties anisotropy: distribution of R_m values for different orientations in the model shape 2124-T351 shown in Fig.1.

The effect of recrystallization on the level, inhomogeneity and anisotropy of properties of aluminum alloy products is also very important. A distinction must be made between the recrystallization of cold deformed products such as drawn tubes or rolled sheet and extrusions. The microstructure of tubes and sheets is usually relatively homogeneous, fine grained and textured. Sheets exhibit anisotropic, but homogeneous, tensile properties through their width. The impact of recrystallization on the properties of hot extruded products is rather different. Highly heterogeneous coarse-grained microstructure may be developed during thermomechanical heat treatment. This unacceptable microstructure has detrimental effect on properties. The existence of a sharp boundary between unrecrystallized and recrystallized structure is connected with a severe decrease of tensile properties in L-direction. The decrease of strength is up to 150 MPa, in extreme cases it can be even 200 MPa. At this boundary anisotropy changes too (Fig.4).

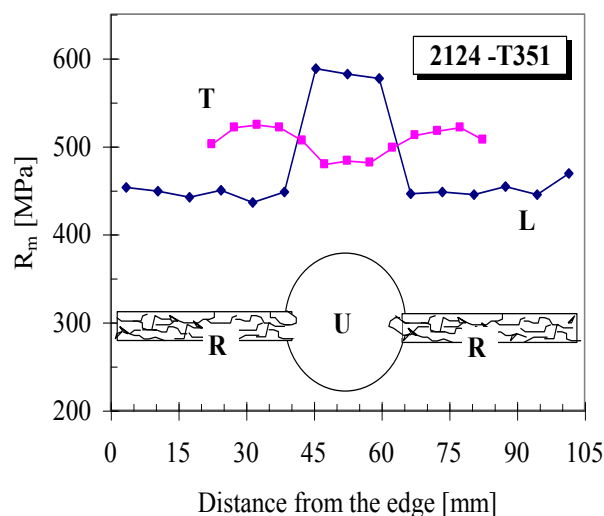


Fig. 4 Influence of recrystallization on R_m anisotropy and inhomogeneity for L- and T-orientations in a model shape 2124-T351



4. CONCLUSIONS

The results of the investigation of heterogeneous and anisotropic properties of aluminum alloys can be summarized in the following conclusions:

- 1) The inhomogeneity and anisotropy of every alloy type and product reflect the microstructure formed during the down-stream technological process of their fabrication. The inhomogeneity and anisotropy result from heterogeneous material flow.
- 2) The differences in properties through extrusion cross-section are not random but are controlled by several well defined rules. There are typical positions in every shape, where minimum (or maximum) values of mechanical properties are usually measured.
- 3) The property inhomogeneity and anisotropy is determined mainly by the texture of the aluminum matrix, the level of solid solution decomposition and the type of matrix softening.
- 4) Softening to O-temper results in an important decrease of inhomogeneity, whereas repeated solution annealing and aging evoke inhomogeneity again.
- 5) The co-existence of recrystallized and unrecrystallized microstructure results both in the important inhomogeneity of the properties in L-direction and in outstanding local gradients in the anisotropic behavior. The local differences of tensile properties in some specific directions can reach values up to 200 MPa.

5. LITERATURE

- [1] E.Hirosawa, J.of the Inst.of Metals, 92 (1963-64) 78-81.
- [2] G.Tempus, W.Calles, G.Schorf, Mat. Sci. and Techn. 7 (1991) 937 - 940.
- [3] W.Tilch, K.H.Matucha, P.Winclerz, Z.Metallkde, 73 (1982) 473-482.
- [4] J.R.Hirsch, M.D.Crowley, Textures and Microstructures, 14 -18, (1991) 133-138.
- [5] N.J.Kim, E.W.Lee, Acta metall.materi., Vol.41, 3 (1993) 941-948.
- [6] H.Klein, H.J.Bunge, Z.Metallkde, 90 (1999) 103-110.
- [7] I.G.Palmer, R.E.Lewis, D.D.Crooks, Aluminum Lithium Alloys, TMS-AIME, Warrendale, PA, 1981, p.241.
- [8] V.Očenášek, K.Šperlink, J.N.Fridlyander, L.N.Leshiner, Aluminium Alloys, Proc. of ICAA-5, Grenoble, France, 1996, p. 1349.
- [9] V.Očenášek, V.Sedláček, M. Slámová, K.Šperlink, Thermomechanical Processing in Theory, Modelling and Practise, Proc. of [TMP]2, Stockholm, Sweden, 1996, p.277.
- [10] V.Očenášek, K.Šperlink, P.Zuna, K.Macek, Aluminium Alloys, Proc. of ICAA-6, Toyohashi, Japan, 1998, p.1313.

..

Acknowledgements

This paper was created within the project "**Creation of an international scientific team and incorporation to scientific networks in the area of nanotechnology and unconventional forming material. CZ.1.07/2.3.00/20.0038**", which is financed by the European Social Fund and state budget of the Czech Republic.





esf european
social fund in the
czech republic



EUROPEAN UNION



MINISTRY OF EDUCATION,
YOUTH AND SPORTS



OP Education
for Competitiveness

INVESTMENTS IN EDUCATION DEVELOPMENT

Possibilities of Utilization of Light Metals in the SPD Process

Stanislav RUSZ^a, Lubomír Čížek^a, Jan KEDROŇ^a, Stanislav TYLŠAR^a, Michal Salajka^a

^a VSB – Technical university of Ostrava, 17. Listopadu 15, CZ 708 33 Ostrava – Poruba, Czech Republic,
stanislav.rusz@vsb.cz

Abstract

Currently, technological progress in many modern industries requires in implementation of new types of technical materials and related development of new manufacturing technologies that bring both enhancement of service properties of final products, as well as their wider implementation into engineering practice, including the associated energy savings. One possibility is also a constant increasing of consumption of light metals. Sustainable development of human society is subject to a maximum economy of non-renewable sources of energy and raw materials, especially metallic ones. One of the ways for achieving this goal, in addition to recycling waste alloys based on aluminium, copper, magnesium, brass ect. is systematic reduction of their consumption by increasing their quality and service life of utility objects and structures made from them. Already for many years, this happens in metallurgical production for example by alloying or by heat treatment. One of the ways to the more effective use of metallic materials is their processing by forming. At present in this the area the use of the process of multiple severe plastic deformation (SPD process), leading to a refinement of the structure (materials with UFG structure) and thus to achievement of higher level of their utility value, is expanding.

Keywords

SPD process, light metals, grain refinement, mechanical properties, structure

1. INTRODUCTION

High deformation at comparatively low homologous temperatures is an efficient method for manufacture of ultrafine grained (UFG) massive materials [1-3]. New technologies, which use high deformation for obtaining the fine-grained structure, are described namely by the following authors [4-6].

Models of ultra fine-grained (nano-crystalline) materials are defined as two-phase composites describing their mechanical properties by the so called rule of mixtures

Yield point is in these materials defined as a proportion of the yield point of the phase in the grain interior and the phase of its edges, which is heavily dependent on the volume fraction of the grain boundary. It is assumed that the yield point of the grain boundary phase is lower than that of the grain interior phase.



Basic theoretical model for nano-structural materials formation:

- Masumura's theoretical model
- Carsley's theoretical model
- Kim's theoretical model
- Ovidko's theoretical model Chokshi's theoretical model

The process of plastic deformation, which leads to a refinement of the structure, depends on several factors. The following factors are involved: the structure before deformation (grain size, microstructure), the second phase particles, strain rate and temperature of deformation, magnitude of deformation, the route of deformation [1,2].

Mechanisms of grain refinement vary depending on the magnitude of deformation divided the influence of the magnitude of an increase of deformation into four areas.

This concerns evaluation of results achieved during deformation of metals with cubic face-centred lattice ECAP (ECAP-principle – see below at description of the proposed project), using the deformation route BC: small strain intensity ($\epsilon_{VM} < 2$), small to moderate strain intensity ($\epsilon_{VM} = 2 - 4$), moderate to high strain intensity ($\epsilon_{VM} = 4 - 6$), extreme strain intensity – SPD ($\epsilon_{VM} > 6$).

Microstructure formed by SPD methods is usually unstable and grain growth and recrystallization can occur at the temperatures lower than $0.3 T_m$

Foreign elements in solid solution can have a beneficial effect by reducing both dynamic and thermal recovery, thereby increasing the strength at ambient temperature and the thermal stability of microstructure at elevated temperatures (Cheng Xu, Kenong Xi, Terence G. Langdon)

Several types of SPD technologies serving for production of UFG metals were developed already at the beginning of the nineties:

This research concerned the whole production of UFG materials using the ECAP and DRECE technology.

2. EXPERIMENTAL PROCEDURES AND MATERIALS

The ECAP technology – Equal Channel Angular Pressing, belongs to technologies of accelerated development and represents top items of severe plastic deformation methods to reach ultra-fine granularity structure. Fig. 1 shows a principle of ECAP.

One of them is new type of equipment called DRECE (Dual Rolling Equal Channel Extrusion), designated for obtaining UFG structure in a strip of sheet. Fig. 2 shows a principle of DRECE. Equipment DRECE is based on process CONFORM, modified for sheet forming.

The prototypes of this equipments were established at the VSB - Technical university of Ostrava. Figs. 3 and 4 show overall view of the prototype of these equipments.

Used ECAP and DRECE process belongs to the group of a progressive type of forming processes making use of severe plastic deformation (SPD). The SPD methods make it possible to process suitable materials to achieve ultrafine grained structure (UFG) with mean grain size of $1\mu m$. After this processing the materials exhibit – in comparison with conventional structure materials – significantly higher mechanical values – especially yield strength, and in limited



extent also ultimate tensile strength. Forming process DRECE is an extrusion technology with limited cross-sectional reduction to achieve high degree of deformation of suitable selected material.

New materials prepared for application of SPD processes

In the case of the first ECAP processing the aluminum alloys and magnesium alloys AZ31, Mg-Zr and WE43 were used. For the future AZ61, AZ80 and Mg-Li alloys were prepared. For ECAP processing solid solution heat treatment –T4 after ASTM of magnesium alloys must be used:

B1-TH1 – pre-heating 375 °C/3 hours + 415 °C/18 hours air cooling,

B2-TH2 – pre-heating 375 °C/3 hours + 415 °C/18 hours, water cooling

Microstructure of these alloys in initial state is shown in Figs. 5-8.

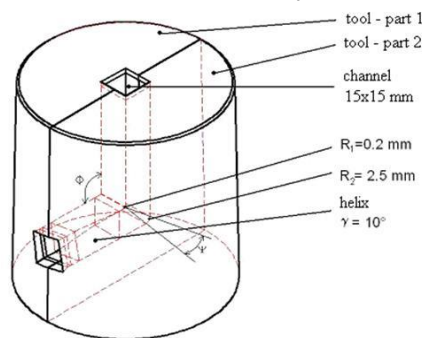


Fig. 1 Principle of ECAP process

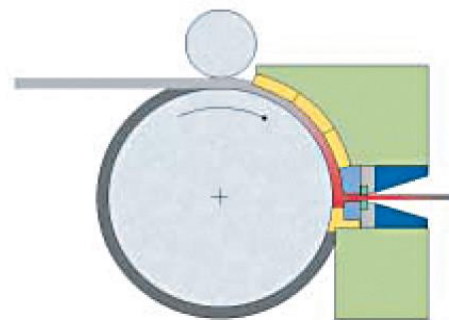


Fig. 2 Principle of DRECE process



a) Working site



b) Control system



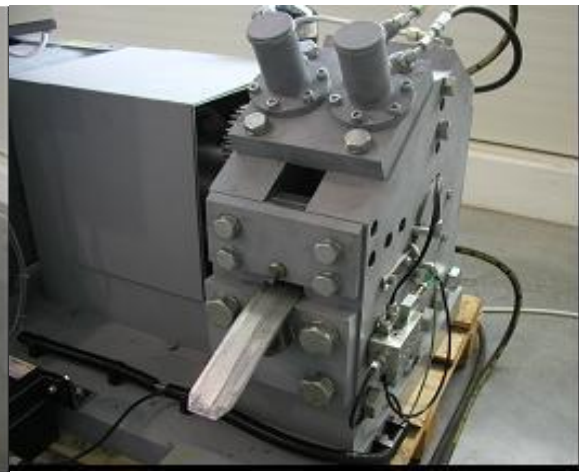
c) Detail of the forming tool with reheating sleeve

Fig. 3 The equipment ECAP





a) working site



b) The detail of the equipment DRECE

Fig. 4 The equipment DRECE

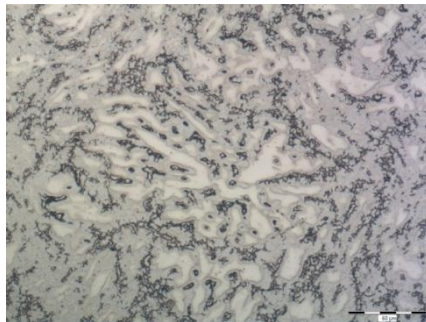


Fig. 5 Microstructure of AZ61



Fig. 6 Microstructure of AZ80

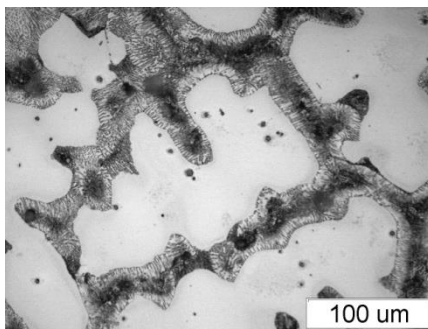


Fig. 7 Microstructure of Mg-4%Li

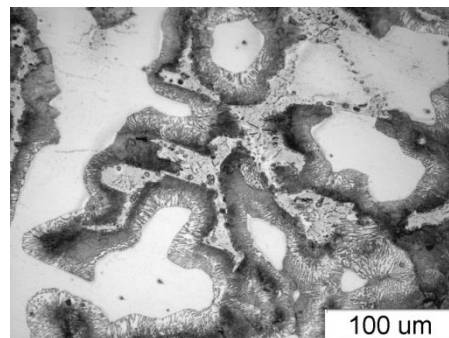


Fig. 8 Microstructure of Mg-7,5%Li

Microstructure in initial as cast state of sample AZ61 and AZ 80 is formed by crystals of matrix on the basis of magnesium, surrounded by minority massive phase of the type $Mg_{17}Al_{12}$ in almost continuous formations in interdendritic areas along grain boundary, which represent places of initiation and propagation of failure at tensile test (Figs. 5 and 6).

Microstructure of used magnesium – lithium alloys are showed in Figs. 7 and 8. The Fig. 7 shows magnesium alloys with 4% Li and the Fig. 8 with 7,5% Li. Alloy containing 4% Li is characterized with one phase microstructure built of solid solution of lithium in magnesium with hexagonal structure and alloy containing 7.5% Li is characterized with two-phase microstructure built of solid solution of lithium in magnesium with hexagonal structure and magnesium in



lithium with regular body-centered structure. The eutectic area E with complex intermetallic phases is present. For detail phases description the SEM analysis will be used.

3. RESULTS AND EVALUATION OF CARBON STEEL BY DRECE PROCESSING

Carbon steel as cold rolled state, without previous heat treatment, in chemical purity corresponding to the relevant Czech standard ČSN 41 1321 was used for investigation in the form of sheet with dimensions 48x2x1000 mm. Chemical composition of investigated steel is given in Tab. 1. Strip of sheet form carbon steel was extruded through the DRECE equipment.

Table 1 Chemical composition (in wt %)

C	Mn	P	S
0.10	0.43	0.03	0.03

Experimental materials have been formed by DRECE process at ambient temperature, without previous heat treatment and operative heating after individual passes. The sheets were rotated by 180° around longitudinal axes between individual passes.

Realised number of passes low carbon steel: 2x - 4x - 6x passes through the DRECE equipment.

Hardness HV10 and mechanical properties (proof stress $R_{p0.2}$, ultimate strength R_m and ductility A_{80}) after tensile test was evaluated in initial state and after application of the DRECE process. Investigation was completed by metallographic evaluation of microstructure of selected samples (see Table 2 and 3).

Table 2 Obtained hardness values

Number of passes	Hardness HV 10 (average value)
Initial state	93
2	122
4	135
6	136

Table 3 Obtained results of mechanical properties of the strip of sheet from low carbon steel grade

Number of passes	$R_{p0.2}$ [MPa]	R_m [MPa]	A_{80mm} [%]
initial state	173	311	38,3
2x	370	391	22,6
4x	383	411	15,8
6x	390	415	14,8

The obtained results of experimental verification of structure refining by DRECE process have confirmed suitability of this technology for production of UFG structure in low-carbon steel, which leads to substantial increase of mechanical properties. Substantial increase of proof stress $R_{p0.2}$ and ultimate strength R_m was achieved, which opens up much broader



possibilities of its use for manufacture of high strength machine components (value of the given steel grade is increased).

4. SUGGESTION FOR NEW POSSIBLE INTERNATIONAL PROJECTS

The main objective of the current project "Creation of an international scientific team and participation in scientific networks in nanotechnology and unconventional forming" is to create a scientific research Nanotým VŠB-TU Ostrava. This project connects to international networks and will be under the help of foreign experts and partners prepare for application of international scientific projects.

Long-lasting contacts between scientists and educators from the VŠB - TU Ostrava with top experts in the field from both academic and research and development institutions in Czech Republic and abroad multiplied by intensive collaboration within the solved project create a very good basis for meeting the objectives of the project. Within the frame of this project overviews of several prospective European projects were prepared that could help the development of the team being prepared. For the basic approach several projects of the Seventh Framework Programme for support research and development (FP7) were selected, namely the projects COST, KONTAKT, EUREKA, INGO, INTERNATIONAL VISEGRAD FUND (IVF), EUROSTARS 2, HORIZON and CEEPUS. In terms of participation in the above projects an opportunity appeared to use the experience of past years gained at the organization of the project CEEPUS (CEEPUS III) and the International Visegrad Fund (IVF). Help from the PAV Krakow at the preparation of the project of MARIA CURIE also appears to be very promising.

5. REFERENCES

- [1] Gutkin, M.Yu., Ovidko, I.A. and Pande, C.S. Theoretical models of plastic deformation processes in nanocrystalline materials, *Reviews on Advanced Materials Science*, September 2001, vol. 2, p. 80 – 102.
- [2] Kobayashi, M. at all. Research and Development of Superplastic Materials „Recent Progresses and Future Prospects“, *Metallurgical Transactions* 18A, 1987, p. 685-695.
- [3] Rusz, S., Čížek, L., Klos, M. Modelling of severe plastic deformation at ECAP technology process, In.:12th International Research/Expert Conference, "Trends in the Development of Machinery and Associated Technology", TMT 2006, Istanbul, Turkey, 26-30 August, p. 1249-1252.
- [4] Valiev, R. Recent developments of severe plastic deformations techniques for processing bulk nanostructured materials, *Materials Science Forum A* 579 (2008) p. 1–14.
- [5] Michenka, V., Gottwald, M., Malaník, K., Rusz, S. Research of influence of extreme deformation conditions on metal sub-microstructure and development of testing methods for evaluation of their technological properties, In. Conference proceeding METAL 2009, TANGER, May 2009, p. 1-9 (CD).
- [6] Rusz, S., Malaník, K., Donič, T., Kedroň, J., Tylšar, S., Salajka, M. Development of Structure at Extrusion of a Strip of Sheet Made of Cu through the DRECE Machinery. *Journal of Materials Science and Engineering A*, November 2011, pp. 844-848. ISSN 2161-6213.

Acknowledgments

The authors would like to acknowledge gratefully the Ministry of Education, Youth and sports of Czech Republic for its support to the project "Creation of an international team of scientist and participation in scientific networks in the sphere of nanotechnology and unconventional forming metal", CZ.1.07/2.3.00/20.0038.





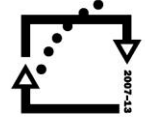
europa
social fund in the
czech republic



EUROPEAN UNION



MINISTRY OF EDUCATION,
YOUTH AND SPORTS



OP Education
for Competitiveness

INVESTMENTS IN EDUCATION DEVELOPMENT

Vacuum surface treatment of heat treated cast light alloys

T. Tański^{a,*}, K. Labisz

^a Division of Materials Processing Technology, Management, and Computer Techniques in Materials Science,

Institute of Engineering Materials and Biomaterials, Silesian University of Technology, ul. Konarskiego 18a,

44-100 Gliwice, Poland

*Corresponding author. E-mail address: tomasz.tanski@polsl.pl

Abstract

In this paper there are presented investigation results concerning surface treatment of Mg-Al-Zn, Al-Si-Cu magnesium and aluminium alloys. In the present work, the emphasis is set on current practices and future trends for nanocomposite thin films and coatings deposited by physical vapour deposition (PVD). The presented results reveals the characteristics of surface treatment as well as the structure and properties of magnesium and aluminium cast alloys, used as constructional materials. The surface treatment of the these alloys was carried out with the use of physical deposition methods, especially the CAE PVD. The results confirms, that the performed standard heat treatment, consisting of solution heat treatment with cooling in water, as well aging with cooling in air, causes strengthening of the MCMgAl9Zn1, MCMgAl6Zn1, AlSi9Cu and AlSi9Cu4 alloy according to the precipitation strengthening mechanism, induced by inhibition of dislocation movement due to the influence of strain fields of the homogeny distributed phase Mg₁₇Al₁₂ as well as Al₂Cu precipitates. The combination of properly chosen heat treatment with the possibilities of structure- and phase composition the PVD vacuum method ensures an additive increase of mechanical and functional properties by significant grain refinement as well as a gradient micro-composite multilayer coating deposited on the material surface. In conventional bulk materials, refining grain size is one of the possibilities for hardness increase. The same is true for nanocomposite films or coatings. It was confirmed in this paper to obtain coating materials with high hardness, higher than the hardness of traditional polycrystalline coatings.

Keywords: Manufacturing and processing; PVD coatings; Light alloys, Heat treatment; Structure; Surface

1. Introduction

The reason of this paper is to present the effect of heat treatment and surface treatment on properties of the cast Mg-Al-Zn and Al-Si-Cu alloys, based on the investigation results published over the last few years. In these works there are presented in detail the research methodology, as well as technical details related to the realised technological processes of heat and surface treatment, as well as chemical composition data of the applied engineering materials. The presented work makes it purposeful to carried out research concerning laser treatment as well coatings technology with appliance of the physical vapour deposition PVD on cast magnesium and aluminium alloys, as one of the fastest growing areas of surface engineering of light metal alloys. To meet the new requirements set by present users and in line with the current tendencies to eliminate technologies that contaminate natural environment, some universal solutions have been searched for, ones that combine inexpensive, light metal alloys and the best possible properties with appropriately selected technology of its surface processing. The gain of simultaneous development of both production

technologies and processing of light materials, including in particular light alloys and technologies of formation and protection of their surfaces, also seem to be the key issue here, which in consequence shall enable the maintenance of balance between the modern base material and new generation coating [1-5].

The generally available reference studies concerning magnesium and aluminium alloys, as well as the annual conferences and symposiums on the production and processing of light materials indicate that magnesium alloys find a more and more extensive circle of followers, both among the manufacturers and users.

Magnesium and aluminium alloys that have been used in various branches of industry for a long time are characterised with combination of low density and high strength. The tendency of contemporary designers to create possibly the lightest vehicles and, in consequence, with possibly the lowest fuel consumption, contributed to the use of light alloys as the structural material for car wheels, engine pistons, housing of transmission gear and clutch, sunroofs and structures of doors, pedals, suction conduits, collectors, housings of drive shafts, differential gears, cantilevers,

radiators and other. The progress that has been made lately in the scope of production and surface engineering of light materials allows for the effective improvement of both the matrix and top layer of the Mg/Al alloys [6-11].

Global tendencies of production of top layers of light materials mainly focus on learning and improvement of the knowledge of the scope of obtaining and depositing coatings with the use of laser beam and physical and chemical vapour deposition techniques. Similarly, deposition of coatings using PVD methods is one of the most efficient methods of coating production providing the option of forming the aesthetic values, in addition to the usable features required, with the undeniable ecological aspect – non-

waste technology meeting clean production requirements[20-26].

2. Investigation procedure

The investigations have been carried out on test pieces of magnesium and aluminium alloys (Table 1). The produced coating was produced by CEA CVD process (Table 2). The substrates were cleaned by argon ion at the pressure 2 Pa for 20 min in bias voltage reaching even 100 V. To improve the adhesion of coatings, a transition Ti interlayer was deposited. The obtained coatings were deposited using argon and nitrogen (N₂) as precursor.

Table 1 Chemical composition of investigated alloys, %

Type of material	Mass concentration of the elements, %							
	Al	Zn	Mn	Si	Mg	Fe	Cu	Rest
magnesium alloy-AZ61	5.92	0.49	0.15	0.04	93.3	0.007	-	0.093
magnesium alloy-AZ91	9.09	0.77	0.21	0.04	89.8	0.011	-	0.079
aluminium alloy-AlSi9Cu	88.86	0.16	0.37	9.1	0.27	0.18	1.05	0.01
aluminium alloy-AlSi9Cu4	85.4	0.05	0.01	9.27	0.28	0.34	4.64	0.01

Table 2 Deposition parameters of the investigated coating

Parameters	Value
Base pressure [Pa]	1x10 ⁻³
Working pressure [Pa]	1.0/1.4-2.3/2.2
Acetylene flow rate [scm]	140, 170
Substrate bias voltage [V]	60-100
Process temperature [°C]	<150

Structure investigation was performed using the light microscope Leica MEF4A supplied by Zeiss in a magnification range of 50 - 500x. The micrographs of the microstructures were made by means of the KS 300 program using the digital camera.

The examinations of thin foils microstructure and phase identification were made on the JEOL 3010CX transmission electron microscope (TEM), at the accelerating voltage of 300 kV using selected area diffraction method (SAD) for phase investigations. Microstructure investigation was performed using scanning electron microscope (SEM) ZEISS Supra 35, with the accelerating voltage of 5-25 KV.

Wear resistance investigations were performed using the ball-on-disk method in dry friction conditions in horizontal settlement of the rotation axis of the disk. As the counterpart there was used a tungsten carbide ball with a diameter of 3 mm. The tests were performed at room temperature by a defined time using the following test conditions: load, Fn-5N, rotation of the disk 200 turns/min, wear radius of 2.5 mm, shift rate of -0, 05 m/s

3. Investigation results

Own investigations results concerning the structure of the cast Mg-Al-Zn alloys after heat treatment are presented in the attached references.

Both the performed investigations as well as literature study confirm, that the structure of the investigated alloys, changes in a way, that in general bigger precipitations occurs for the higher additional chemical additive like Al in case of the magnesium alloy and copper in case of the aluminum alloy. Depending on the alloy component concentration, particularly in the aluminium alloys changing within the range from 6 to 9%, and on the applied heat and surface treatment of the material the amount of additional phases increases to, particularly the amount of the matrix coherent Al₂Cu phase (Fig. 1, 2). According to the mentioned literature the occurrence of this phase is responsible for enhancement of the mechanical properties. The heat treatment carried out, composed of super saturation with cooling in water and ageing with cooling in air causes reinforcement of the MCMgAl9Zn1, MCMgAl6Zn1 magnesium alloys, according to the mechanism of precipitation hardening reinforcement caused by stopping dislocation slip due to interaction of the stress fields of evenly located precipitations of □-□Mg₁₇Al₁₂ phase, which, according to the expectations, causes additional growth of strength properties, wear resistance and resistance to the corrosion factor impact. In case of the aluminium alloys the main precipitation phase is the Al₂Cu phase.

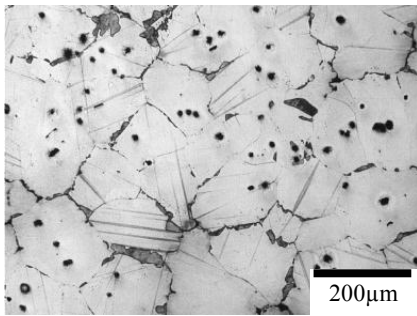


Fig. 1 Structure of the MCMgAl9Zn1 alloy after aging at the temperature of 190 C for 15 hours

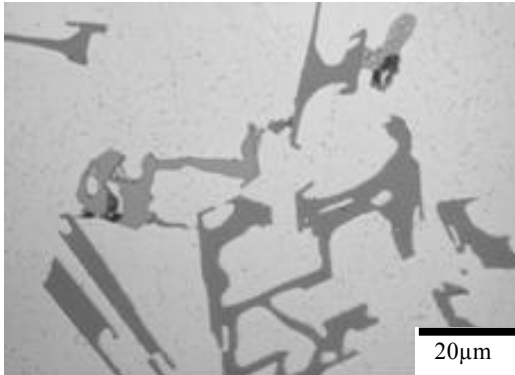


Fig. 2 Structure of the AlSi9Cu alloy in as cast state

In case of the investigated aluminium cast alloys the heat treatment was carried out in the electric resistance furnace U117, with two holds at 300°C/s and 450°C/s performed for 15 minutes. Cooling of the samples after heat treatment was performed in air for the ageing process and in water for the solution heat treatment process, like it is stand of the art for this types of light aluminium alloys.

The coatings obtained in selected variants, reinforced by solution, produced as a result of synthesis of non-balance (metastable) phases of the following configuration Ti/Ti(C,N)-gradient/CrN; and coatings Cr/CrN-gradient/CrN; are characterised with distinct heterogeneity of the surface, related to the occurrence of numerous micro-particles in the structure, their shapes of drops fallen out of the shield during coating deposition process and hollows produced as result of some drops falling out during the solidification (Figs. 3,4,6-11).

The increase of the exploitation time and hardness enhancement of elements made with Mg-Al-Zn alloys is only possible with the use of their surface layer purification in the vapour deposition, which was also proven upon extensive tests made by the authors, contrary to the common opinion that coating magnesium alloys with PVD coatings is pointless, due to their low hardness.

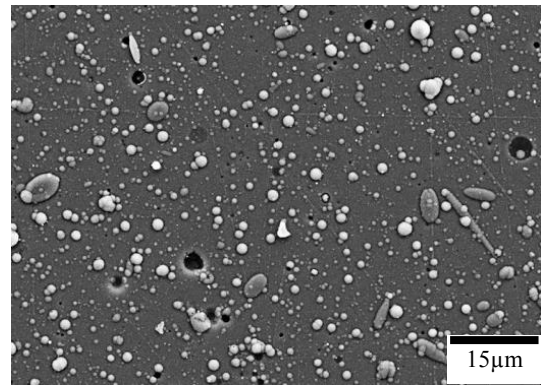


Fig. 3 Surface morphology of the Ti/Ti(C,N)/CrN layer coated on the MCMgAl6Zn1 cast magnesium substrate

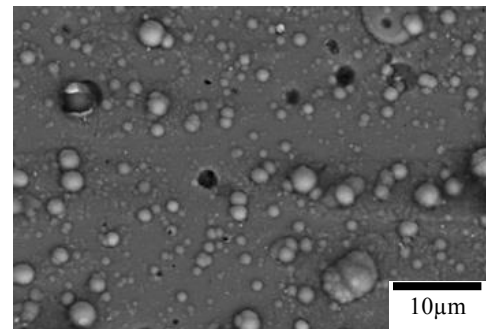


Fig. 4 Surface morphology of the Ti/Ti(C,N)/CrN layer coated on the AlSi9Cu cast aluminium substrate

In the solid solution as the matrix of cast magnesium alloys after aging there are present also clusters of dislocations in form of dislocation networks with a density much higher compared to the supersaturated state of the material. Formation of these dislocations (Fig. 5) is associated with stain generated in the matrix by precipitation of the □ phase particles.

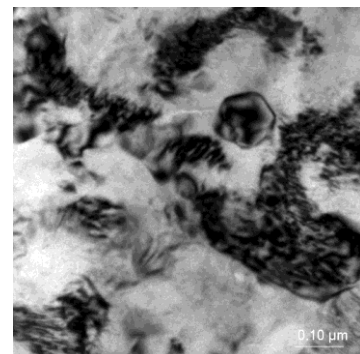


Fig. 5 Dislocation density revealed using TEM investigations

The above effect is undoubtedly related to the differences in thermal conductivity coefficients and tension difference between the coating and the set drops of metal produced during the cooling of the substrate surface, upon completion of the coating deposited.

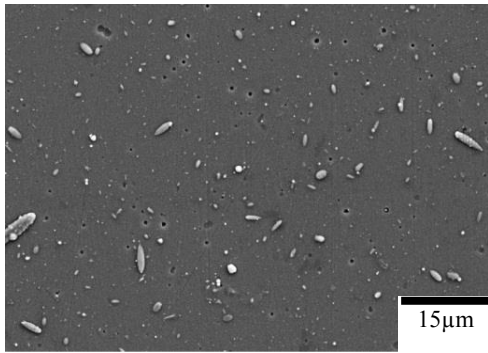


Fig. 6 Surface morphology of the Cr/CrN/CrN layer coated on the MCMgAl9Zn1 cast magnesium substrate

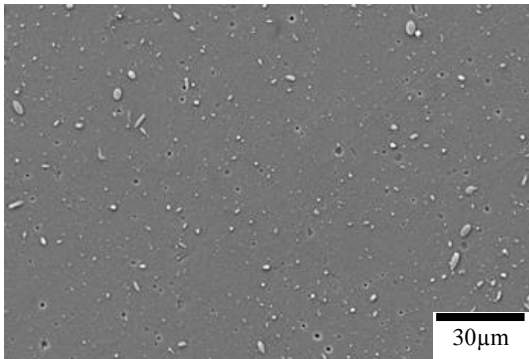


Fig. 7 Surface morphology of the Cr/CrN/CrN layer coated on the Al-Si9Cu cast aluminium substrate

As a result of fracture investigations carried out in electron scanning microscope on the PVD coatings analysed, it was found that the deposition coatings are characterised with one- two- or multi-layered structure, depending on the layer system applied.

As a result of fracture investigations carried out in electron scanning microscope on the PVD coatings analysed, it was found that the deposition coatings are characterised with one- two- or multi-layered structure, depending on the layer system applied. The particular layers are applied evenly and tightly adhere to the substrate and one another (Figs. 8-10).

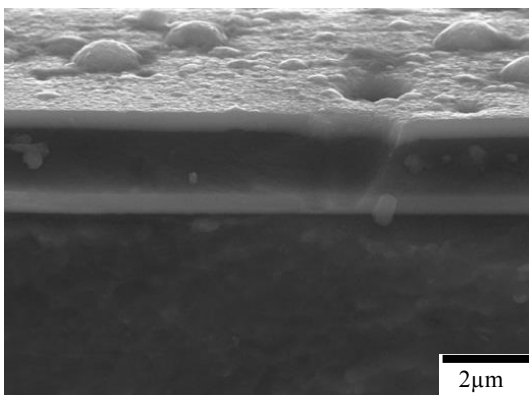


Fig. 8 Fracture of the Ti/Ti(C,N)/CrN coating deposited on the MCMgAl9Zn1 cast magnesium alloy

a)

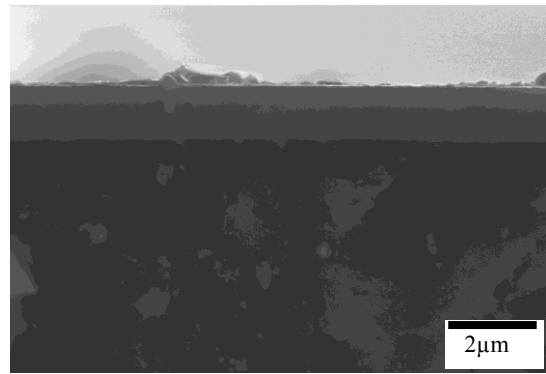


Fig. 9 Fracture of the Cr/CrN/CrN coating deposited on the MCMgAl6Zn1 cast magnesium alloy

The structure of the (Ti, Al)N layers depends in particular on the type and conditions of the process and the type of the deposition coating. Based on the structure investigations obtained with dark field TEM imaging technique, it was established that the coatings are characterised with compact structure of high grain homogeneity and a size reaching even 30 (Figs. 12b, 13b).

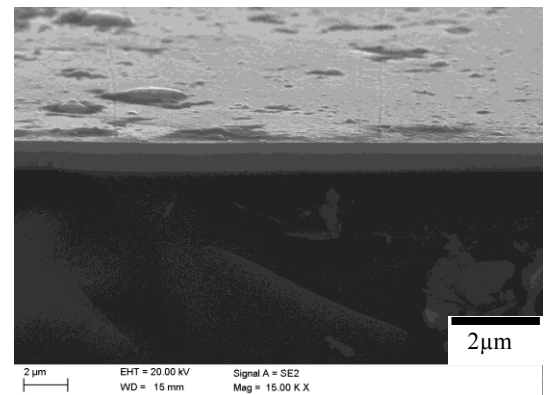


Fig. 10 Fracture of the Cr/CrN/CrN coating deposited on the AlSi9Cu1 cast aluminium alloy

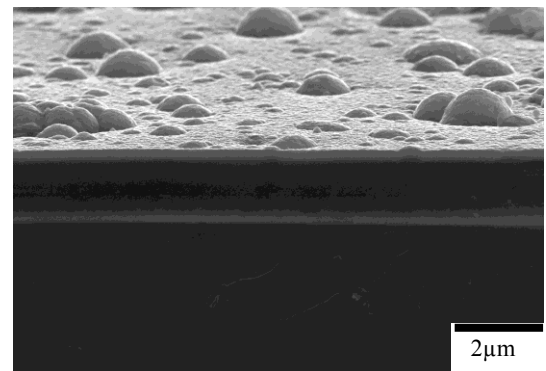
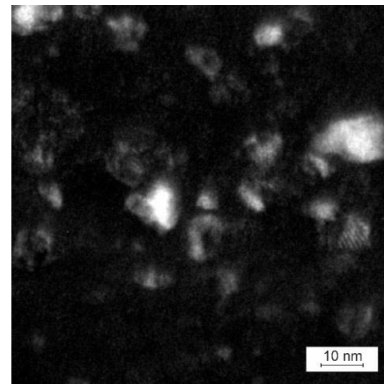
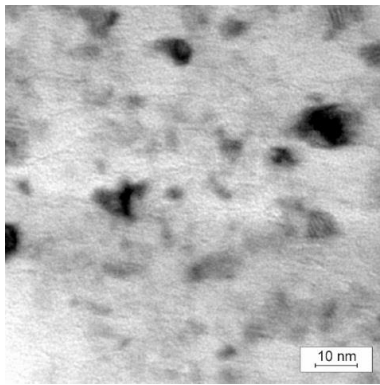
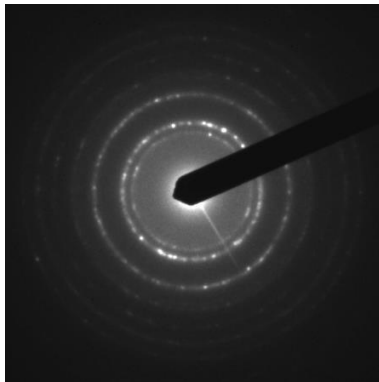


Fig. 11 Fracture of the Ti/Ti(C,N)/CrN coating deposited on the AlSi9Cu1 cast aluminium alloy

b)



c)



d)

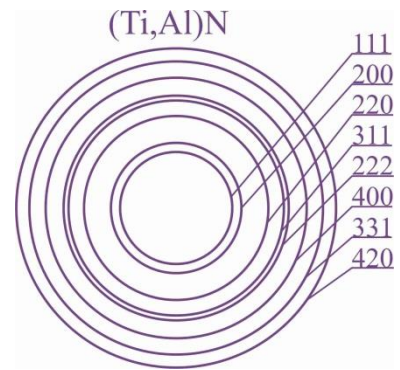
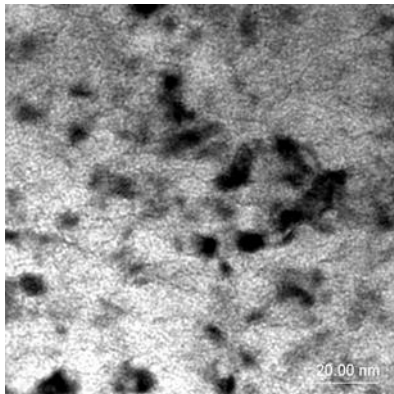
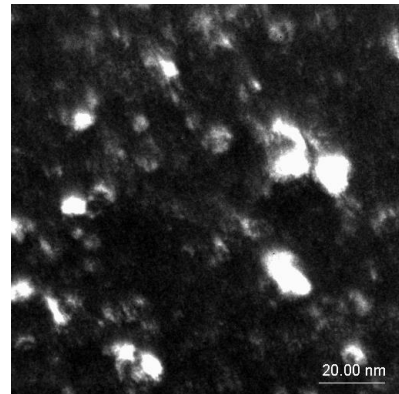


Fig. 12 Structure of the thin foil from Ti/Ti(C,N)/(Ti,Al)N surface layer fracture deposited on the MCMgAl6Zn1 cast magnesium alloy: a) bright field, b) dark field, c) diffraction pattern of the surface layer presented on fig. a and b, solution of the diffraction pattern presented on fig. c), TEM

a)



b)



c)

d)

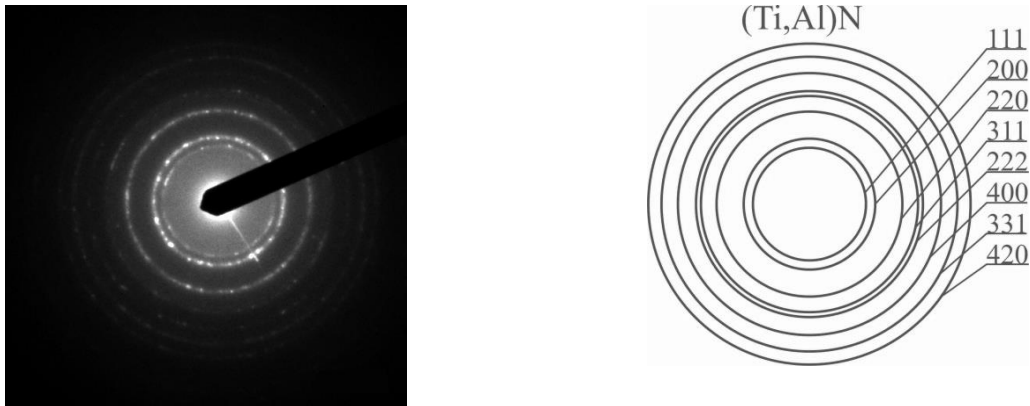


Fig. 13 Structure of the thin foil from Ti/Ti(C,N)/(Ti,Al)N surface layer fracture deposited on the AlSi9Cu4 aluminium alloy: a) bright field, b) dark field, c) diffraction pattern of the surface layer presented on fig. a and b, solution of the diffraction pattern presented on fig. c), TEM

7. Summary

Structure and properties of the investigated cast Mg-Al-Zn and Al-Si-Cu alloys, are varied depending on substrate material as well as the alloying additive used – Cu or Zn, as well as the treatment, for example in as cast state before heat treatment, after aging or surface treatment. The aging process, which was confirmed on the basis of thin foils investigations, causes clear change in the structure resulting from the uniform precipitation process of dispersed Al_2Cu in a bulk form or $\text{Mg}_{17}\text{Al}_{12}$ phase particles in a needle form, forming large agglomerates inside the grains, which are also present in the form of pseudo eutectic areas. In such a case, due to the low content of the solution compound in the matrix - in this case aluminium - causes a softening effect by precipitation of the Al_2Cu phase.

In general refining of the obtained structure is possible using the presented methods by creating coatings on the surface from the gas phase, partially solution hardened, coated in the system of soft substrate - gradient transition layer, with a continuous change of one or more of components from the substrate to the outer surface - and an outer layer, as a result of cathodic arc evaporation as well in the process of plasma assisted chemical vapour deposition, characterized by a homogeneity, compact structure, without visible delamination and structural defects, evenly and tightly coated and adherent to each other as well as to the light alloy substrate.

Generally for both types of substrate material it can be stated that:

- the coatings are homogeneity without any pores or cracks and of uniform thickness,
- the structure of the surface layer has a polycrystalline character,
- for the Ti/Ti(C,N)/CrN type of coating there can be distinguished between the three layers of the coatings, revealed as a with strips on the SEM microstructures,
- the coating consists of nanoscale crystallites in the range of ca. 30 nm in size,
- the obtained layer in the PVD process is of excellent uniformity and high quality.

References

- [1] T. Tański, Synergy effect of heat and surface treatment on properties of the Mg-Al-Zn cast alloys, Habilitation thesis not published, Žilinska Univerzita v Žiline, Žilina 2012.
- [2] L.A. Dobrzański, T. Tański, J. Domagała, Microstructure analysis of MCMgAl16Zn1 MCMgAl8Zn1 MCMgAl4Zn1 magnesium cast alloy, Archives of Foundry Engineering, 7/4 (2007) 33-38.
- [3] L.A. Dobrzański, T. Tański, L. Čížek, J. Domagała, Mechanical properties and wear resistance of magnesium casting alloys, Journal of Achievements in Materials and Manufacturing Engineering, 31/1 (2008) 83-90.
- [4] L.A. Dobrzański, T. Tański, L. Čížek, Z. Brytan, Structure and properties of the magnesium casting alloys, Journal of Materials Processing Technology, 192-193 (2007) 567-574.
- [5] L. Čížek, M. Greger, L. Pawlica, L.A. Dobrzański, T. Tański, Study of selected properties of magnesium alloy AZ91 after heat treatment and forming, Journal of Materials Processing Technology, 157-158 (2004) 466-471.
- [6] L.A. Dobrzański, T. Tański, L. Čížek: Microstructure of MCMgAl12Zn1 magnesium alloy, Archives of Foundry Engineering, 7/1 (2007) 179-182.
- [7] L.A. Dobrzański, T. Tański, Influence of aluminium content on behaviour of magnesium cast alloys in bentonite sand mould, Solid State Phenomena, 147-149 (2009) 764-769.
- [8] L.A. Dobrzański, T. Tański, J. Trzaska, Optimization of heat treatment conditions of magnesium cast alloys, Materials Science Forum, 638-642 (2010) 1488-1493.
- [9] M. Krupiński, T. Tański, Prediction of mechanical properties of cast Mg-Al-Zn alloys, Archives of Materials Science and Engineering, 56/1 (2012), 30-36.
- [10] L.A. Dobrzański, T. Tański, J. Domagała, Sz. Malara, M. Król, Effect of high power diode laser surface melting and cooling rate on microstructure and properties of magnesium alloys, Journal of Achievements in Materials and

- Manufacturing Engineering, 37/2 (2009) 238-257.
- [11] A.D. Dobrzańska-Danikiewicz, T. Tański, S. Malara, J. Domagała-Dubiel, Assessment of strategic development perspectives of laser treatment of casting magnesium alloys, Archives of Materials Science Engineering, 45/1 (2010) 5-39.
- [12] W. Ozgowicz, K. Labisz, Analysis of the state of the fine-dispersive precipitations in the structure of high strength steel Weldox 1300 by means of electron diffraction, Journal of Iron and Steel Research, International 18, 135-142 (2011).
- [13] L.A. Dobrzański, K. Labisz, E. Jonda, A. Klimpel, Comparison of the surface alloying of the 32CrMoV12-28 tool steel using TiC and WC powder, J. Mater. Process. Technol. 191\ 1/3, 321-325 (2007).
- [14] J. Konieczny, L.A. Dobrzański, K. Labisz, J. Duszczyk, The influence of cast method and anodizing parameters on structure and layer thickness of aluminum alloys. Journal of Materials Processing Technology 157–158, 718-723 (2004).
- [15] T. Tański, K. Labisz, Electron microscope investigation of PVD coated aluminium alloy surface layer, Solid State Phenomena 186 (2012) 192-197
- [16] L.A. Dobrzański, M. Krupiński, K. Labisz, B. Krupińska, A. Grajcar, Phases and structure characteristics of the near eutectic Al-Si-Cu alloy using derivative thermo analysis, Materials Science Forum, Vols. 638-642 (2010) 475-480
- [17] M. Piec, L.A. Dobrzański, K. Labisz, E. Jonda, A. Klimpel: „ Laser alloying with WC Ceramic Powder in hot work tool steel using a High Power Diode Laser (HPDL), Advanced Materials Research, vol. 15-17 (2007) 193-198

Acknowledgements

This project, headed by Dr Eng. Krzysztof Labisz, was funded by the National Science Centre (NCN) on the basis of Decision No. 2011/01/B/ST8/06663.

This contribution was created within the project **Creation of an international scientific team and incorporation to scientific networks in the area of nanotechnology and unconventional forming material. CZ.1.07/2.3.00/20.0038**, which is financed by the European Social Fund and state budget of the Czech Republic.



europa
esf
european
social fund in the
czech republic



EUROPEAN UNION



MINISTRY OF EDUCATION,
YOUTH AND SPORTS



OP Education
for Competitiveness

INVESTMENTS IN EDUCATION DEVELOPMENT

Selected metal forming methods for obtaining ultrafine-grained microstructure

Marek TKOCZ, Franciszek GROSMAN, Eugeniusz HADASIK, Dariusz KUC, Kinga RODAK

*Silesian University of Technology, Faculty of Materials Science and Metallurgy, Krasińskiego 8, 40-019
Katowice, Poland, E-mail address: marek.tkocz@polsl.pl*

Abstract

The paper presents opportunities to obtain ultrafine-grained microstructure in metallic materials by forming with controlled strain path. A number of unique laboratory devices have been developed and launched at the Faculty of Materials Science and Metallurgy in the Silesian University of Technology for studying unconventional forming methods of such kind. The devices permit to perform experiments with three various loading systems: compression with oscillatory torsion, forging with transverse motion of a punch and rolling with transverse motion of rolls. The results of experiments and numerical simulations obtained so far have proved that repetitive changing of the strain path provided by cyclic change of loading system leads to significant grain refinement and controlled improvement of functional properties of a product. Moreover, the flow stress of materials deformed in these conditions is lower than in conventional processes. As a result, it enables for reduction of the force required to perform cold forming operations without preheating a workpiece. On a basis of the obtained results and experience gained during the experiments, perspectives for continuation of the studies and possible industrial applications areas are discussed in conclusion.

Keywords

Ultrafine-grained, strain path, compression, torsion, forging, oscillatory, shear stress

1. INTRODUCTION

It has been shown in many experiments that metal forming methods utilizing cyclic changes of the strain path cause severe plastic deformation of a workpiece. As a result, significant grain refinement and controlled improvement of functional properties of a product are possible [1,2]. Cyclic strain path changes can be obtained by application of the additional force that acts with oscillatory manner in orthogonal direction to the compression force. This force induces additional shear stress in a workpiece. There are various loading systems of this kind which can be used in practise, e.g. compression with oscillatory torsion [3,4], extrusion with oscillatory torsion [5], compression with transverse motion of a punch [6] and rolling with transverse rolls motion [7]. Although forming operations utilizing these loading systems are continuous, cyclic changes of the strain path make it possible to divide the forming operation into a number of specific steps, considering that in every step the strain is monotonic. The accumulated effective strain in a workpiece after n steps can then be estimated according to the general formula:



$$\varepsilon_{eff} = \frac{1}{\sqrt{3}} \sum_{i=1}^n \sqrt{3 \cdot \varepsilon_{ci}^2 + \varepsilon_{ti}^2} \quad (1)$$

The component ε_{ci} in the Equation (1) denotes strain due to compression at a step i while the component ε_{ti} stands for strain due to transverse motion of a die at the step i . The both components can be expressed as functions of the amplitude and the frequency of transverse die motion as well as the compression/extrusion/rolling velocity. The higher both parameters of transverse motion and the lower velocity, the higher value of the accumulated effective strain can be obtained.

2. COMPRESSION WITH OSCILLATORY TORSION

To date, compression with oscillatory torsion is the most commonly investigated loading system with cyclic strain path change at the Faculty of Materials Science and Metallurgy in the Silesian University of Technology. A dedicated laboratory device is presented in Fig. 1. It is mounted in the working space of a typical material strength testing machine with the maximum load of 300 kN. Strain path can be controlled by changing proportions of the kinematic test parameters. The lower punch torsion frequency can be adjusted within 0 to 1.8 Hz, the amplitude of torsion angle - in the range of 0° to 16° and the lower punch vertical velocity – from 0 to 0.4 m/min.



Fig. 1 A device for compression with oscillatory torsion: as mounted in the material strength testing machine (left), a close-up view (center) and a schematic view (right)

The series of experiments with various combinations of kinematic parameters were conducted, inter alia, for cylindrical test pieces (9 mm in height and 6 mm in diameter) made of pure copper and aluminum. Due to the nature of torsion, a gradient of the accumulated effective strain is obtained after the test along the workpiece radius. The strain is largest at the workpiece outer contour and the lowest – at the centre. Therefore, investigations of the microstructure after compression with oscillatory torsion tests were conducted for a representative area – located in the middle of the test piece height and in a distance ca. 0.8 of the test piece radius from its centerline. It can be assumed that the microstructure in this area corresponds to the accumulated effective strain calculated by the Equation 1. The results prove that the grains can be significantly refined by this forming method. They also suggests that the accumulated effective strain is not a decisive factor because the intensity of grain refinement depends strongly on the strain path applied. For instance, the Fig. 2 shows that the strain increase (achieved by increasing torsion frequency) to some extent causes a progress in grain refinement. There were two indicators of grain refinement used: the area fraction of grains with size smaller than $1 \mu\text{m}$ and the fraction of high-angle boundaries. Both of them reached the higher values (almost 40%) in the representative area at the frequency of 1.6 Hz.



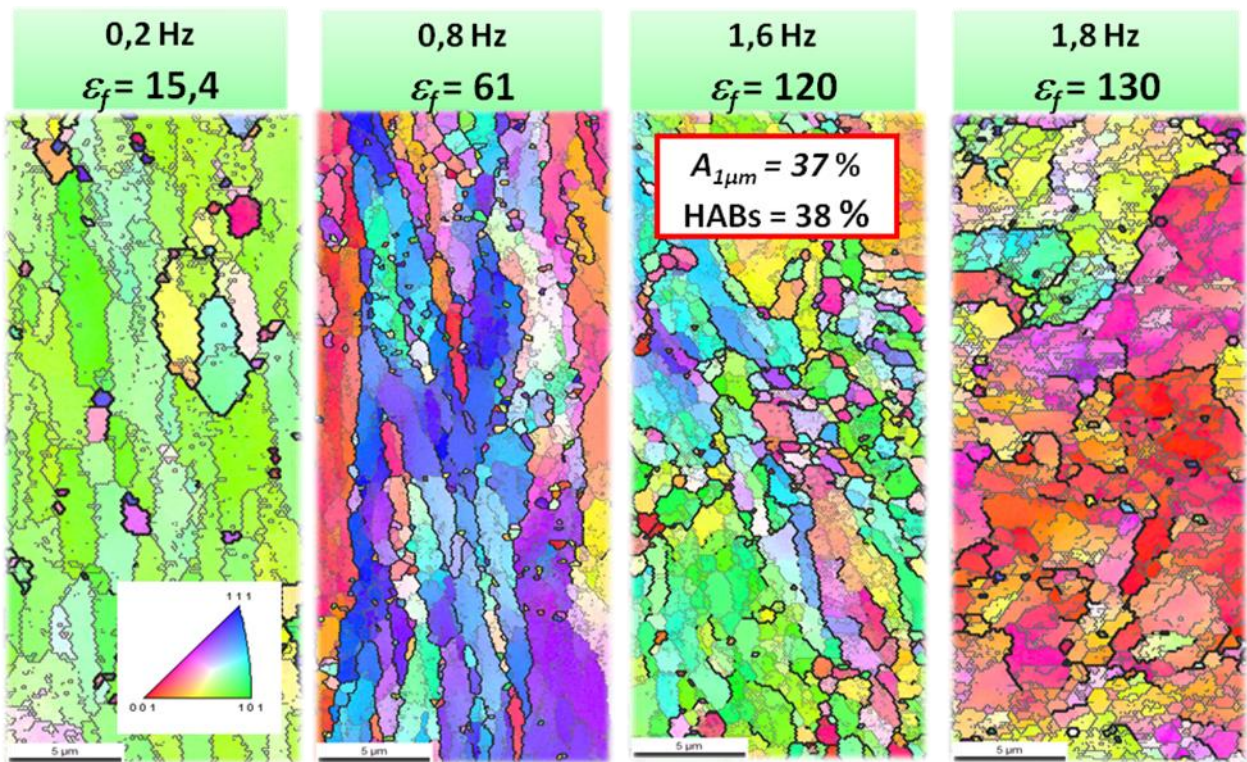


Fig. 2 An effect of the torsion frequency on the accumulated effective strain and grain refinement in the representative area of the aluminum test piece (results obtained for the torsion amplitude $\pm 6^\circ$, the compression velocity 0.015 mm/s and 7 mm height reduction)

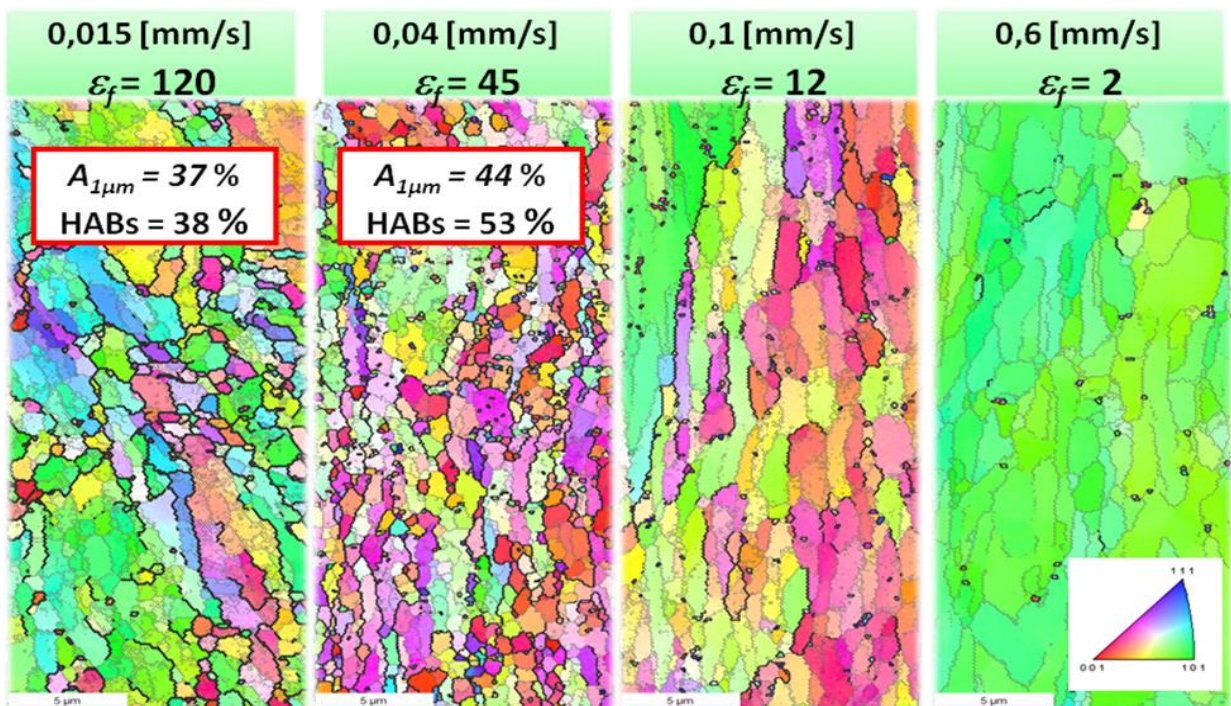


Fig. 3 An effect of the compression velocity on the accumulated effective strain and grain refinement in the representative area of the aluminum test piece (results obtained for the torsion amplitude $\pm 6^\circ$, the torsion frequency 1.6 Hz and 7 mm height reduction)



Although the accumulated effective strain rises for higher torsion frequency, intensive recovery process begins to dominate causing considerable restrictions in grain refinement. It should be also noticed that a relatively small change of the compression velocity had a considerable impact on grain refinement (Fig.3). Increasing the compression velocity to 0.04 mm/s, caused the delay of the microstructure recovery process. However, the further increase of the compression velocity does not foster grain refinement.

In the most advantageous variants of conducted experimental trials the grain/subgrain size of 300 nm / 200 nm and 600 nm / 300 nm was obtained for pure Cu and Al respectively, the fraction of high-angle boundaries of Cu and Al is about 50 % and the fraction area of the ultrafine grains is about 60 % and 45 % for Cu and Al respectively. It is expected that these indicators can be higher for Cu and Al alloys.

3. COMPRESSION WITH TRANSVERSE MOTION OF A PUNCH

Experience gained during the tests of compression with oscillatory torsion was the basis for development of the other laboratory devices for forming with controlled strain path. In the laboratory device shown in Fig. 4 compression is not accompanied with cyclic torsion but with the reciprocating, horizontal motion of a lower punch. For many product shapes this loading system can be more advantageous. The kinetic parameters of a lower punch transverse motion is controlled by two hydraulic cylinders. The frequency within 0-3 Hz and the peak-to-peak amplitude up to 2 mm can be applied.

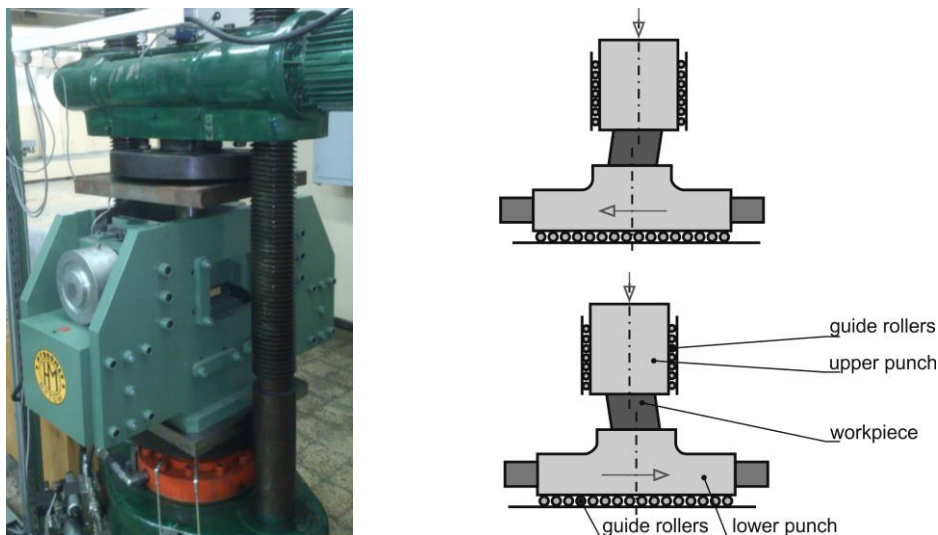


Fig. 4 A device for compression with transverse motion of a punch: as mounted in the hydraulic press (left) and a schematic view (right)

As a result of this cyclic, additional motion of the lower punch, significant increase of local strains can be achieved in comparison with conventional forging. The accumulated effective strain, calculated by means of the Equation 1 for various combinations of the process parameters, is compared on a diagram in Fig. 5. In the same figure, distributions of the accumulated effective strain in workpieces upsetted conventionally and by the investigated method are presented as well [6]. The results prove that, in addition to high strain values, also more uniform strain distribution is possible to achieve in the transverse direction to horizontal punch motion when using a proper combination of process parameters.

The numerical simulations confirmed the opportunity of press load reduction as well [6]. For the process parameters indicated in Fig.5 the compression force required to obtain 50% reduction in height in the investigated process was ca. 30% lower than in the conventional upsetting.



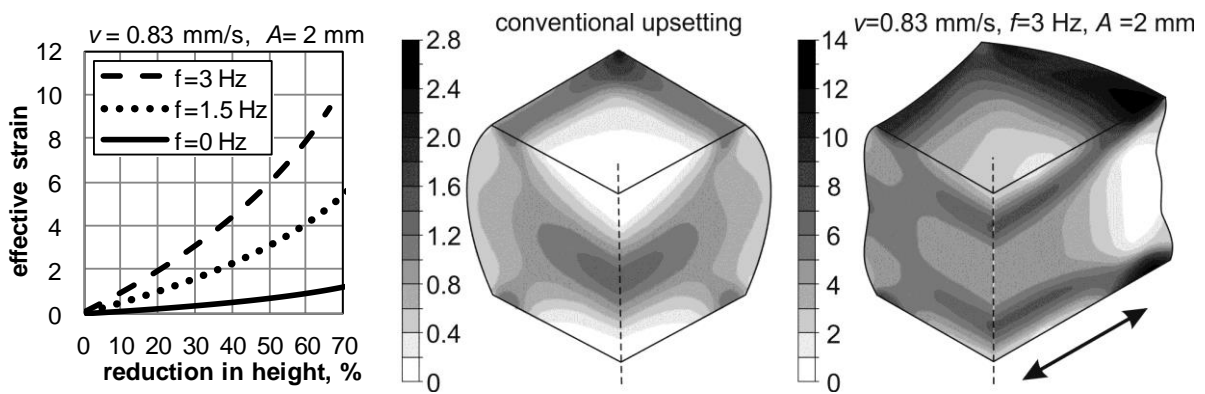


Fig. 5 Comparison of the estimated accumulated effective strain after compression with transverse punch motion for various process parameters (left) and strain distributions in copper workpieces after conventional upsetting and compression with transverse punch motion (right) - direction of transverse punch motion is indicated with the arrow; reduction in height: 50%

4. ROLLING WITH TRANSVERSE ROLLS MOTION

The concept presented in chapter 3 has been adapted also for the rolling process. A developed laboratory rolling stand (Fig.6) consists of two rolls, a power unit and a mechanism to control cyclic motion of both rolls that is transverse to the rolling direction. The mechanism is driven by gear-motor controlled by an inverter, that allows to adjust the frequency of transverse rolls motion in the range of 0 to 3Hz and the amplitude ± 2 mm for each roll. The rolling velocity can be adjusted in the range of 0 to 3.7 rpm. The individual reduction in height is adjusted by a screw mechanism. The device is equipped with a set of sensors that provides acquisition of the key process parameters.



Fig. 6 A laboratory stand for rolling with transverse rolls motion (left), a close-up view on the rolls and a workpiece during the test (center) and a schematic view (right)

5. SUMMARY

The three metal forming methods were presented that can be used to obtain the products with ultrafine-grained microstructure. Experimental trials and simulations performed so far prove that process parameters significantly influence the material flow, accumulated effective strain and its distribution, grain size and load required.

Expected benefits that can be obtained by means of the methods are as follow:

- significant increase of effective strain and grain refinement,
- more homogenous strain distribution,
- significant reduction of press load or rolling force in comparison to corresponding



- conventional processes,
- opportunity to consolidate porous materials,
- creating advantageous conditions for closing and welding of voids in stock material,
- obtaining better functional properties of the products than after conventional processes.

The presented laboratory devices can be used for:

- estimating the effects of cyclic change of strain path on the microstructure and properties of products,
- determining material formability under specific forming conditions,
- producing small forgings for demonstration purposes,
- preparation of stock for other forming processes.

6. LITERATURE

- [1] K. Rodak, J. Pawlicki, M. Tkocz. Deformation-induced grain refinement in AlMg5 alloy, *Solid State Phenom.* 191, 2012, 37-44.
- [2] K. Rodak, J. Pawlicki, M. Tkocz, Mechanical and microstructural aspects of severe plastic deformation of austenitic steel, *IOP Conf. Series: Mater. Sci. Eng.* 35, 2012.
- [3] K. Rodak. Structure and mechanical properties of the Cu and Al forming by compression with oscillatory torsion method. *Wyd. Politechniki Śląskiej, Gliwice 2012, ISBN 978-83-7335-958-1.*
- [4] J. Pawlicki. The effect of deformation history on flow stress during cold metal forming. *Wyd. Politechniki Śląskiej, Gliwice 2012, ISBN 978-83-7335-904-8.*
- [5] W. Bochniak, K. Marszowski, A. Korbel. Theoretical and practical aspects of the production of thin-walled tubes by the KOBO method. *J. Mater. Process. Technol.* 169, 1, 2005, 44-53.
- [6] M. Tkocz, Z. Cyganek, F. Grosman. The potential and application areas of forging aided by shear stress. *Solid State Phenom.*, 212, 2014, 91-94.
- [7] Z. Cyganek, K. Rodak, F. Grosman. Influence of rolling process with induced strain path on aluminium structure and mechanical properties. *Arch. Civ. Mech. Eng.* 13, 1, 2013, 7-13.

Acknowledgements

This paper was created within the project "**Creation of an international scientific team and incorporation to scientific networks in the area of nanotechnology and unconventional forming material. CZ.1.07/2.3.00/20.0038**", which is financed by the European Social Fund and state budget of the Czech Republic.

Financial support of Structural Funds in the Operational Programme – Innovative Economy (IE OP) financed from the European Regional Development Fund – Project "**Modern material technologies used in aerospace industry**", No. **POIG.0101.02-00-015/08** is gratefully acknowledged.





esf european
social fund in the
czech republic



EUROPEAN UNION



MINISTRY OF EDUCATION,
YOUTH AND SPORTS



OP Education
for Competitiveness

INVESTMENTS IN EDUCATION DEVELOPMENT

Microstructure and properties of ultrafine grained and nanocrystalline metals and alloys.

Gerhard Wilde

Institute of Materials Physics, University of Münster, Wilhelm-Klemm-Str. 10, 48149 Münster, Germany

Abstract

Our research interest is focused on the basic properties of interfaces and their interaction with other lattice defects leading to complex defect reactions that have a large impact on materials properties and performance. In our laboratory, materials are synthesized by different methods and the main characterization methods are based on scanning and transmission electron microscopy, calorimetry and thermal analysis, mechanical testing and indentation, low-temperature transport and optical properties and radiotracer diffusion. The combination of a large range of complementing characterization tools allows for an in-depth analysis of microstructure-property relationships.

Keywords

nanocrystalline, nanostructured, ultrafine grained, microstructure, mechanical properties, thermodynamics, diffusion kinetics

1. INTRODUCTION

Nanostructured materials offer particular promise for new and potentially very useful products since they can have very different and often superior properties that crucially depend on the atomistic details of interior or exterior interfaces. The nanostructures may be used in a wide range of contexts; most of these are ones in which ensembles of nanostructures are assembled into complex, functional arrangements. As nanostructured materials are structures far away from thermodynamic equilibrium and since they have short transport pathways, fast diffusion and rapid transformation kinetics often lead to coarsening and to the deterioration of the microstructure and the associated properties. Thus, ensuring the stability of the nanoscale structures, e.g. by utilizing a composite approach, is a key issue. This approach, however, imposes additional constraints on processing-related issues as well as on the stability of phases and phase mixtures and on phase transformations within the nanoscale structural units due to size confinement and due to the presence of internal heterophase interfaces. In order to address this complex spectrum of issues, a concise research program including the synthesis, processing, microstructural analysis and the characterization of different materials properties including the mechanical performance has been designed after the chair professorship has been taken by Prof. Wilde. The general objective of the research work aims at a general understanding of the underlying physical phenomena in order to develop a predictive understanding of the complex processing-microstructure-properties relationships.



2. INSTITUT OF CHEMISTRY AND MATERIALS OF EAST-PARIS

2.1 Research topics and equipments

The IMP (Institute of Materials Physics of University of Münster) is an integral part of the „Nanoscience“ focus area of the department of physics. The institute is composed of two professorships (one with and the other without leadership function). Including permanent and non-permanent researchers and staff, about 85 people work at the IMP.

The research at the institute is primarily focused on basic materials physics issues involving the relationship between the microstructure including the atomic level structure and the resulting mesoscopic and macroscopic properties of a wide spectrum of materials. The materials classes studied include metallic glasses, nanocrystalline and ultrafine grained metals and alloys, liquid metals, nanostructured surfaces, semiconductor heterostructures and polymer electrolytes. The institute es are focused on 4 mains transversal topics including energy, ecology, health science and advancencompasses several dedicated means for materials synthesis and processing, such as rapid melt quenching, single crystal and bi-crystal growth facilities, r.f. induction melting, arc melting, rolling, high-pressure torsion and several deposition methods including PVD, CVD, ALD and electrodeposition. In addition to the conventional characterization techniques (XRD, DSC, DTA) the institute has high standard transmission electron microscopes (TEM-STEM) equipped with HAADF, EELS, EDX mapping, and a new FE-SEM with EBSD/EDX, AFM and digital and analog optical microscopy. Metallurgical researches are also supported by a mechanical testing machine (Instron) equipped with a high temperature furnace, a nano-indenter with scratch test, TMA, several micro-tensile testing machines, a custom-designed micro-chip calorimeter, a high-sensitivity isothermal microcalorimeter, a device for measuring low-temperature heat capacity, transport properties and magnetic properties (PPMS) and a fully equipped radiotracer laboratory with the permission to store and handle solid and liquid radiotracers for diffusion measurements including many furnaces, detectors and special devices for parallel sectioning.

2.2 Staff involved in UFG

Currently the activities on UFG and nanocrystalline metals and alloys are focused on the analysis of so-called “non-equilibrium” grain boundaries in Cu, Ni, Ti and binary alloys after severe plastic deformation.

Prof. Gerhard Wilde is the director of the institute of Materials Physics and is heading the group on Materials Physics. Dr. Harald Rösner is a senior scientist at the institute and is responsible for the electron microscopy equipment. He has about 15 years of experience in high resolution and analytical transmission electron microscopy and is a specialist for defect analysis and for analyzing deformed microstructures. PD Dr. Sergiy Divinski is a senior scientist at the institute with about 15 years of scientific experience and is responsible for the diffusion laboratory. He is a specialist for grain boundary diffusion and for interface properties. Dr. Martin Peterlechner is working on his habilitation and he is in charge of the surface nanostructuring unit. He is a specialist for martensitic transformations and for cold rolling.

2.3 Teaching activities

The expertise of the staff involved in the UFG activities is in the broader area of materials physics and physical metallurgy, including synthesis, processing, microstructure analysis and characterization. The staff involved in the UFG activities covers the entire area of materials



science and materials physics on the Master level and additionally the area of experimental physics on the Bachelor level.

3. INTERFACES IN ULTRAFINE GRAINED MATERIALS BY SEVERE PLASTIC DEFORMATION

Ultrafine grained materials have been synthesized by high pressure torsion and by equal channel angular pressing. In addition to pure metals such as Cu, Ni and Ti as model systems, segregation-stabilized systems as well as concentrated alloys have been investigated [1-12]. Diffusion analyses have unequivocally shown that the interaction of the extreme dislocation densities with grain boundaries lead to modified structures of the internal interfaces that result in a strong enhancement of the grain boundary diffusion rates by more than 6 orders of magnitude [1, 2, 4-6, 9, 12]. Microstructure analyses by geometric phase analysis that is based on high-resolution electron microscopy have additionally revealed that these materials include internal interfaces that are exceptionally wide and have large strain fields associated to the grain boundary near regions [3, 4, 8, 9]. These microstructure characteristics have been found for all materials processed by SPD methods. Moreover, a quantitative model was developed based on these studies that can predict the processing range of ultrafine grained materials by severe plastic deformation in order to produce materials with a useful ductility and high strength [7]. Moreover, the inherent interactions between large densities of lattice dislocations with elements of the microstructure, particularly with grain boundaries and triple junctions have been analyzed and a new mechanism for microstructure stabilization based on rotational defects has been suggested [8].

Achieving a reasonable ductility in bulk high-strength UFG materials is still a challenge and current research is focused on strategies for simultaneous improvement in the strength and ductility of metallic materials. The different approaches proposed to improve ductility are: (i) bimodal grain size distribution; (ii) controlled precipitation through ageing of SPD-processed alloys; (iii) introduction of nanoscale twins; (iv) through transformation/twinning-induced plasticity; and (v) control of the grain boundary character. In our recent work [10], we demonstrated an approach for retaining high strength while recovering ductility. For this study, we selected a Cu–Ag alloy, which is a precipitation-hardened material due to the very limited solubility of Ag in Cu at room temperature (RT). Additionally, this alloy has medium stacking fault energy, and therefore twin formation is expected during both deformation and annealing. It has already been reported that a bimodal or multimodal grain size distribution developed following short-time annealing at temperatures below recrystallization. Cu–Ag alloys are therefore suitable for combining approaches (i)–(iii) listed above in order to achieve high strength and ductility. In the present investigation, sequential cold rolling at RT and cryogenic temperature (at liquid N₂ temperature (LNT)) followed by short-time annealing was employed to introduce fine deformation/annealing twins and precipitates in the microstructure. The microstructure and mechanical properties after rolling and annealing were studied and the optimum parameters for achieving high strength with reasonable tensile ductility were identified.

4. CONCLUDING REMARK AND OBJECTIVES

Our work on UFG metals is focused today on the analysis of the complex and intricate coupling between high dislocation densities, structure modification of interfaces and the modification of (mostly) mechanical properties. In addition, we now focus our attention on a directed



modification of the internal interfaces to achieve a new type of „interface engineering“ to obtain nanocrystalline materials with high thermal stability and enhanced mechanical performance.

5. REFERENCES

- [1] Wilde, G. (Ed.): Nanostructured Materials First volume in the series: Frontiers of Nanoscience, by R.E. Palmer (Ed.), ISBN 978-0-08-044965-4, Elsevier, Oxford, (2009).
- [2] Divinski, S.V., Ribbe, J., Reglitz, G., Estrin, Y., Wilde, G.: Percolating network of ultra-fast transport channels in severely deformed nanocrystalline metals. *Journal of Applied Physics*, 106 (2009), 063502.
- [3] Rösner, H., Boucharat, N., Padmanabhan, K.A., Markmann, J., Wilde, G.: Strain mapping in a deformation-twinned nanocrystalline Pd grain. *Acta Materialia*, 58 (2010), 2610-2620.
- [4] Wilde, G., Ribbe, J., Reglitz, G., Wegner, M., Rösner, H., Estrin, Y., Zehetbauer, M., Setman, D., Divinski S.: Plasticity and grain boundary diffusion at small grain sizes. *Advanced Engineering Materials*, 12 (2010) 758-764.
- [5] Divinski, S.V., Reglitz, G., Rösner, H., Estrin, Y., Wilde, G.: Ultra-fast diffusion channels in pure Ni severely deformed by equal channel angular pressing. *Acta Materialia*, 59 (2011) 1974-1985.
- [6] Fiebig, J., Divinski, S., Rösner, H., Estrin, Y., Wilde, G.: Diffusion of Ag and Co in ultrafine grained α -Ti deformed by equal channel angular pressing. *Journal of Applied Physics*, 110 (2011) 083514.
- [7] Divinski, S.V., Padmanabhan, K.A., Wilde, G.: On the theoretical limits of Microstructure Evolution During Severe Plastic Deformation. *Philosophical Magazine*, 91 (2011) 4574-4593.
- [8] Rösner, H., Kübel, C., Ivanisenko, Y., Kurmanaeva, L., Divinski, S.V., Peterlechner, M., Wilde, G.: Strain mapping of a triple junction in nanocrystalline Pd. *Acta Materialia*, 59 (2011) 7380–7387.
- [9] Sauvage, X., Wilde, G., Divinski, S.V., Horita, Z., Valiev, R.Z.: Grain boundaries in ultrafine grained materials processed by severe plastic deformation and related phenomena. *Materials Science and Engineering A*, 540 (2012), 1-12.
- [10] Raju, K.S., Sarma, V.S., Kauffmann, A., Hegedus, Z., Gubicza, J., Peterlechner, M., Freudenberger, J., Wilde, G.: High strength and ductile ultrafine-grained Cu–Ag alloy through bimodal grain size, dislocation density and solute distribution. *Acta Materialia*, 61 (2013) 228–238.
- [11] Prokoshkina, D., Esin, V.A., Wilde, G., Divinski, S.V.: Grain boundary width, energy and self-diffusion in nickel: Effect of material purity. *Acta Materialia* 61 (2013) 5188-5197.
- [12] Wegner, M., Leuthold, J., Peterlechner, M., Setman, D., Zehetbauer, M., Pippan, R., Divinski, S., Wilde, G.: Percolating Porosity in Ultrafine Grained Copper Processed by High-Pressure Torsion. *Journal of Applied Physics*, 114 (2013) 183509.

6. STRATEGY AND CONTENT OF POSSIBLE COLLABORATION WITHIN THE CONSORCIUM

The field of metallurgy (chemistry, physics, mechanics and engineering) is the subject of intense discussions for development of projects in the domains of research and education since it appears as much necessary for industrial development in Europe. Our group is involved in these metallurgy initiatives and strengthen its activities on materials physics with melting, solidification, processing and mechanical properties of metals and alloys. UFG materials are among the materials of interest.

We are willing to keep connections in this framework in particular through organising joint scientific meetings, laboratory visits and welcoming visiting researchers. We also support



collaborations with co-supervising PhD students within EU programs or industry financial supports.

Acknowledgement

This contribution was created within the project **Creation of an international scientific team and incorporation to scientific networks in the area of nanotechnology and unconventional forming material. CZ.1.07/2.3.00/20.0038**, which is financed by the European Social Fund and state budget of the Czech Republic.



CZ.1.07/2.3.00/20.0038



esf european
social fund in the
czech republic



EUROPEAN UNION



MINISTRY OF EDUCATION,
YOUTH AND SPORTS



OP Education
for Competitiveness

INVESTMENTS IN EDUCATION DEVELOPMENT

Prior structure modification on grain refinement and mechanical properties of medium carbon steel

Jozef ZRNÍK^a, Sergey V. DOBATKIN^b, George RAAB^c, Libor KRAUS^a

^a COMTES FHT Inc., Průmyslová 995, Dobřany, Czech Republic, jzrník@comtesfht.cz

^b Baikov Institute of Metallurgy & Materials Science, RAS, Moscow, Russia, dobatkin@ultra.imet.ac.ru

^c Institute of Physics of Advanced Materials, Ufa, Russia, G.I.Raab@mail.

Abstract

The work presents the results on grains refinement of steel containing 0.45 wt pct. carbon resulted from severe plastic deformation (SPD). Different steel structures resulting from prior solutioning and/or thermomechanical (TM) treatment were prepared for deformation experimental. A coarse grain ferrite-pearlite structure was achieved applying solutioning. By application of TM control forging process, performing multistep open die forging, the refined ferrite-pearlite mixture was resulted. Final steel structure refinement, having different initial structure, was then accomplished applying warm Equal Channel Angular Pressing (ECAP) at 400°C. Employment of this processing route resulted in extensive deformation of ferrite grains and cementite lamellae fragmentation. Applying the highest shear stress ($\epsilon_{ef} - 4$) the mixture of subgrains and ultrafine grains was found in former equiaxed ferrite grains. On the other side, in pearlite grains, modification of cementite lamellae due to shearing, bending, twisting and breaking was found efficient in pearlite lamellae refining. The coarse cementite lamellae spheroidization was more efficient when prior TM treatment modified steel microstructure. The tensile deformation records then confirmed strength increase and diversity in strain hardening behaviour.

Keywords

Medium carbon steel, solutioning, TM treatment, SPD, SPD, ECAP, microstructure, properties.

1. INTRODUCTION

The severe plastic deformation (SPD) technology of metallic materials is capable of producing ultrafine grained (UFG) structures with submicrometer or even nanometer grain size [1,2]. Since ECAP and the others deformation technologies were introduced to refine structure of bulk metallic materials, many research works were devoted to analyse the processing method details, but also to study the microstructural evolution and deformation respond of ultrafine grained materials. Continuously significant interest has shifted to the use of ECAP in processing of UFG low carbon steels [3,4]. This interest has been motivated in part by the fact that UFG low carbon steels can be used in many applications as structural materials, and in particular by ECAP capability to improve the strength of these steels without a need to change their chemical composition [5]. It was observed that the ultimate tensile strength (UTS) increased with



increased straining. On the other hand, the number of research works as to SPD of commercial medium carbon steels is still limited because SPD processing is relatively difficult in steels with higher flow stress [6]. To clarify the evolution of the deformation microstructures in medium carbon steels subjected to an effective strain ϵ_{ef} of 4 and higher, the warm or hot ECAP is recommended, to provide the deformation required for the onset of dynamic recrystallization under larger strain [7,8].

In present study at first the effect of initial structure modification of ferrite-pearlite microstructure of AISI 1045 steel (0.45 wt % C) due to solutioning and TM treatment is described. Subsequently the effect of initial structure modification in steel was correlated with development of ultrafine grain microstructure in condition of severe plastic deformation (ECAP) at increased temperature. Finally, resulting microstructure development was related to deformation behaviour and mechanical properties of steel.

2. MATERIALS AND EXPERIMENTAL PROCEDURES

2.1 Initial steel microstructure characterization

To study an influence of initial structure characteristics of steel on formation of ultrafine grain structure in condition of severe plastic deformation in medium carbon steels, different initial structural states of steels were prepared applying thermal and/or thermomechanical treatment. The experimental material for this study was commercial medium carbon steel grade AISI 1045, (Fe-0.45%C-0.23 Si-0.63 Mn-0.18 Cr-0.43 Al).

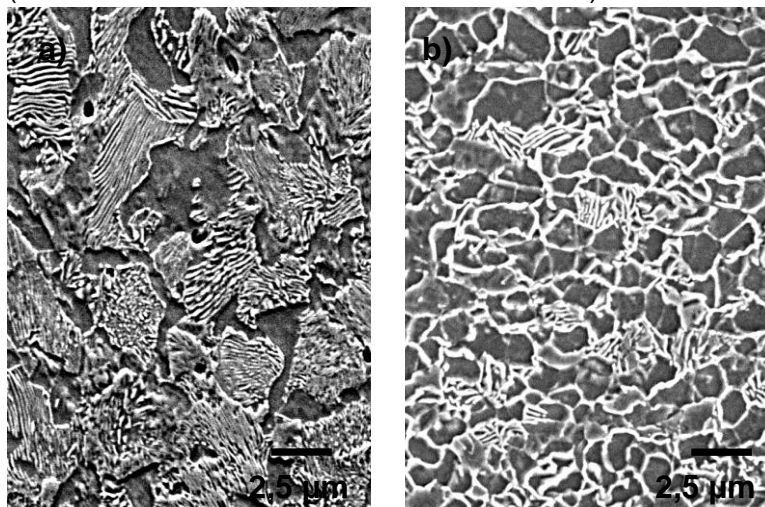


Fig. 1 Microstructure resulting from steel solutioning (a) and TM treatment (b).

The mixture of ferrite and pearlite phases resulting from soaking treatment at 960°C for 1h and air cooling is presented in Fig. 1a. Pearlite grains with size of ~ 50 μm are lined by the finer ferrite grains (~10 μm in size). In order to achieve, prior ECAP deformation, preliminary refined ferrite and pearlite structure, the TM processing 900 – 700°C with aim to refine the coarse ferrite – pearlite structure. The resulting microstructure in the centre of deformed specimen is shown in Fig. 1b. The average grain size in deformed specimen was in range of 5 μm .

For ECAP deformation experimental the prior soaked and TM treated cylindrical bars of 9 mm in diameter and 50 mm in length were machined. The warm ECAP pressing at 400°C was performed and billets were subjected to N = 4, 5 and 6 passes respectively. The ECAP channels had a round shape and the angle of channels intersection was of $\phi = 120^\circ$, yielding for each pass an effective strain $\epsilon_{ef} = 0,67$. For ECAP experimental the route Bc was chosen. The heating of bars prior pressing was done inside pre-heated ECAP die until samples reached the pressing temperature of 400°C.



The microstructural examination of thermally treated samples was carried out by scanning electron microscopy (SEM) and development of deformed microstructure in ECAP deformed bars by transmission electron microscopy (TEM). Thin foils for TEM observation were sliced normal to the longitudinal axis of ECAPed billets.

Uniaxial tensile tests at room temperature were conducted using an Instron 5882 testing machine. Tensile specimens with gauge length of $l_0 = 20$ mm were tested at a constant crosshead displacement of 0,016 mm/s until failure. From received tensile data the engineering stress-strain curves were constructed for both initial structural states of steel.

3. EXPERIMENTAL RESULTS AND DISCUSSION

3.1 Initial steel microstructure characteristics

It is generally known, that medium carbon steel when thermally treated in annealing condition consists of ferrite and lamellae pearlite constituents. Deformation behaviour and properties of carbon steel then depends on morphology and volume fraction of phases present in steel. In this work two different procedures, specifically solutioning and/or thermomechanical treatment of steel, were carried out with aim to prepare different initial ferrite-pearlite microstructure characteristics in steel, as regards morphology and distribution of ferrite and pearlite constituents. Subsequently, the effect of structure modification was verified with regard to ultrafine grain formation in condition of severe plastic deformation (ECAP) and from aspect of deformation behaviour modification of steel.

The steel microstructure resulting from solutioning treatment at 900°C and air cooling was the mixture of lamellae pearlite and equiaxed ferrite grains. The average size of pearlite grains is about of 50 μm . The pearlite grains are lined by fine ferrite grains, Fig. 1a. The volume fraction of pearlite in structure is ~80 vol.% and the rest was ferrite phase. The mean linear intercept size of larger and smaller ferrite grains is ~ 2 and ~ 5 μm respectively.

In order to modify the coarse initial steel ferrite-pearlite structure resulting from solutioning treatment at 900°C, the TM treatment of steel bars was then conducted using forging. Applying this treatment the ferrite-pearlite structure was then apparently modified as presented in Fig. 1b.. Two different morphologies of ferrite grains were present in microstructure. The first, fine equiaxed grains, which resulted from the transformation of deformed austenite with size of ~ 2 μm , and the second, the elongated grains of already transformed ferrite, which was deformed passing intercritical $\alpha+\gamma$ region and down below this critical temperature region of austenite. These ferrite grains were larger with size of about 5 μm . In the central part of specimens, the pearlite grains were comparable to that of ferrite grains and their distribution was uniform there. Some spheroidized cementite rods were found scattered along ferrite grains boundaries. Towards the specimens edge the size of pearlite colonies increased and microstructure heterogeneity, as regards pearlite grains size and distribution, was increased as well.

3.2 Prior steel solutioning treatment and ECAP deformation process

Initial microstructure of steel prior ECAP processing was modified applying solution treatment at 900°C for 1h and air cooling. Thermally treated steel bars were then deformed in ECAP die. Performing ECAP pressing the individual steel bars were then experienced $N= 4, 5$ and 6 passes through the die. Finishing ECAP deformation the corresponding effective strain in dependence of number of passes was $\epsilon_{\text{ef}} = 2.7, 3.4$ and 4 respectively for individual samples. The microstructural characteristics of deformed ferrite and pearlite structure, experienced $N= 4$ and 6 ECAP passes are presented in Fig. 2. Performing $N= 4$ passes ($\epsilon_{\text{ef}}= 2.7$) the resulting



deformed structure was found heterogeneous and diverse along deformed bar. The equiaxed ferrite grains, resulting from solution treatment, were found only partly deformed. The cementite lamellae were curved, bowed and only slightly distorted, preserving lamellar morphology, as shown in Fig. 2a. Executing $N = 6$ passes the ferrite and pearlite grains were substantially stretched in shear direction, as shown in Fig. 2b. More effective straining caused to larger extent lamellae pearlite breakage. However locally in some pearlite grains the modified lamellae morphology was preserved.

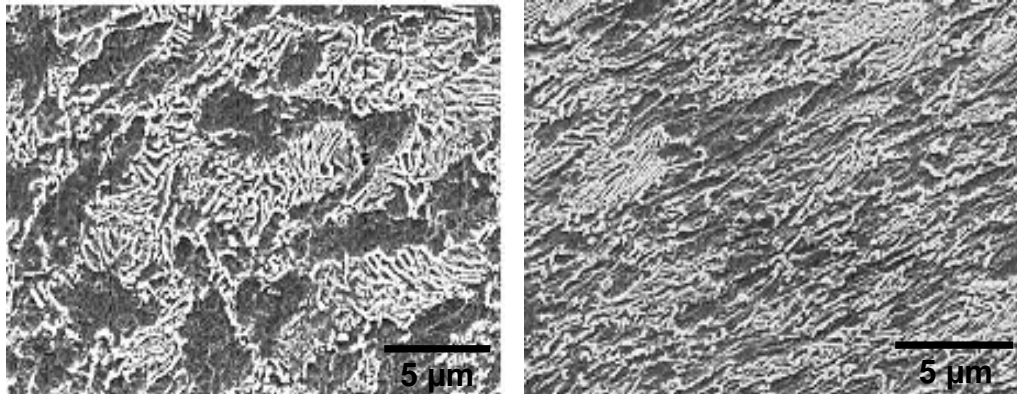


Fig. 2 Deformed ferrite-pearlite microstructure experienced: a) N4 passes and b) N6 passes through die. Initial microstructure resulted from steel solutioning prior ECAP.

The effect of straining on deformed microstructure formation was also investigated using TEM of thin foils on the plane parallel with billet longitudinal axis. The deformed substructures of ferrite and pearlite, experienced different straining performing $N = 4, 5$ and 6 passes are presented in Fig. 3. Formation of ultrafine grain structure in initially coarse ferrite and pearlite grains was only of low efficiency when experienced the lower effective strain ($\epsilon_{ef} = 2.7$, $N = 4$). Dense dislocation network and subgrain structure were preferentially formed within ferrite grains, Fig. 3a. The cementite lamellae morphology was predominant and in majority of grains preserved. The cementite lamellae in pearlite areas was predominant in majority, however the crushed cementite lamellae were also found in case when a larger effective straining was applied ($\epsilon_{ef} = 3.4$, $N = 5$). Due to higher level of straining in former deformed ferrite grains the new grains of submicron sizes appeared sporadically, Fig. 3b. Fine grains of submicron size in deformed ferrite grains together with shear bands in cementite lamellae areas were found more frequently as strain was increased to $\epsilon_{ef} = 4$, which corresponds to execution of $N = 6$ passes, Fig. 3c. As records show in pearlite grains the shear bands deforming cementite lamellae were found locally as well.



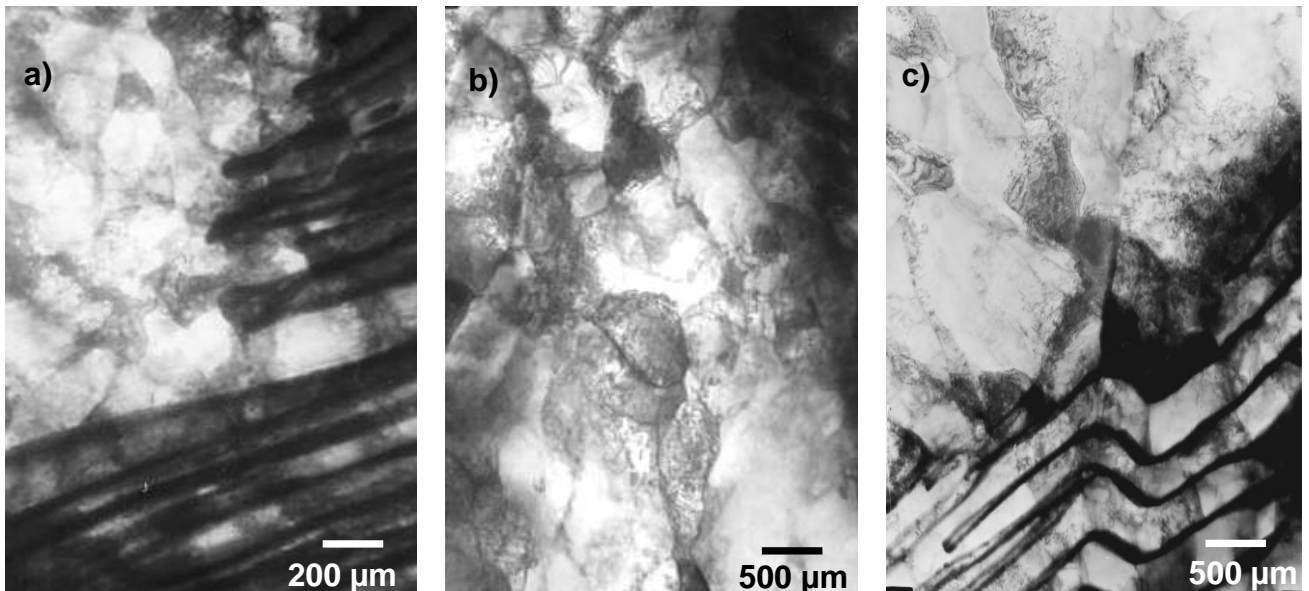


Fig. 3 TEM of ECAP deformed microstructure experienced straining : a) N-4, b) N-5, c) N-6 passes. Initial steel micro structure resulted from steel solutioning.

3.3 Prior steel TM treatment and ECAP processing.

In order to refine initial ferrite-pearlite structure in medium carbon steel a preliminary structure refinement was carried out applying thermo-mechanical processing. It was then expected, that by execution of TM processing of steel prior ECAP deformation and by support of spontaneous recrystallization process at higher temperature will result in more effective austenite grain refining and subsequently to refine and modify ferrite and pearlite structure characteristics in time of repetitive ECAP deformation process.

When executing TM multiaxial step pressing of steel bar prior ECAP, it caused in advance ferrite grains refinement and pearlite (cementite lamellae) morphology modification. Applying repetitive pressing deformation it also influenced, due to temperature gradient and strain distribution heterogeneity across deformed peg, the ferrite grain size heterogeneity and cementite lamellae morphology modification (lamellae fracturing). It was then expected, that development and formation of ultrafine grain structure, when ECAP processed performed, will be then subsequently modified to some extent, due to preliminary initial structure modification resulting from prior TM steel treatment. As structure results showed, formation of ultrafine grain structure was preferential in former ferrite grains and critical factor for structure refinement was level of applied effective strain ϵ_{ef} . Only small contribution from prior microstructure modification due to TM treatment execution was observed, as concerned ferrite grains refinement and pearlite lamellar morphology modification. The deformed microstructure, which resulted from different ECAP straining of steel, related to different number of passes through die channel (N= 4 and N= 6 passes) is presented in Fig. 4 a,b.. The microstructure changes resulted from prior TM treatment applied prior ECAP provided only small contribution as to structure modification, especially lamellar pearlite morphology modification, and also on strengthening effect and deformation behaviour of experimental steel.

In order to characterize deformed microstructure of steel resulting from different ECAP straining at 400°C in details the TEM micrographs are presented in Fig. 5 a,b. Conducted ECAP deformation with channel angle of 120° the deformed structure was found heterogeneous across the billets regardless the strain applied (N-4 and N-6 passes). The areas of severe defor-



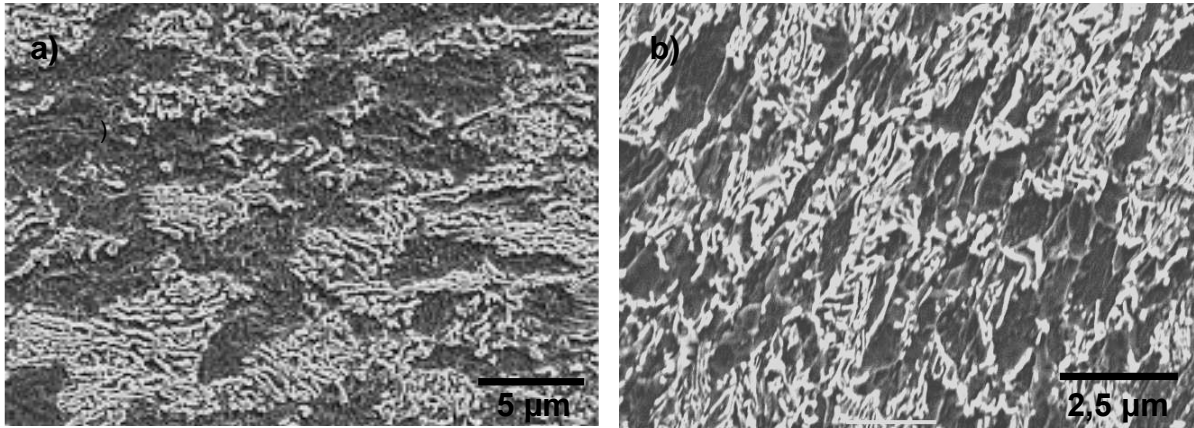


Fig. 4 ECAP deformed ferrite-pearlite microstructure experienced: a) microstructure. Microstructure resulting from steel solutioning (a) and TM treatment (b).

mation, where cementite fragmentation and formation of dislocation network in ferrite are evident, were found next to polygonized microstructure due to the deformation extended ferrite grains. Investigating deformation substructure also a progress in cementite lamellae spheroidization due to increased temperature of deformation is apparent as well. The dislocation substructure in deformed ferrite grains was modified upon effective dynamic polygonization process. However, next to this refined grains sites, the low angle boundaries are still apparent in ferrite grains. Submicrocrystalline structure is formed within ferrite grains as well. As ECAP straining increases reaching $\epsilon_{ef} = 4$, ($N = 6$) the progress in dynamic polygonization proceeded and formation of submicron size grains, having high angle boundaries, was observed in ferrite and also between fractured residues of cementite lamellae. This observation on substructure development indicates that progress in formation of more UF grains is less effective due to insufficient straining of specimen resulting from six passes using ECAP die with angle of 120° .

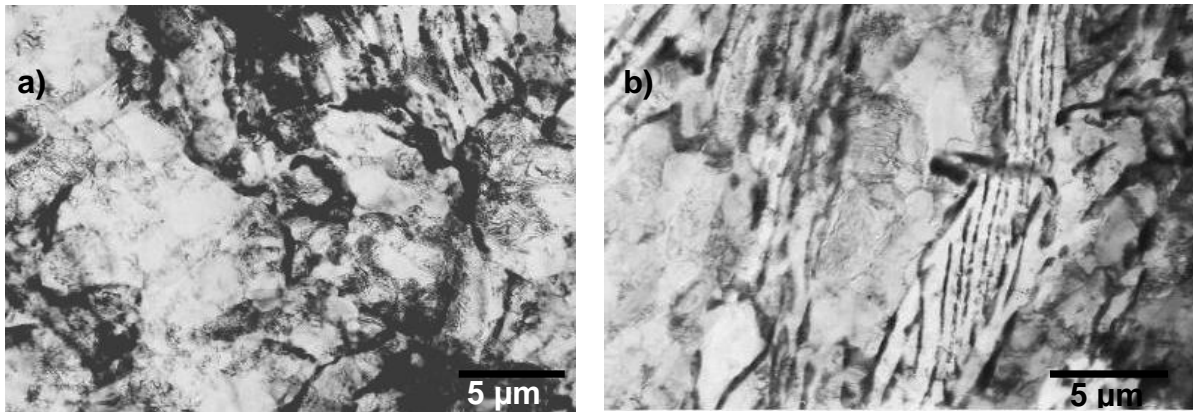


Fig.5 ECAP deformed ferrite-pearlite microstructure experienced: a) microstructure. Microstructure resulting from steel solutioning (a) and TM treatment (b).

3.4 Mechanical properties of prior solutioned steel

When to relate structural characteristics and resulted mechanical properties of the steel having modified structural states, which resulted from applied prior solutioning and then applying additional TM treatment, the hardness values were in good conformity with recorded course of deformation behavior of steel. The results underlined so the good agreement with change of structural state of steel resulting from the applied thermal and thermomechanical treatment of medium carbon steel.



3.5 Mechanical properties of prior solutioned steel

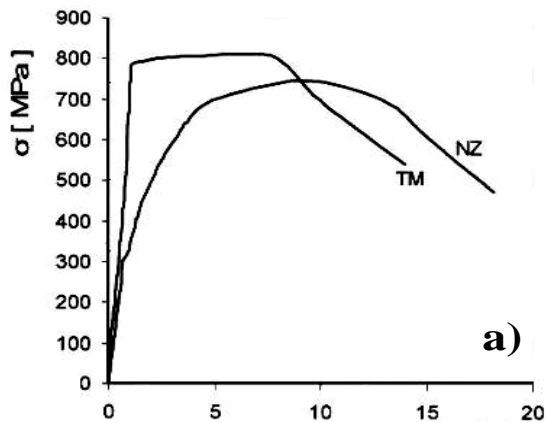


Fig.7 Stress – strain curves for steel experienced soaking and TM treatment.

The mechanical properties of experimental steel which was subjected to thermal and thermo-mechanical treatment prior severe plastic deformation were evaluated in condition of tensile deformation and by hardness (HV30). The tensile deformation results for initial structure states of steel modified by solutioning and TM treatment were carried out at room temperature and they are shown in Fig. 6a. In case of the initial steel solutioning (S) there was a distinctive period of work hardening resulting in quite large elongation to failure. In the same figure the deformation curve corresponding to TM-treated steel, which results in considerable

grains refinement and structure homogenization, shows slight work hardening course and resulted in shorter deformation course to failure. The records of deformation behaviour also confirmed that additional TM treatment of steel slightly improved strength of the steel, probably due to ferrite structure refinement and cementite lamellae modification. Hardness values are in good conformity with course of deformation behaviour and correspond to structural steel state resulting from applied steel treatment.

When to relate structural characteristics and resulted mechanical properties of the steel having modified structural states, which resulted from applied prior solutioning and then applying additional TM treatment, the hardness values were in good conformity with recorded course of deformation behavior of steel. The results underlined so the good agreement with change of structural state of steel resulting from the applied thermal and thermomechanical treatment of medium carbon steel.

3.6 Mechanical properties of prior solutioned and ECAP processed steel.

The mechanical properties of steel subjected to thermal treatment (soaking) prior SPD were evaluated by tensile test and by hardness measurement (HV30). The deformation behaviour of soaked and ECAP steel specimens was very similar for all three initial structural states of deformed specimens. Regardless the different ECAP straining (ϵ_{ef}) resulting from deformation conditions, it was then found only negligible small difference in effective stress value (effect of strengthening). The tensile deformation results received for all different initial structural steel states of soaked and ECAP steel specimens is very similar for all three initial states of deformed specimens. Regardless the different ECAP straining (ϵ_{ef}) resulting from deformation condition that was found only small difference in effective stress reaching ϵ_{ef} value. The tensile deformation results received for all initial structure states of steel exposed to different ECAP straining (N-4,5 and 6 passes) carried out at room temperature are shown in Fig. 7. There is, as deformation records show, after reaching the yield stress, section of slight hardening similar for all three initial states, which is extending slightly as straining is increased. However, on the other side, the strength values are of the same level for all specimens, regardless the effective



strain level introduced. This is probably incurred by quite large fraction of pearlite lamellar

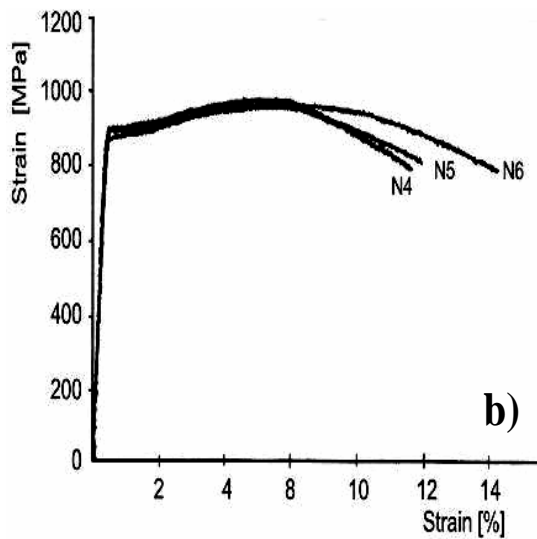


Fig. 7 Stress – strain curves for steel experienced soaking and ECAP deformation to different ϵ_{ef} .

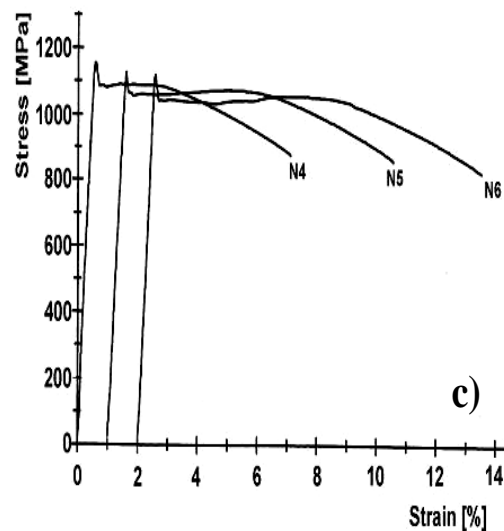


Fig. 8 Stress-strain curves for steel after soaking (NZ) and TM treatment

morphology preserved in structure. The contribution of this preserved pearlite lamellae is inexpressive, probably due to its small volume fraction when compared with steel structure characteristics resulting from TM treated steel.

3.7 Mechanical properties of prior TM treatment and ECAP processed steel.

As concern the deformation behaviour of the medium carbon steel, which was TM processed prior to ECAP, the tensile test records are shown in Fig. 8. For all specimens subjected to different straining the deformation behaviour is very similar. After discontinuous yielding (sharp stress drop reaching the yield stress), there is a region of "creep-like" deformation behaviour, where work hardening period is not appearing on deformation records. The section is extended as straining increases. Due to this sharp drop of stress the ultimate tensile strength is lower than "upper" yield stress. The sharp drop of plastic behaviour of steel is noticeable different from that appearing at deformation behaviour of the low carbon steel, where the effect of aging (carbon atmosphere) can modify the process of yielding. However, this phenomenon can be a result of cementite particle dissolution in ferrite and carbon atoms saturation in lattice as well. The appearance of short flat region on the deformation curves, (which appeared for all ECAP deformed samples), could be then attributed to a balance of strengthening effect, caused by increased portion of newly formed fine submicrocrystalline grains, and on the other side, (with high probability), due more effective progress of dynamic recovery and recrystallization in time of deformation process. These processes, as microstructure results show up and confirmed, actually could participate in structure transformation process and contributed to steel deformation behaviour.

4. SUMMARY

Medium carbon steel AISI 1045 was subjected to severe plastic deformation using ECAP deformation technology at increased temperature of 400 °C. The aim of investigation was to



explore formation of ultrafine grain structure in dependence of the different initial steel structure, which was resulting from prior thermal and/or TM treatment.

Applying warm ECAP to initially coarse ferrite-pearlite structure led to formation of deformed microstructure regardless of the effective shear strain applied. In dependence of straining conditions, within the pearlite grains deformation and fragmentation of cementite lamellae were less productive to modify pearlite lamellar structure, regardless the initial steel structure treatment. As regards ferrite phase deformation, in dependence of applied level of the effective straining, formation of mixture of subgrains and ultrafine grain structure was already observed for solutioned structure when applying lower effective strain, experience two ECAP passes.

In case the initial steel structure was modify by TM treatment prior ECAP processing the steel structure modification was more effective as regards both, pearlite lamellae grains and larger pearlite colonies, were modified, fragmented and refined. Such structure modification resulted in different deformation behaviour of steel, regardless the level of straining.

5. REFERENCES

- [1] W. M. Segal: Materials Science Engineering A, 197, 1995, 157.
- [2] R. Z. Valiev et al.: Materials Science Engineering A, 168, 1993, 141.
- [3] S. V. Shin, J. J. Park, Y.S. Park: Materials Science Engineering A, 375, 2002, 178.
- [4] K. T. Park, Y. S. Kim, D. H. Shin: Metallurgical & Materials Transactions A, 32, 2001, 492.
- [5] Y. Fukuda et al.: Acta Materialia Transactions, 50, 2002, 1359.
- [6] N. Tsuji et al.: Scripta Materialia, 47, 2003, 893
- [7] S. M. Sastry, S. V. Dobatkin, V. Sidorova: Russian Metals, 2, 2004, 139
- [8] J. Zrník, S. Dobatkin, L. Kraus: Key Engineering Materials Vols. 592-593, 2014, 307.

Acknowledgement

This paper was created within the project "**Creation of an international scientific team and incorporation to scientific networks in the area of nanotechnology and unconventional forming material. CZ.1.07/2.3.00/20.0038**", which is financed by the European Social Fund and state budget of the Czech Republic.

